Science Results of 9 Years of Measurements from CALET Operation on the International Space Station

Calorimetric Electron Telescope (CALET)

SuGAR MADISON 2024
SEARCHING FOR THE SOURCES OF GALACTIC COSMIC RAYS

John Krizmanic
NASA Goddard Space Flight Center
for the CALET Collaboration

The CALET Collaboration

O. Adriani,[1,2] Y. Akaike,[3,4] K. Asano,[5] Y. Asaoka,[5] E. Berti,[2,6] G. Bigongiari,[7,8] W. R. Binns,[9] M. Bongi,[1,2] P. Brogi,[7,8] A. Bruno,[10] N. Cannady,[11,12,13] G. Castellini,[6] C. Checchia,[7,8] M. L. Cherry,[14] G. Collazuol,[15,16] G. A. de Nolfo,[10] K. Ebisawa,[17] A. W. Ficklin,[14] H. Fuke,[17] S. Gonzi,[1,2,6] T. G. Guzik,[14] T. Hams,[11] K. Hibino,[18] M. Ichimura,[19] W. Ishizaki,[5] M. H. Israel,[9] K. Kasahara,[20] J. Kataoka,[21] R. Kataoka,[22] Y. Katayose,[23] C. Kato,[24] N. Kawanaka,[25,26] Y. Kawakubo,[14] K. Kobayashi,[3,4] K. Kohri,[26,27] H. S. Krawczynski,[9] J. F. Krizmanic,[12] P. Maestro,[7,8] P. S. Marrocchesi,[7,8] A. M. Messineo,[8,28] J. W. Mitchell,[12] S. Miyake,[29] A. A. Moiseev,[12,13,30] M. Mori,[31] N. Mori,[2] H. M. Motz,[32] K. Munakata,[24] S. Nakahira,[17] J. Nishimura,[17] M. Negro,[14] S. Okuno,[18] J. F. Ormes,[33] S. Ozawa,[34] L. Pacini,[2,6] P. Papini,[2] B. F. Rauch,[9] S. B. Ricciarini,[2,6] K. Sakai,[11,12,13] T. Sakamoto,[35] M. Sasaki,[12,13,30] Y. Shimizu,[18] A. Shiomi,[36] P. Spillantini,[1] F. Stolzi,[7,8] S. Sugita,[35] A. Sulaj,[7,8] M. Takita,[5] T. Tamura,[18] T. Terasawa,[5] S. Torii,[3] Y. Tsunesada,[37,38] Y. Uchihori,[39] E. Vannuccini,[2] J. P. Wefel,[14] K. Yamaoka,[40] S. Yanagita,[41] A. Yoshida,[35] K. Yoshida,[20] W. V. Zober[9]

PI: Japan
Co-PI: Italy
Co-PI: USA

1) University of Florence, Italy
2) INFN Sezione di Firenze, Italy
3) RISE, Waseda University, Japan
4) JEM Utiliziation Center, JAXA, Japan
5) ICRR, University of Tokyo, Japan
6) IFAC, CNR, Italy
7) University of Siena, Italy
8) INFN Sezione di Pisa, Italy
9) Washington University in St. Louis, USA
10) Heliospheric Physics Laboratory, NASA GSFC, USA
11) University of Maryland, Baltimore County, USA
12) Astroparticle Physics Laboratory, NASA GSFC, USA
13) CRESST II, NASA GSFC, USA
14) Louisiana State University, USA
15) University of Padova, Italy
16) INFN Sezione di Padova, Italy
17) ISAS, JAXA, Japan
18) Kanagawa University, Japan
19) Hirosaki University, Japan
20) Shibaura Institute of Technology, Japan
21) ASE, Waseda University, Japan
22) NIPR, Japan
23) Yokohama National University, Japan
24) Shinshu University, Japan
25) Tokyo Metropolitan University
26) NAO, Japan
27) IPNS, KEK, Japan
28) University of Pisa, Italy
29) KOSEN, NIT, Japan
30) University of Maryland, College Park, USA
31) Ritsumeikan University, Japan
32) GCSE, Waseda University, Japan
33) University of Denver, USA
34) NICT, Japan
35) Aoyama Gakuin University, Japan
36) Nihon University, Japan
37) Osaka Metropolitan University, Japan
38) NITEP, Osaka Metropolitan University, Japan
39) QST, Japan
40) Nagoya University, Japan
41) Ibaraki University, Japan

Calorimetric Electron Telescope (CALET) Science Goals

- **Search for nearby sources of trans-TeV $e^{\pm}$, i.e. Tevatrons, dark matter**
  - *Measurement:* **All-Electron observation (1 GeV – 20 TeV)**
  - *Instrument:* **Design optimized for electron detection with highly effective electron/hadron separation and nuclei measurement capability**

    Electromagnetic shower containment with 30 radiation length depth
    → **Fine energy resolution**

    versus 1.3 proton interaction length depth
    → **Effective electron/hadron separation**

    with good charge measurement from Z=1 thru Z=40
    → **Efficient measurement of cosmic ray nuclei**

A.K. Harding et al 2018 ApJL 869 L18

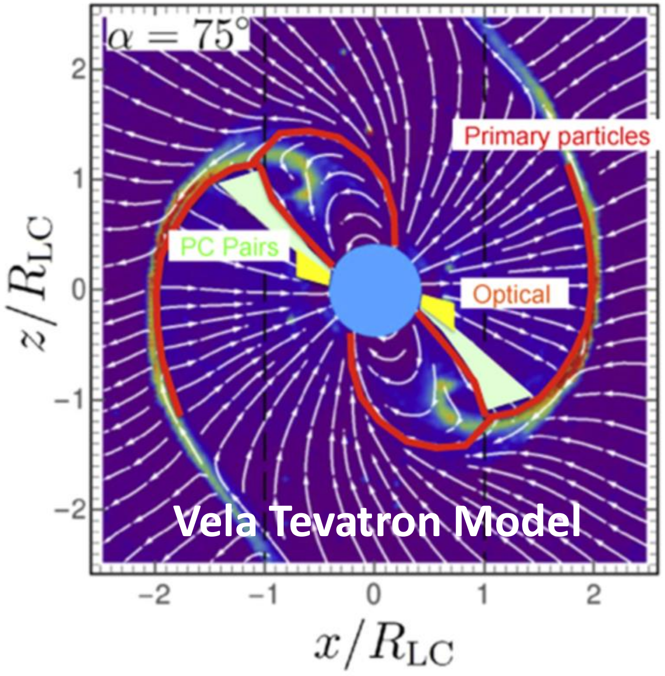

- **Unravel CR acceleration and propagation**
  - *Measurement:* **Cosmic-ray spectra for light & heavy nuclei (10 GeV – 1 PeV)**
  - *Measurement:* **Abundances of UHGCR (Z=30 thru Z=40)**

- **Detection of astrophysical/solar/magnetosphere transient phenomena**
  - Gamma-ray bursts
  - Gravitational wave counterparts
  - Solar modulation of electrons and protons
  - Space weather phenomena

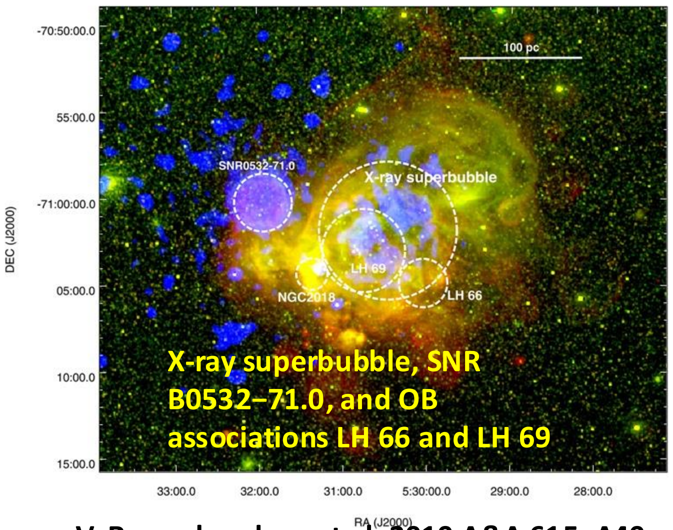

V. Ramachandran et al. 2010 A&A 615, A40

Calorimetric Electron Telescope (CALET) Science Measurements

Scientific Objectives	Observable Quantity	Energy Range
Cosmic-ray origin and acceleration	Electron spectrum	1 GeV – 20 TeV
	Elemental spectra	10 GeV – 1 PeV
	Ultra-heavy abundances	> 600 MeV/n
	Gamma rays (diffuse & point source)	1 GeV – 1 TeV
Galactic CR propagation	B/C and sub-Fe/Fe ratios	Up to some TeV/n
Nearby CR sources	Electron spectrum	100 GeV – 20 TeV
Dark matter	Signatures in electron/gamma spectra	100 GeV – 20 TeV
Heliospheric physics	Electron flux	1 GeV – 10 GeV
Gamma-ray transients	LE gamma rays and x-rays	7 keV – 20 MeV

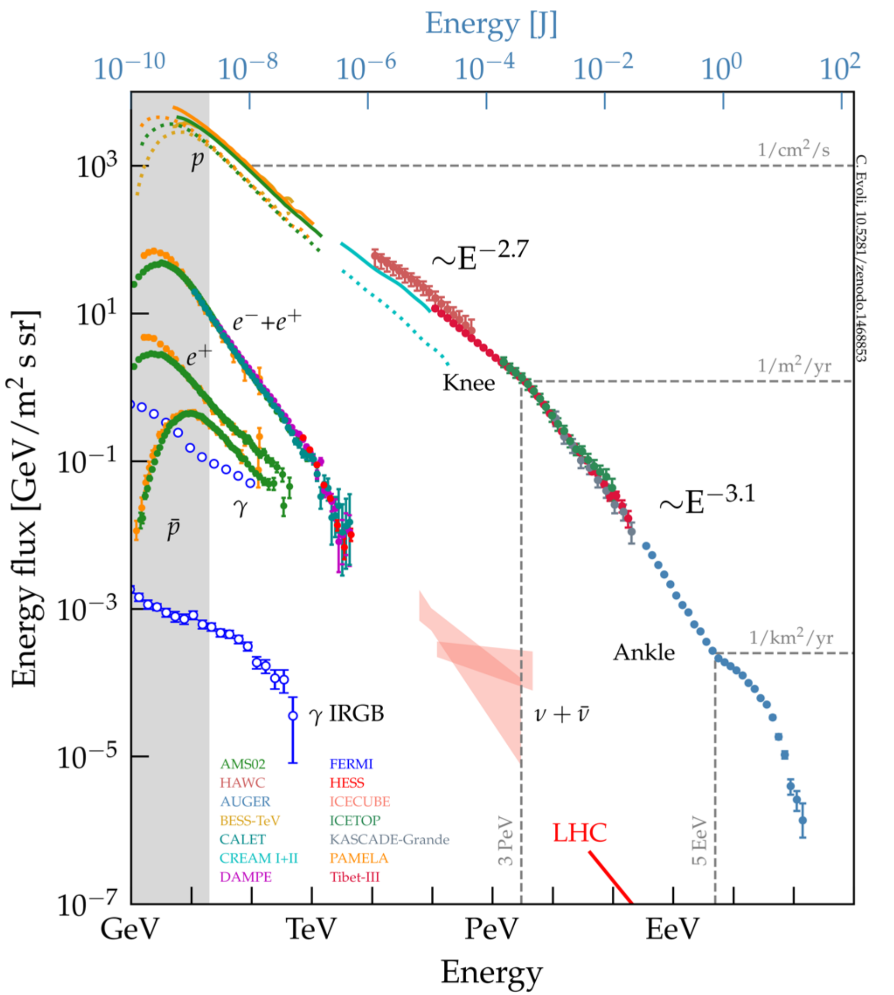

Carmelo Evoli (GSSI)
DOI 10.5281/zenodo.1468852

Science Measurements require CALET to be well calibrated

The CALET Payload

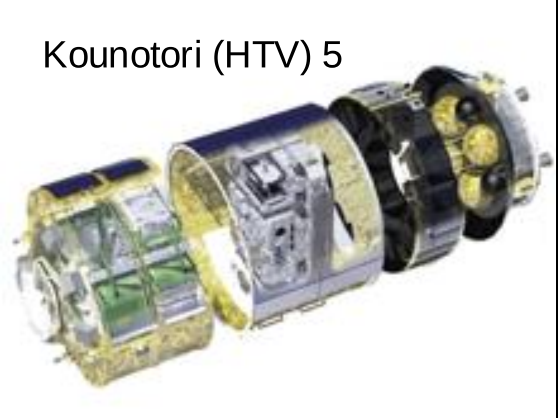

Launched on Aug. 19th, 2015 by the Japanese H2-B rocket

Attached on JEM-EF port #9 on Aug. 25th, 2015

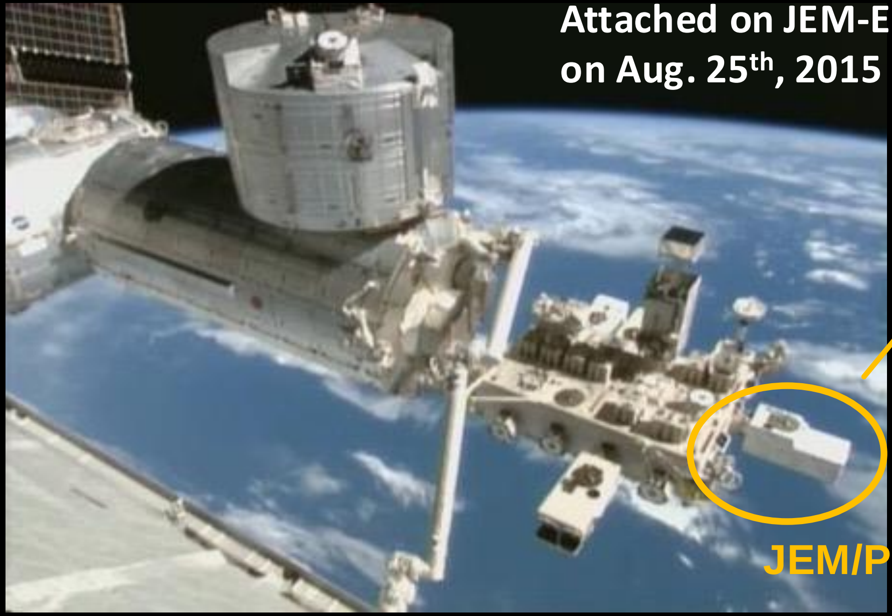

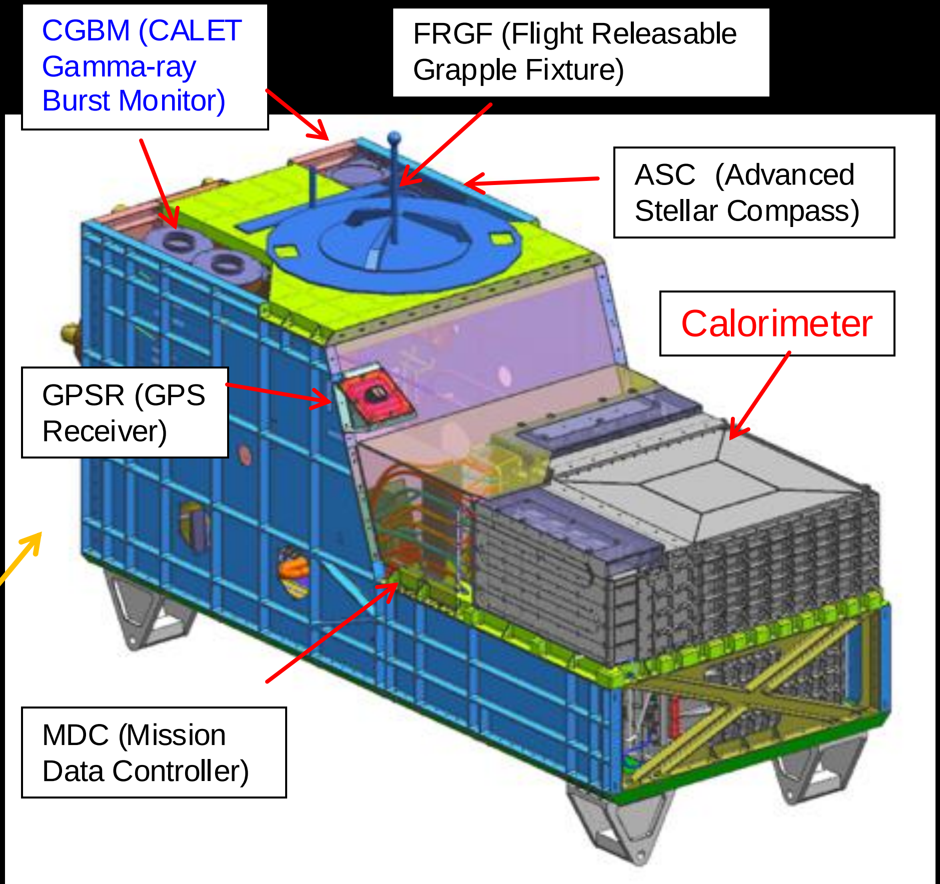

- Mass: 612.8 kg
- JEM Standard Payload Size:
  1850mm(L) × 800mm(W) × 1000mm(H)
- Power Consumption: 507 W （max）
- Telemetry:
  Medium 600 kbps (6.5GB/day) / Low 50 kbps

The CALET Calorimeter

CHD – Charge Detector
- 2 x 14 plastic scintillating paddles
- Charge measurement Z = 0 → 40+

IMC – Imaging Calorimeter
- 8 x 2 x 448 plastic scintillating fibers
- 7 tungsten sheets
- Shower development and imaging
- 3 electron radiation lengths normal incidence depth

TASC – Total Absorption Calorimeter
- 6 x 2 x 16 lead tungstate ($PbWO_4$) logs
- Electromagnetic shower absorption
- 27 electron radiation lengths normal incidence depth

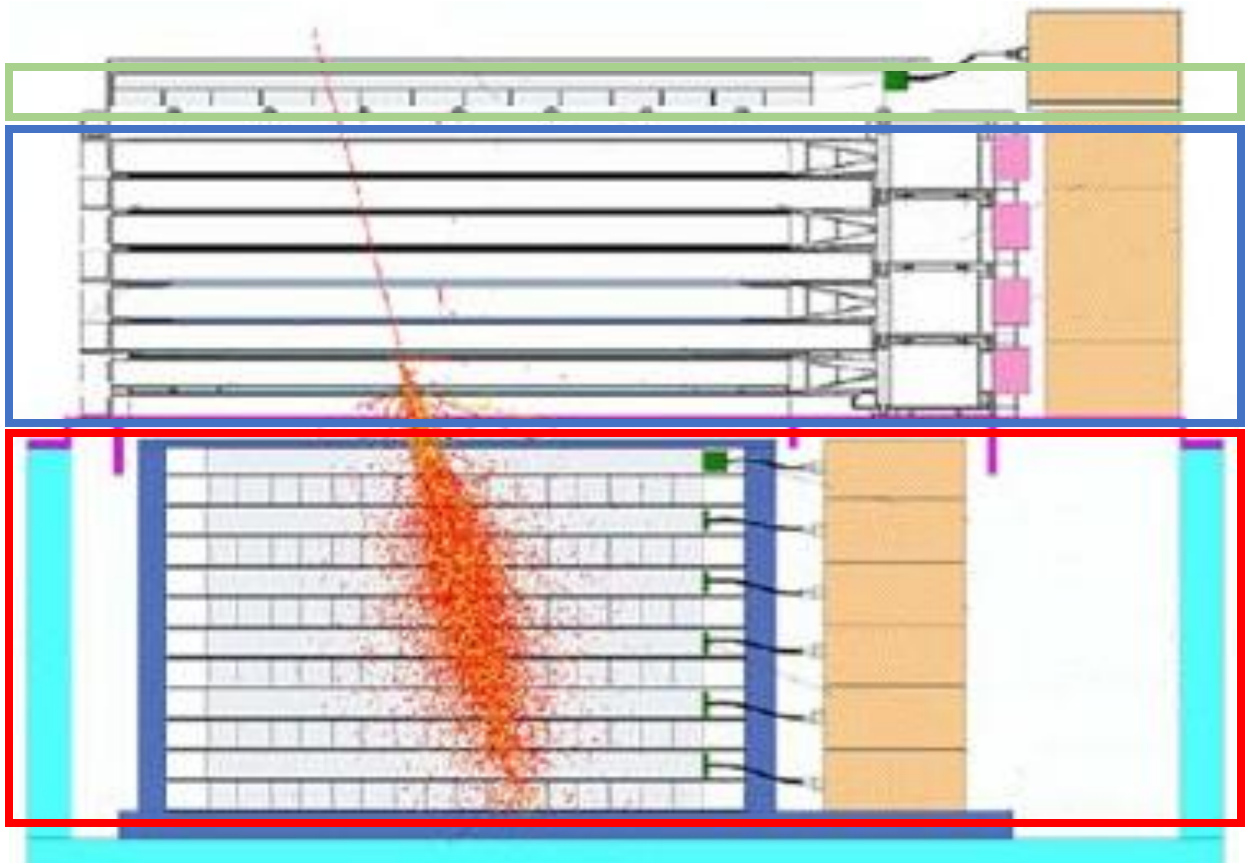

Image: simulated 1 TeV electron event in CALET

- **Geometrical Factor:**
  1040 cm^2 sr for electrons, light nuclei
  1000 cm^2 sr for gamma-rays
  4000 cm^2sr for ultra-heavy nuclei

- **ΔE/E:**
  ~2 % (>10GeV) for e , γ
  ~30-35% for protons, nuclei

- **e/p separation:** ~10^5
- **Charge resolution:** 0.15-0.3 e (p-Fe)
- **Angular resolution:**
  0.2° for gamma-rays > ~50 GeV

The CALET Calorimeter

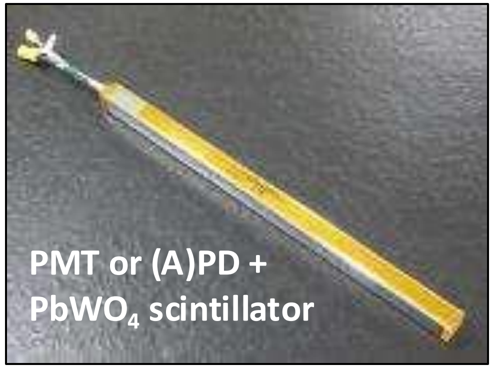

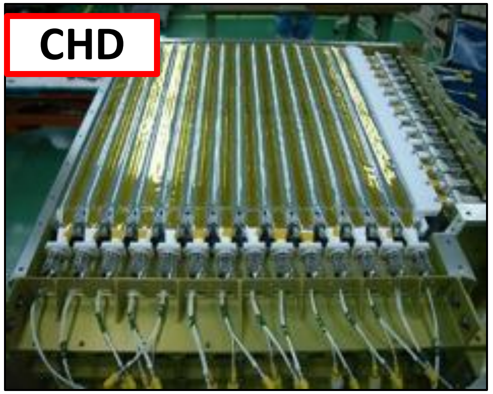

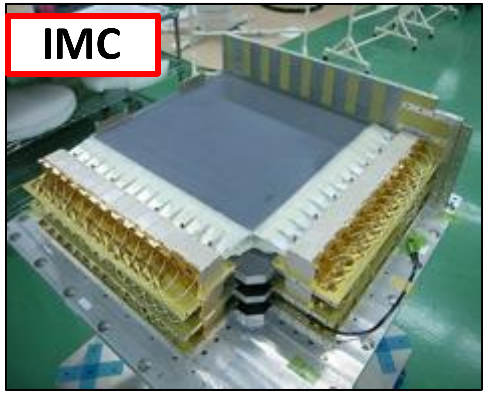

HTV (Kounotori) 5

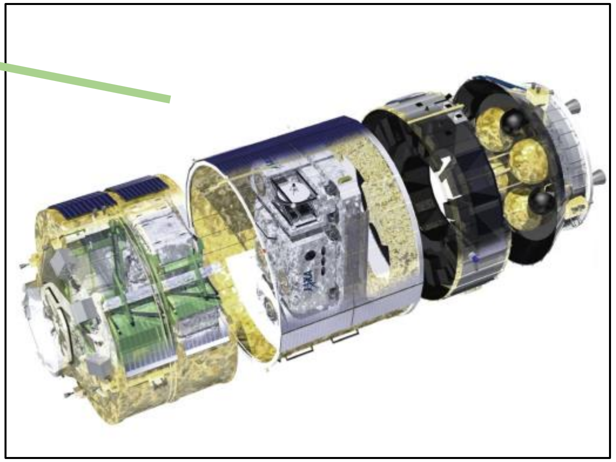

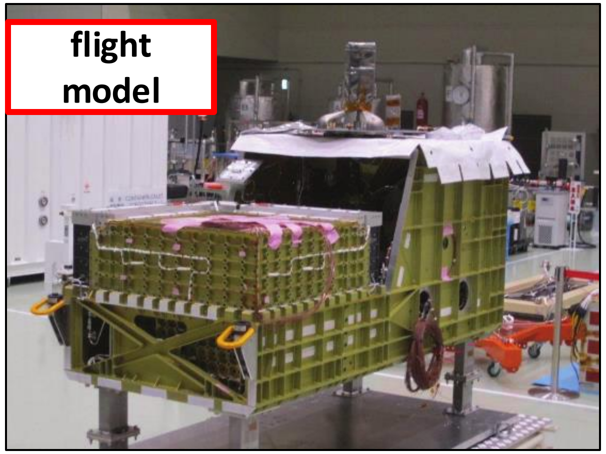

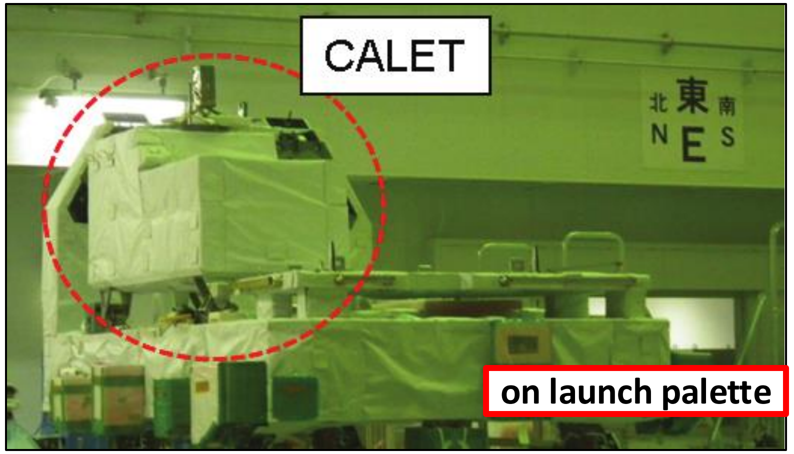

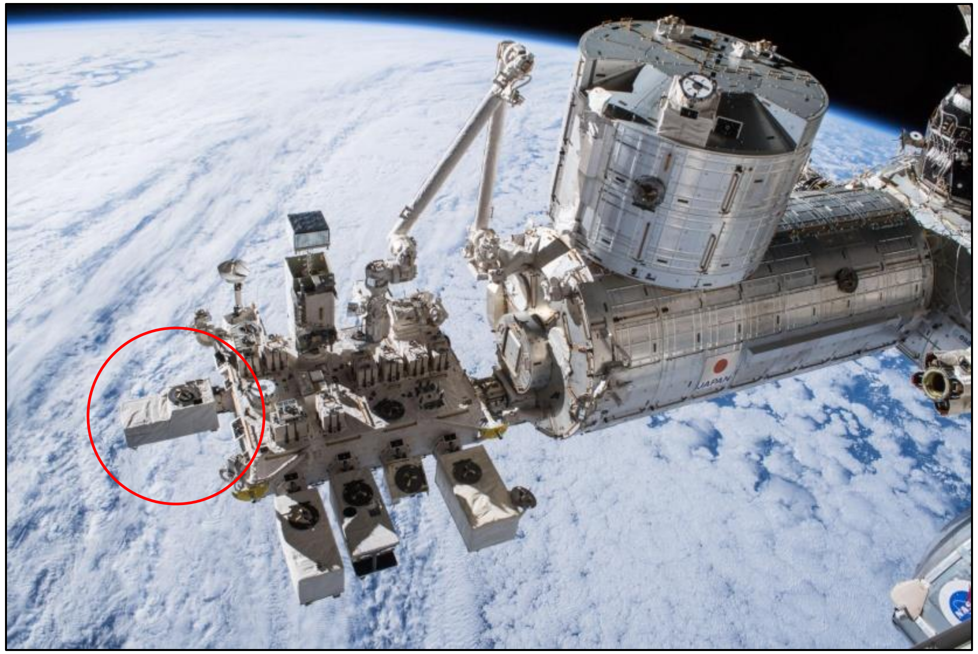

Pre-launch calibration of the TASC

Asaoka et al. 2017, Astropart. Phys. 91, 1—10

UV laser injection to calibrate adjacent gain ranges

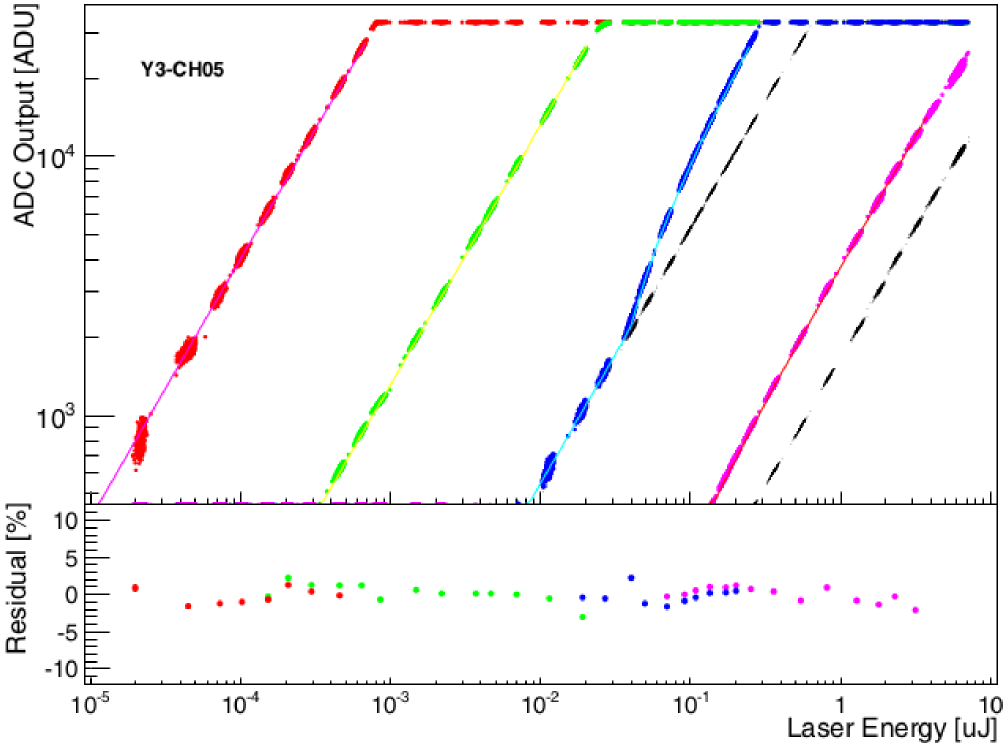

Laser-injected energy distribution in a TASC log

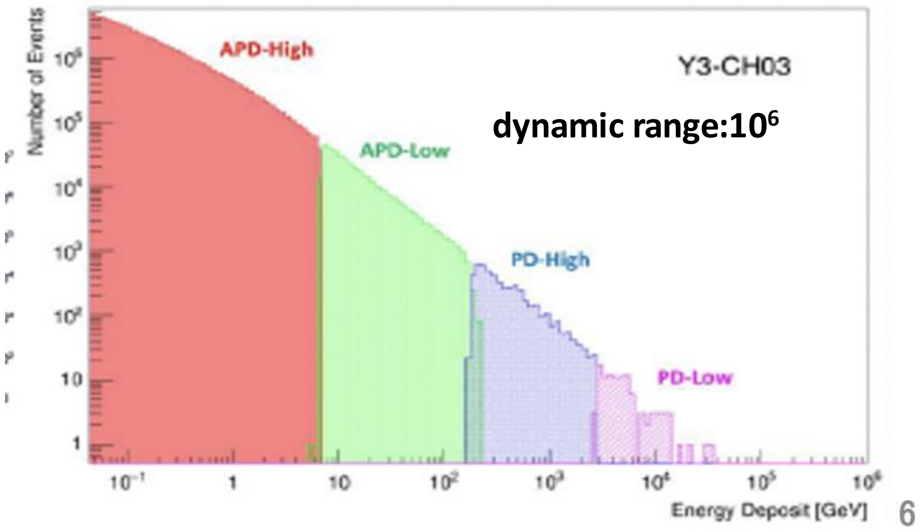

Crosstalk causes increase in PD signal when APD saturated

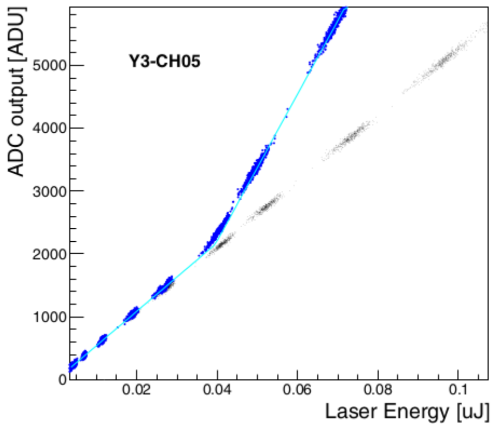

Analyzed on orbit to characterize changes from new environment:

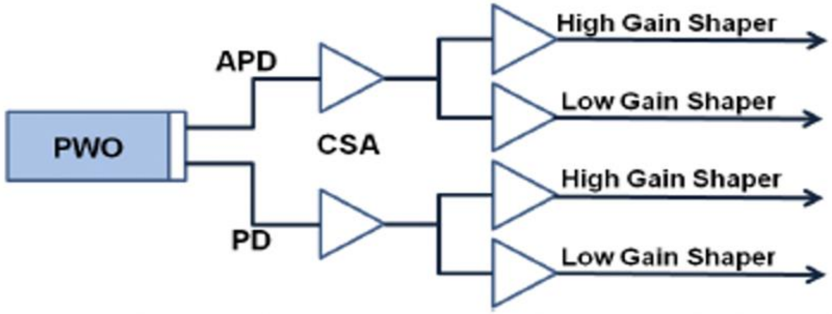

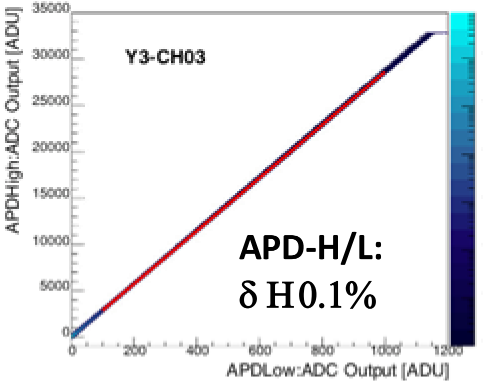

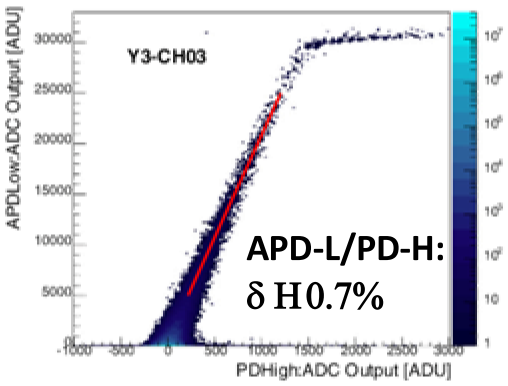

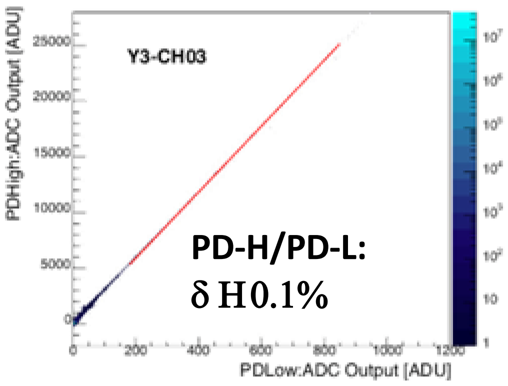

CERN calibration of the calorimeter

Asaoka et al. 2017, Astropart. Phys. 91, 1—10

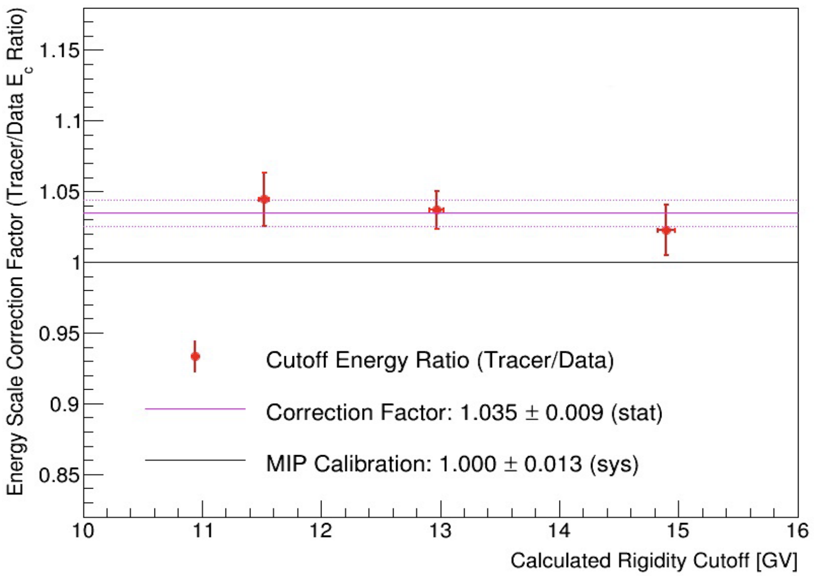

ELECTRONS

Absolute energy scale calibration for electrons using rigidity cutoff + beam calibration at CERN-SPS

Simulated energy dependence of electron energy resolution: < 2% above 20 GeV using both TASC and IMC Including the calibration errors

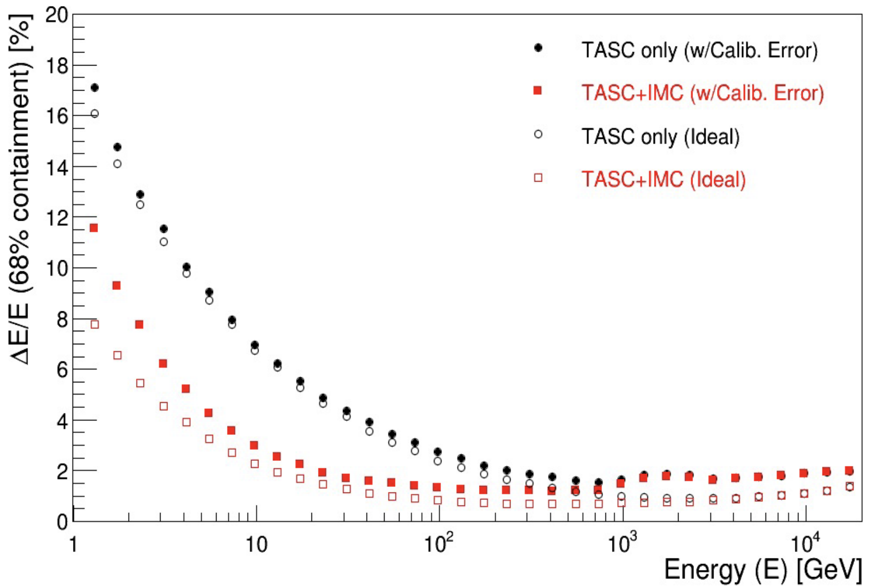

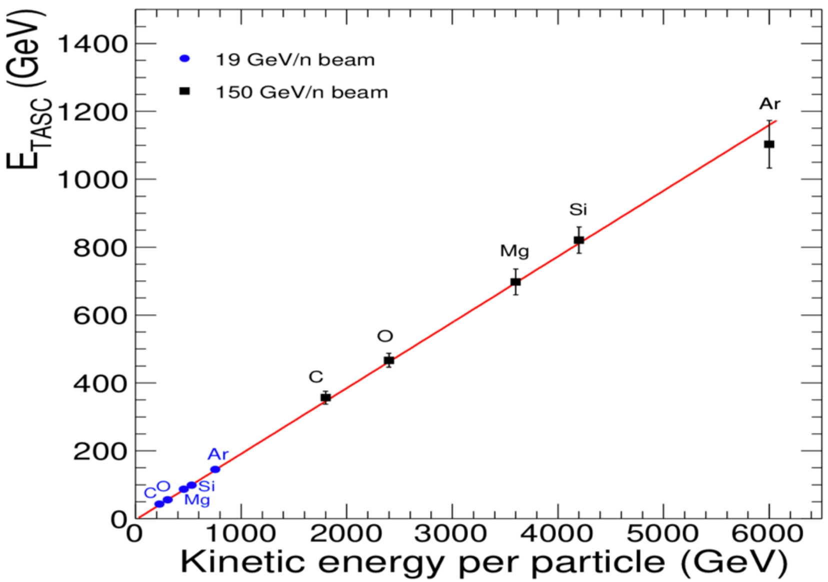

HADRONS

Beam calibration at CERN-SPS with Ion fragments at 13, 19, 150 GeV/n

Linearity assessed up to ~6 TeV with primary beam of 40Ar at 150 GeV/n

Energy resolution ~30%

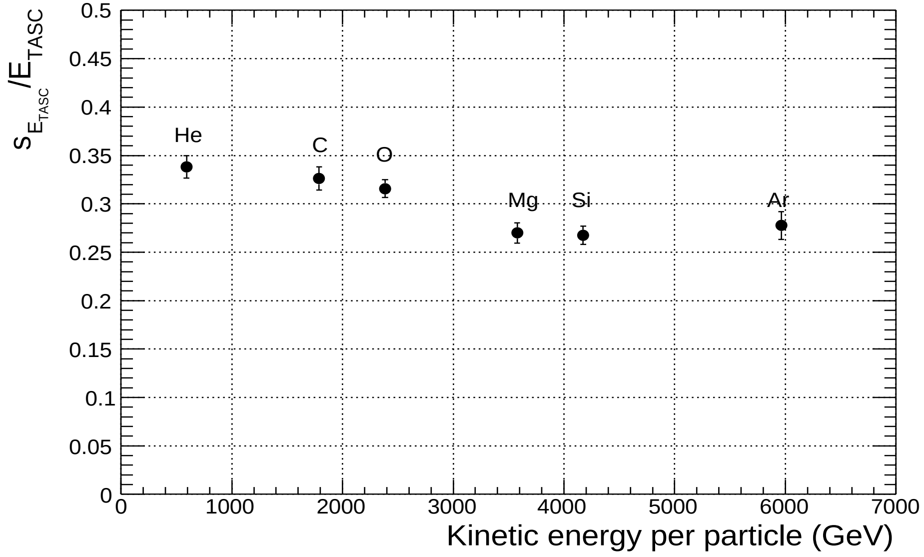

On-orbit calibration of the calorimeter

Asaoka et al. 2017, Astropart. Phys. 91, 1—10

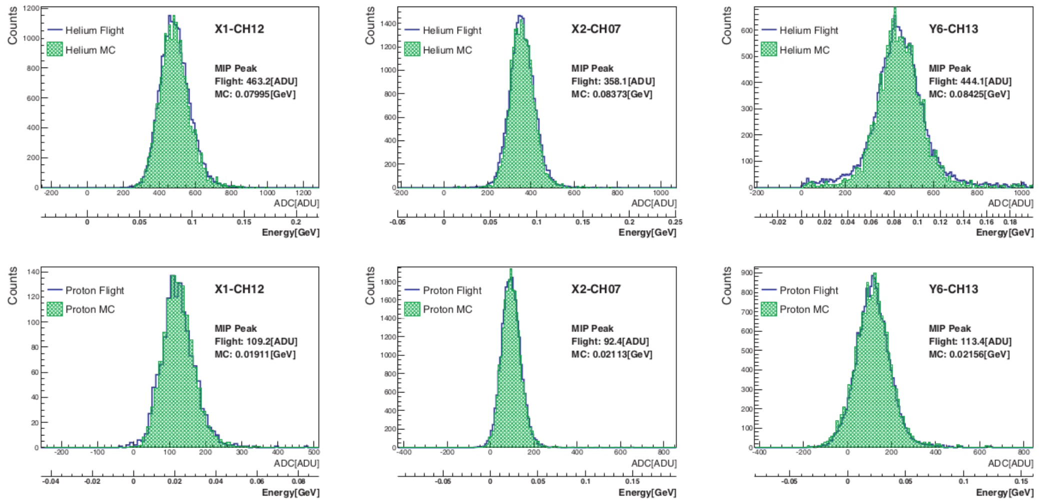

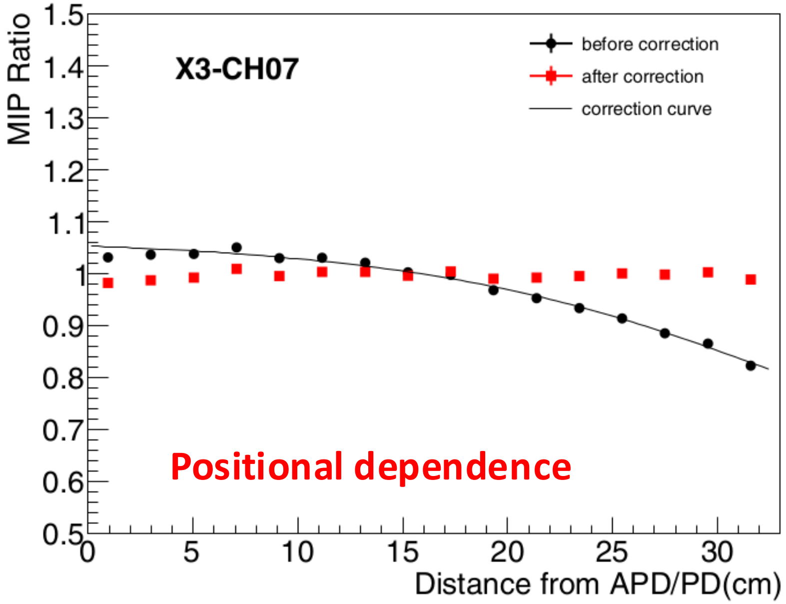

Temperature dependence

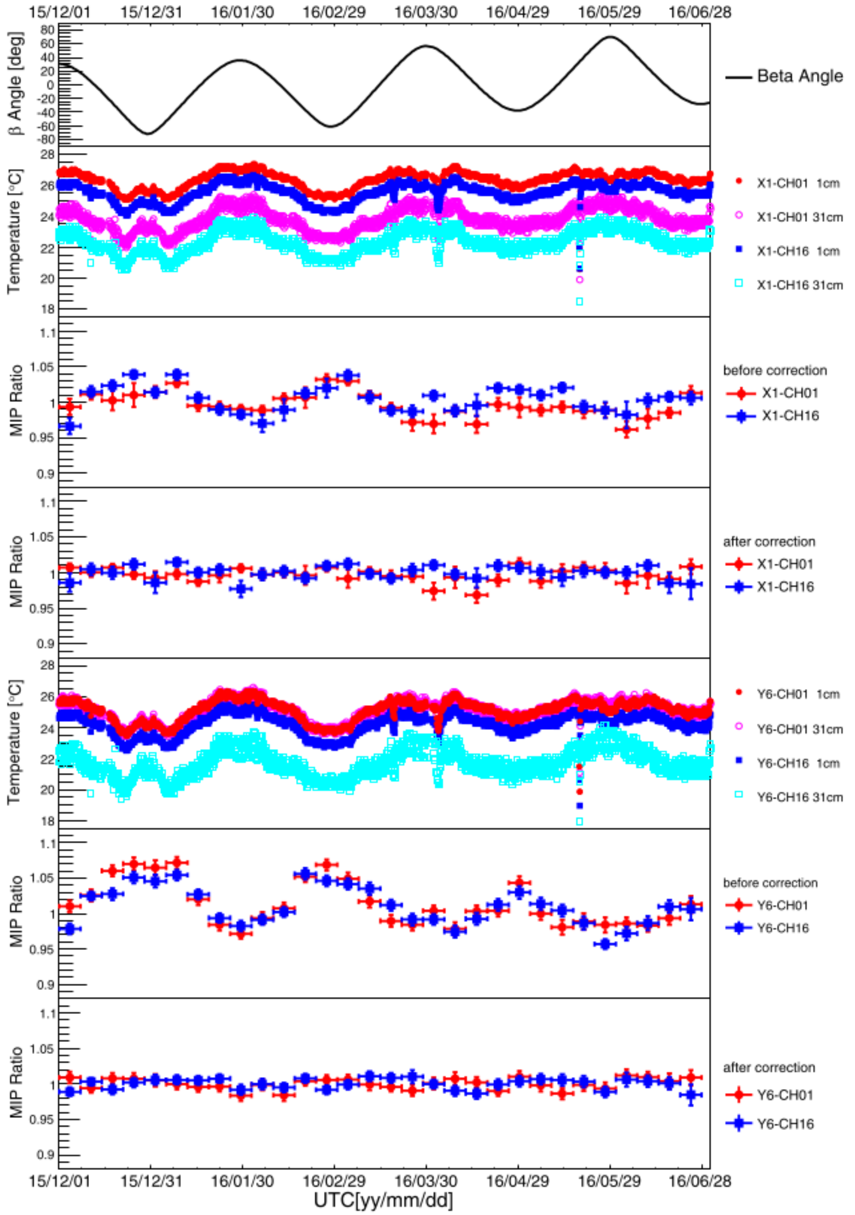

HE trigger observation summary Comparison to LE γ Trigger

Accumulated observation time (live, dead)

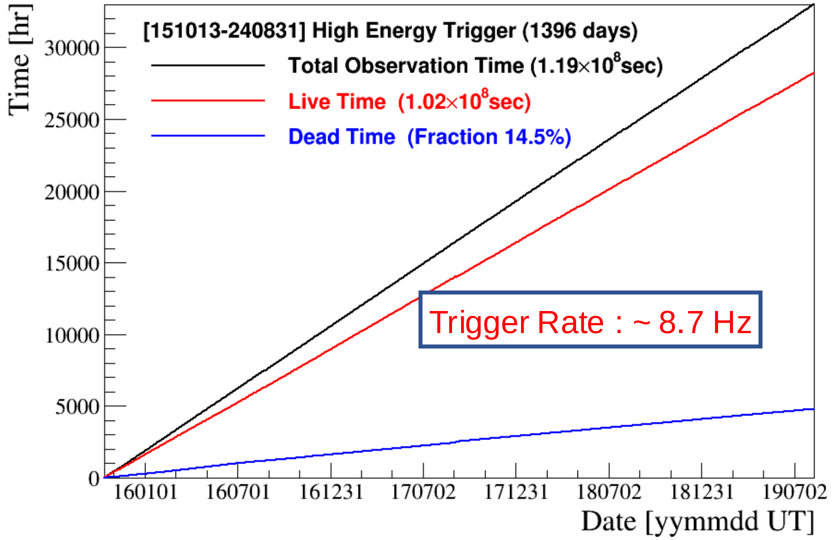

Energy deposit (in TASC) spectrum

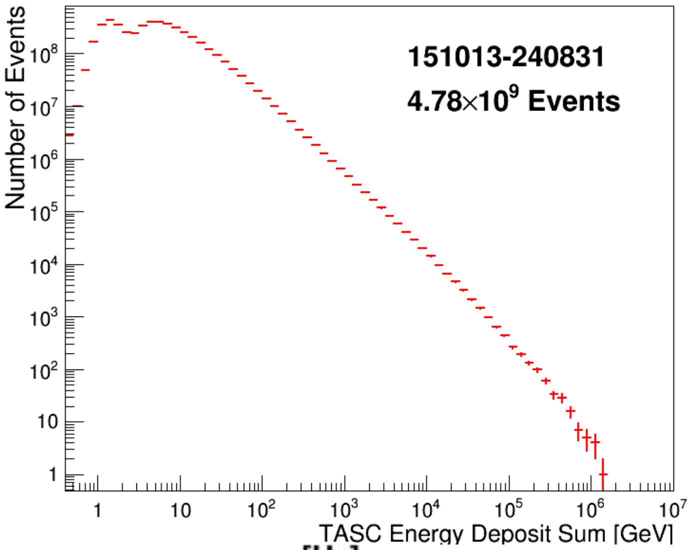

High-energy trigger statistics:

Operational time: >**3250 days**

Live time fraction: **>85%**

Exposure of HE trigger: **~300 m^2 sr day**

Number of HE events: **~2.15 billion**

Total number of >GeV triggers: **~4.77 billion**

HE-gamma point source exposure:

~5.5 m^2 day (for Crab, Geminga)

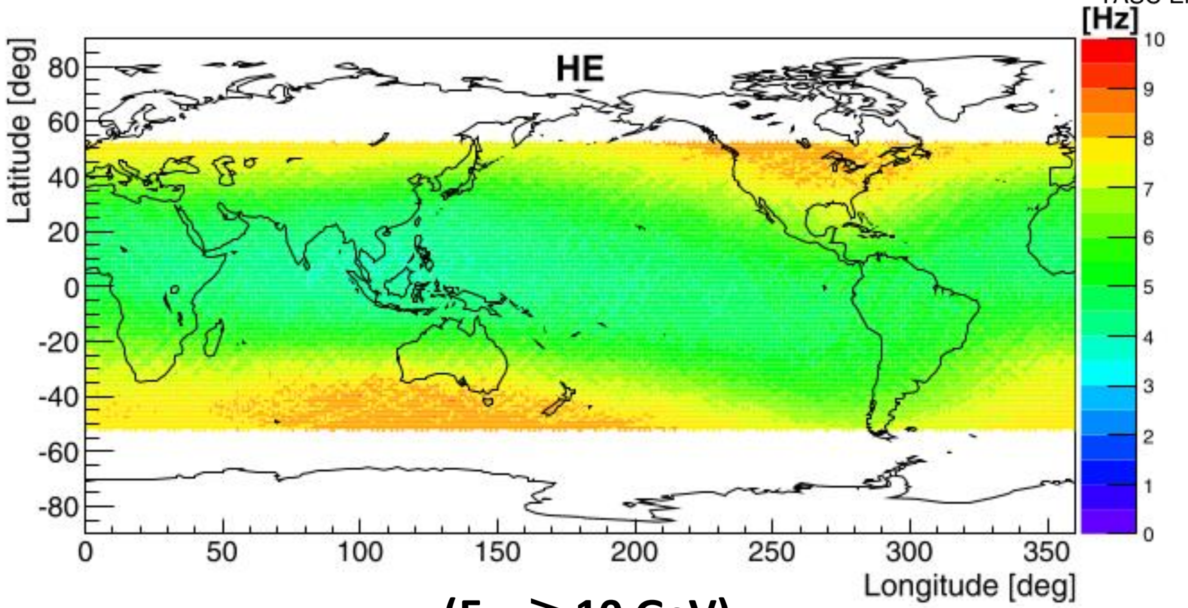

($E_{HE} \gtrsim 10$ GeV)

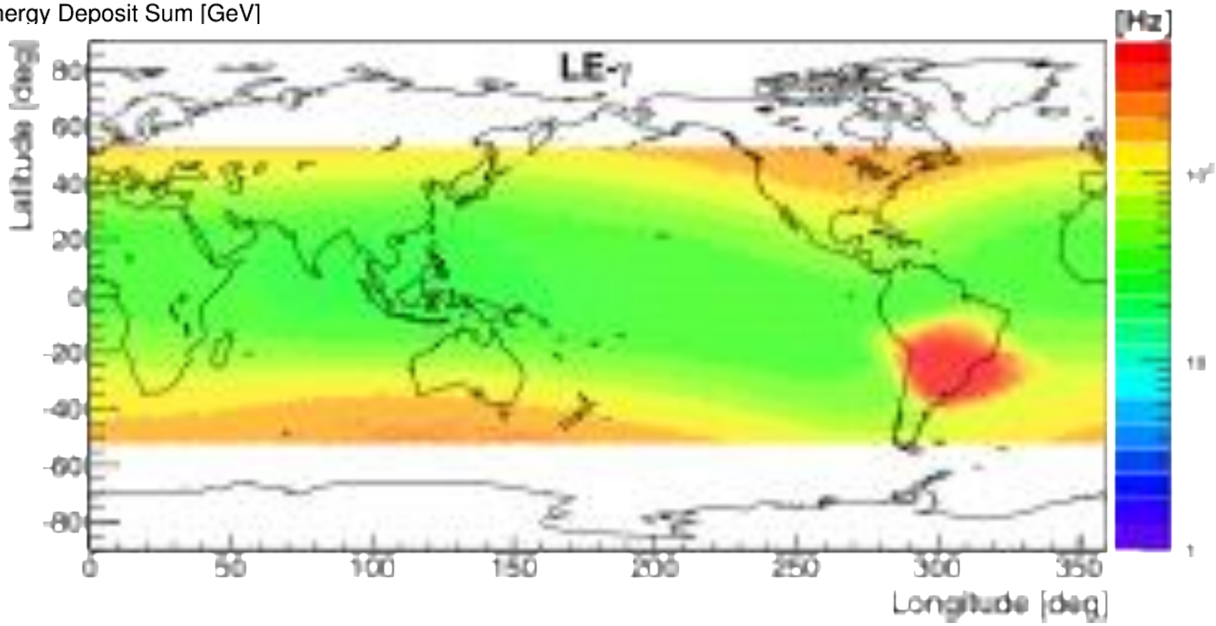

Asaoka et al. 2018, Astropart. Phys. 100, 29—37

($E_{LE\gamma} \gtrsim 1$ GeV)

Observed events in CALET flight data

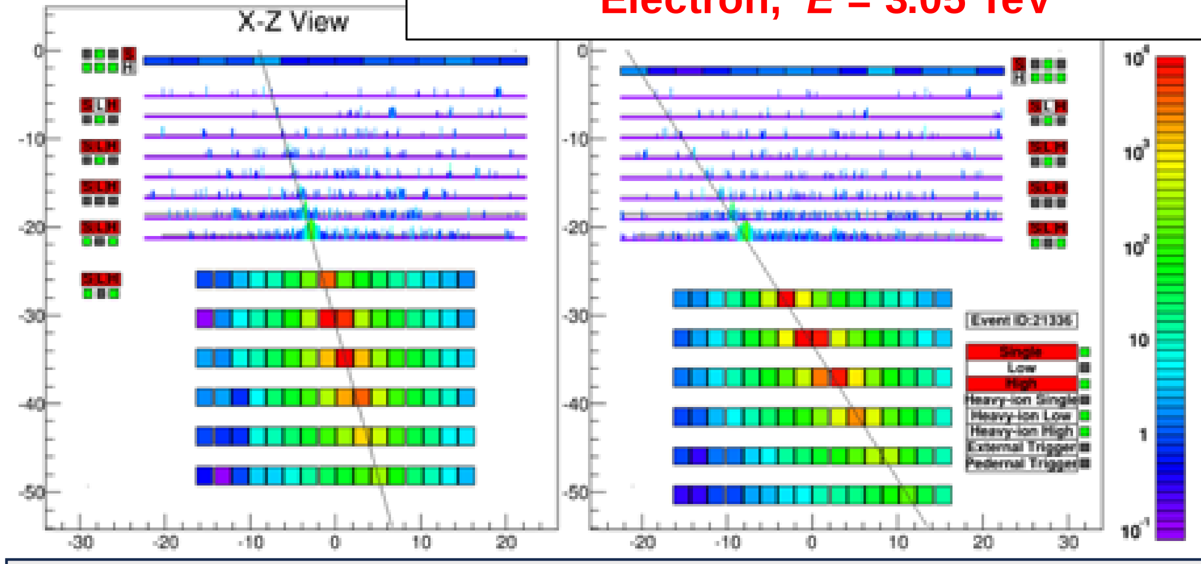

Electron, E = 3.05 TeV

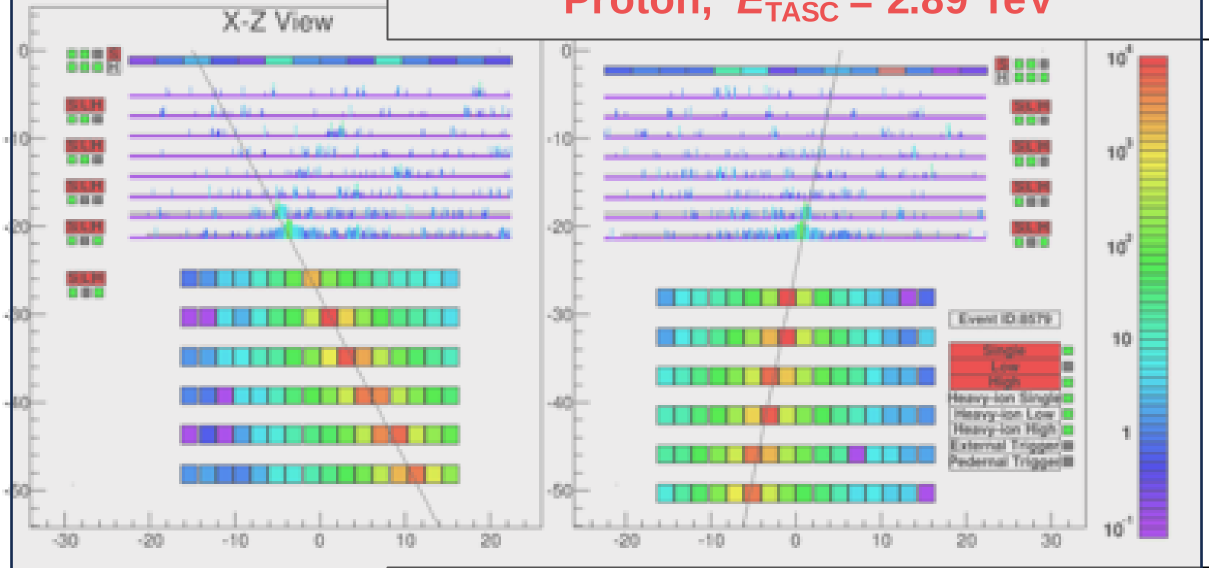

Proton, E_{TASC} = 2.89 TeV

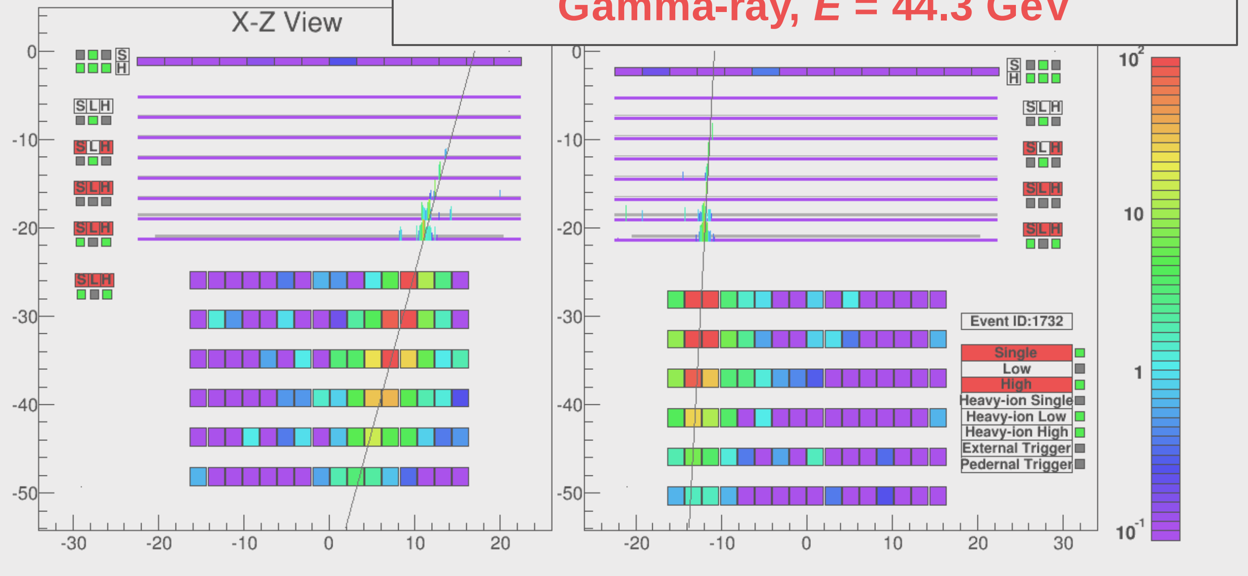

Gamma-ray, E = 44.3 GeV

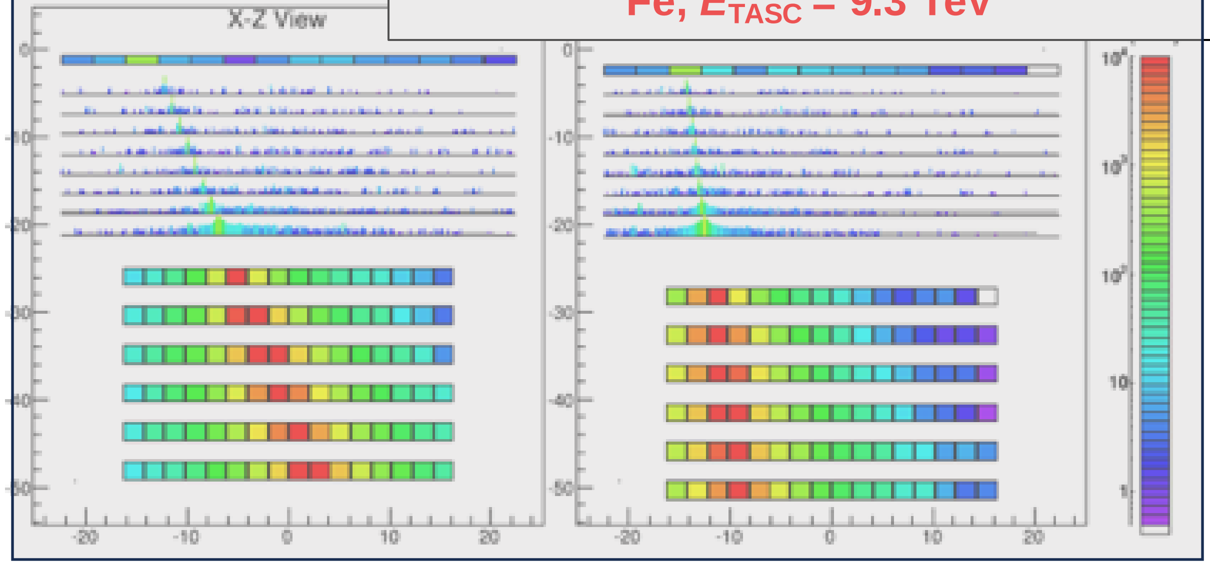

Fe, E_{TASC} = 9.3 TeV

Cosmic-ray all-electron spectrum

Corr: S. Torii, Y. Akaike, H. Motz, N. Cannady

PRL 131, 191001 (2023)

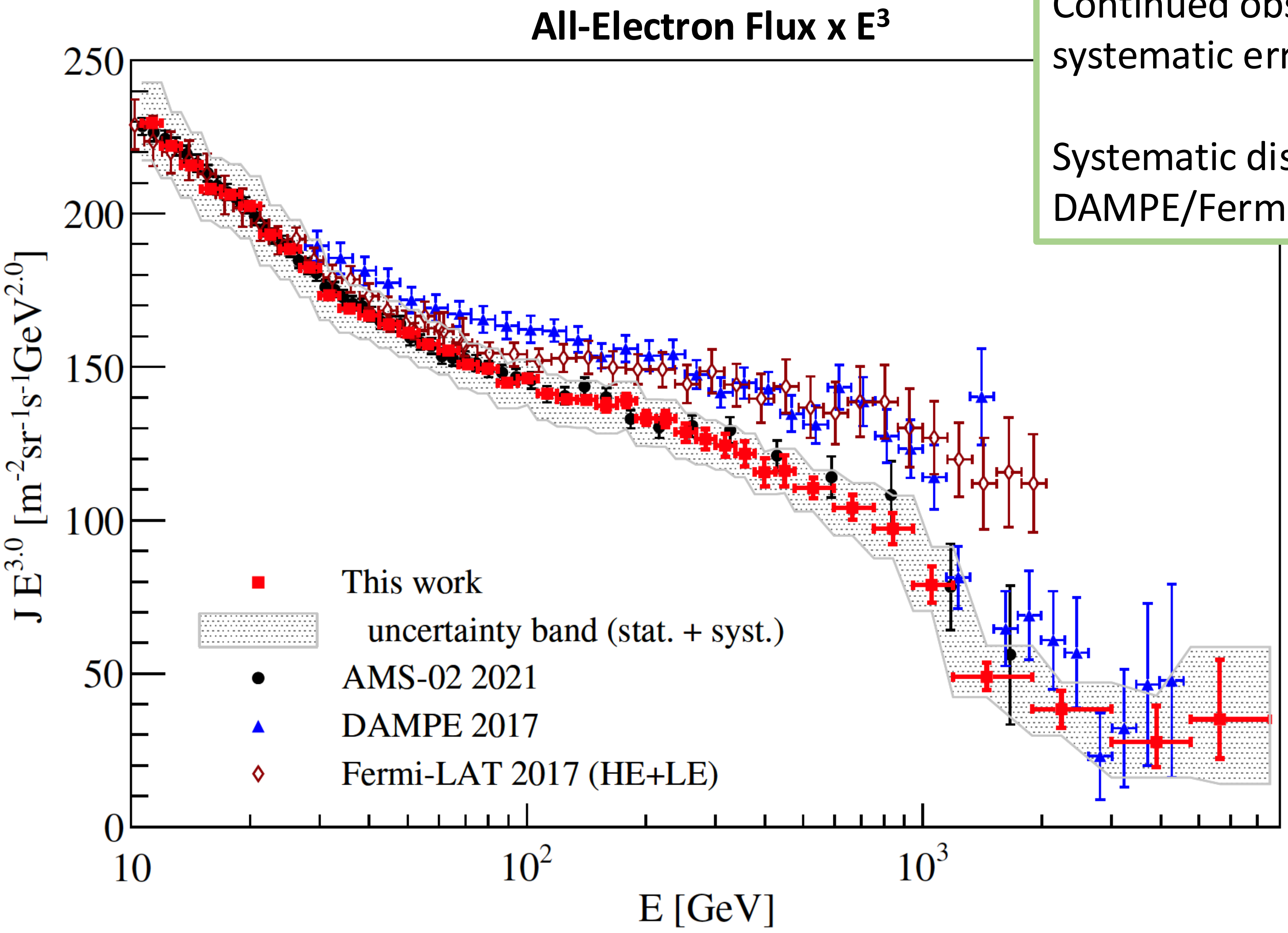

Continued observation has reduced statistical and systematic errors in the all-electron spectrum.

Systematic discrepancy between CALET/AMS-02 and DAMPE/Fermi-LAT persists beyond tabulated error.

At ~1 TeV energies, electrons have…
- diffusion length ~ 1 kpc
- characteristic lifetime ~ 100 kyr

(both decreasing with energy)

→ Expected cutoff around 1 TeV based on decrease in number of contributing sources significant in measurement

- Nearby accelerators could leave observable features in the spectrum in the TeV region

CALET TASC E_{Res} and e/p Separation

Corr: S. Torii, Y. Akaike,
H. Motz, N. Cannady

PRL 131, 191001 (2023)

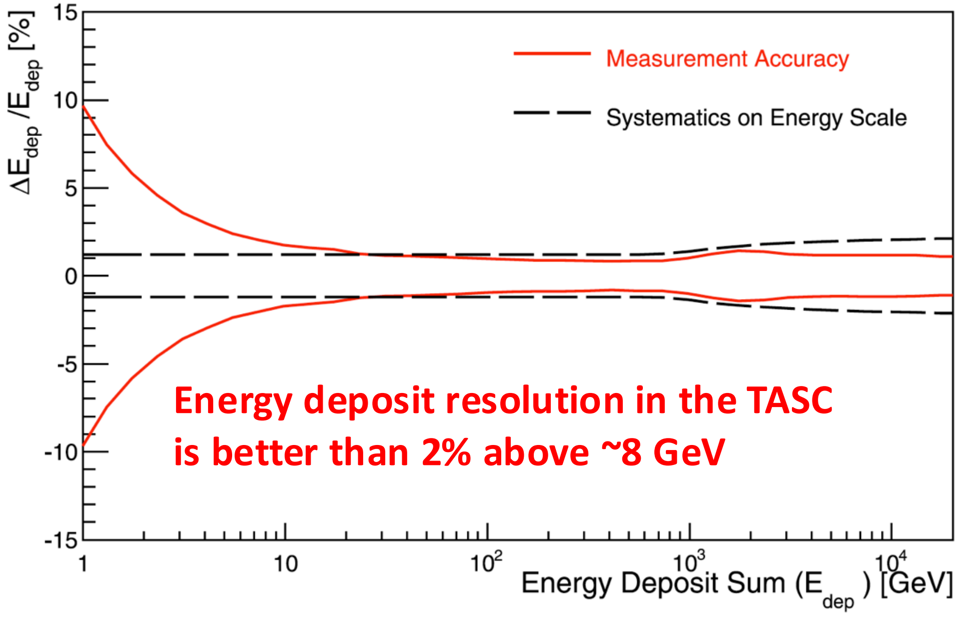

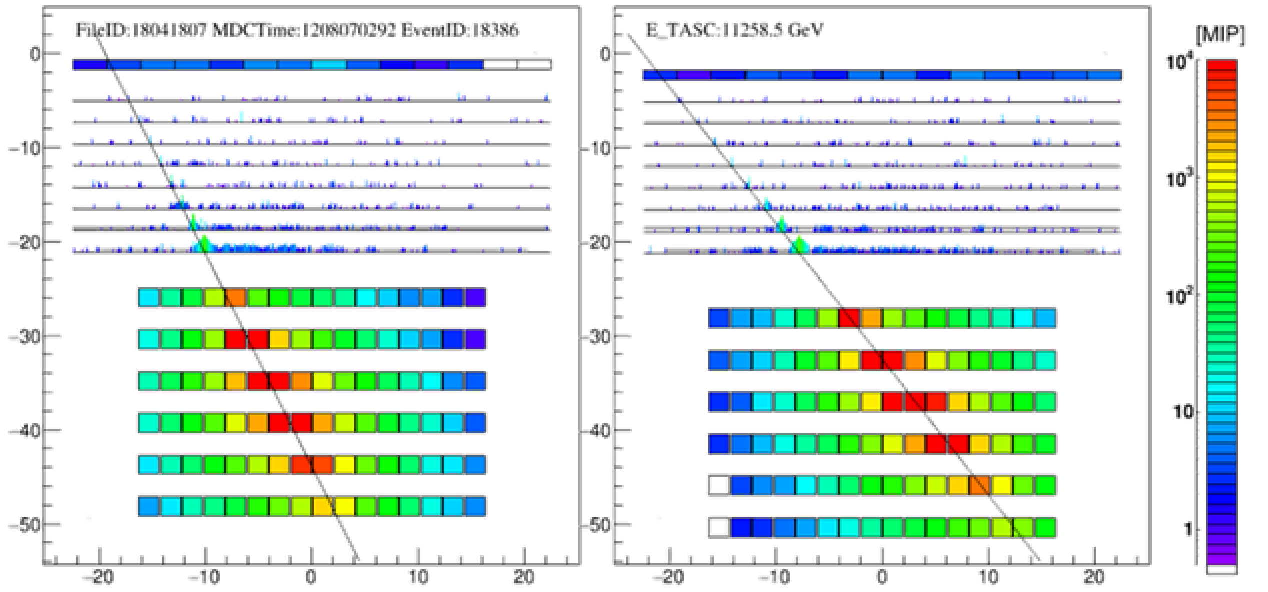

12.04 TeV electron candidate

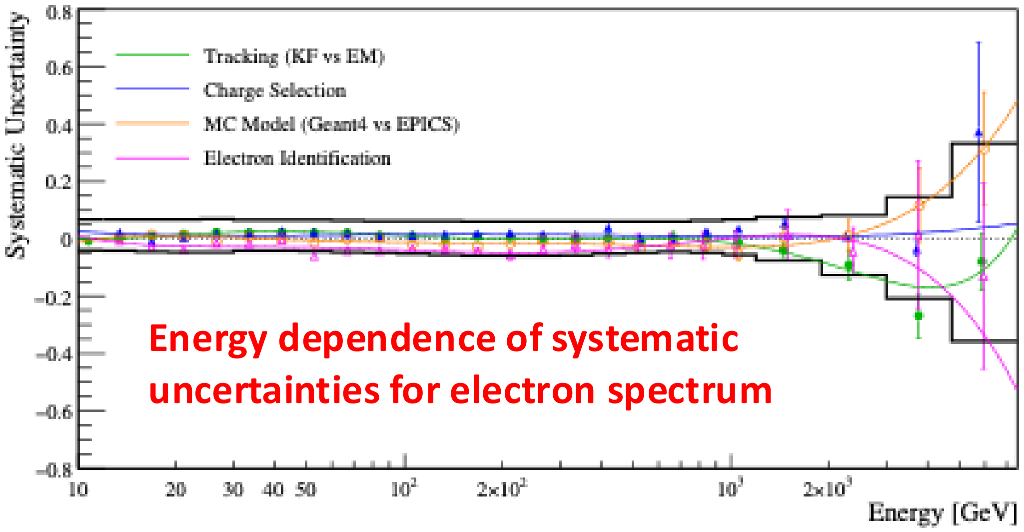

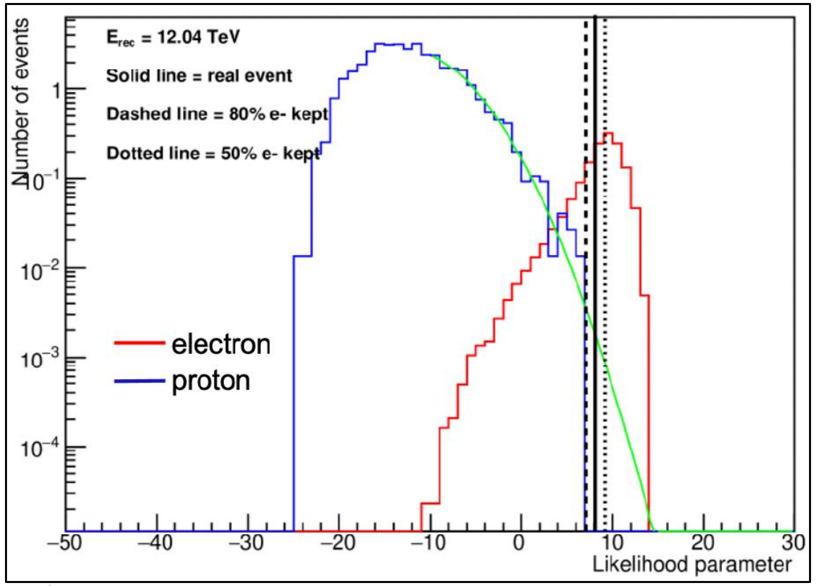

Cosmic-ray all-electron spectrum

Corr: S. Torii, Y. Akaike, H. Motz, N. Cannady

PRL 131, 191001 (2023)

All-Electron Flux x E^3

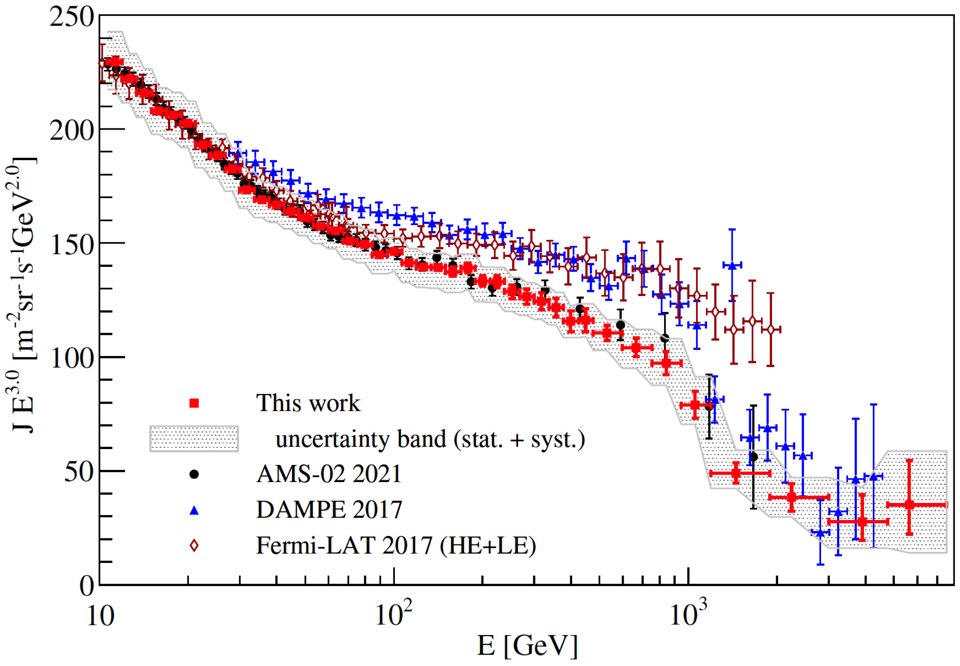

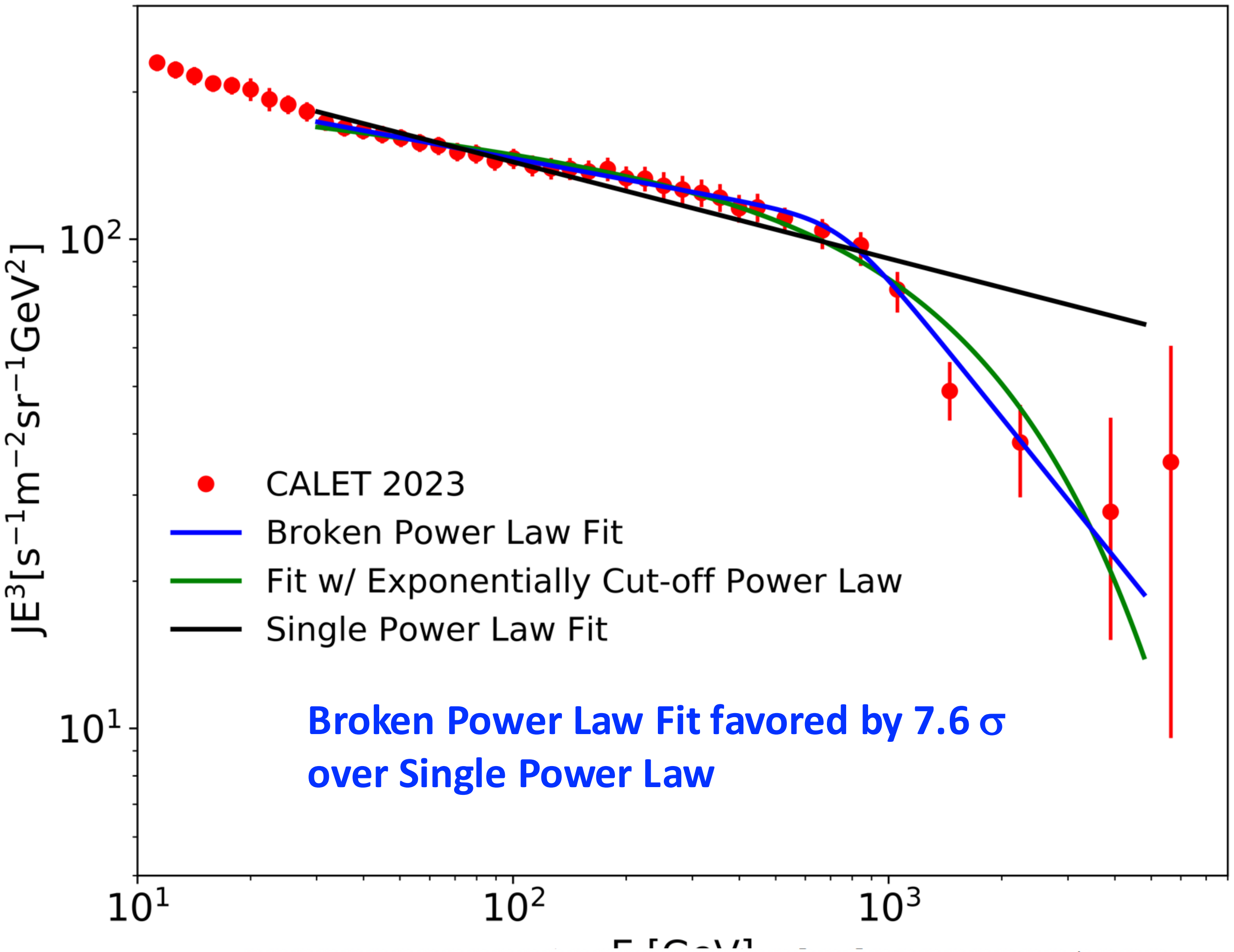

$$J(E) = C(E/100\ GeV)^{\gamma}(1 + (E/E_b)^{\Delta\gamma/s})^{-s}$$

$\gamma = -3.14 \pm 0.01$, $\Delta\gamma = -0.81 \pm 0.20$, $E_b = 755 \pm 107$ GeV

Cosmic-ray all-electron spectrum

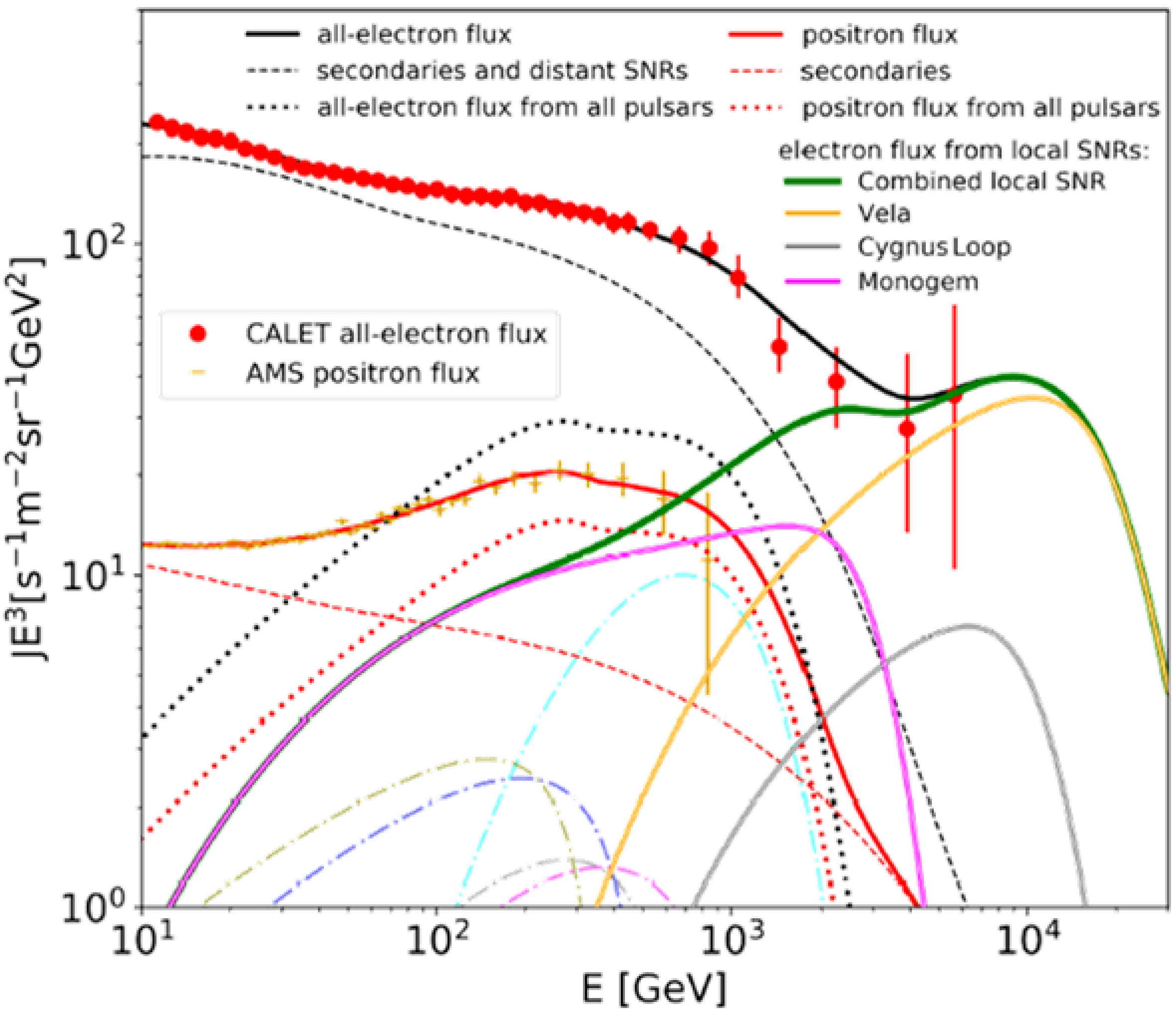

Spectral fit over the whole region of the CALET observation **with** the contributions from nearby SNRs.

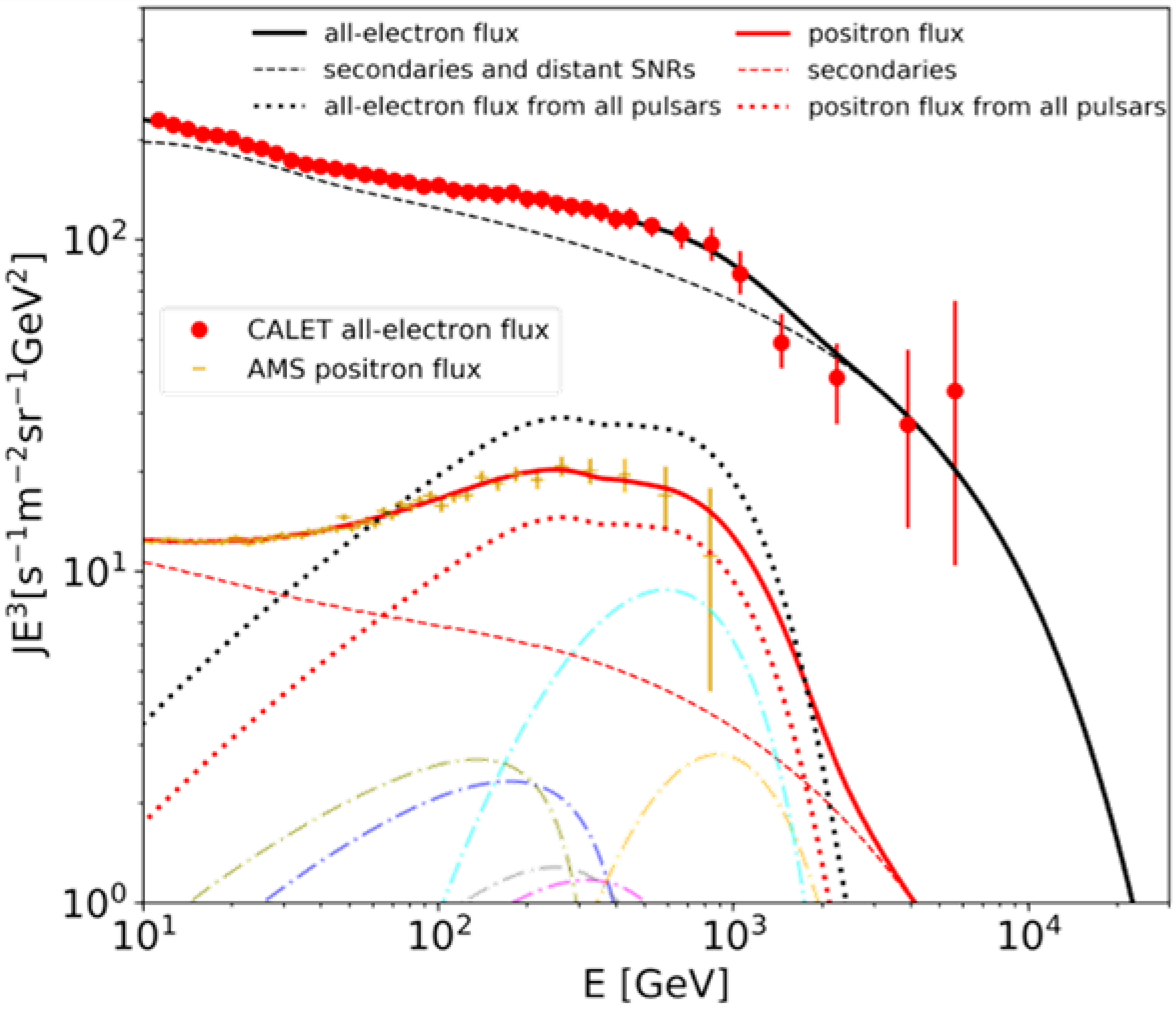

Spectral fit over the whole region of the CALET observation **without** the contributions from nearby SNRs.

Observed events in CALET flight data

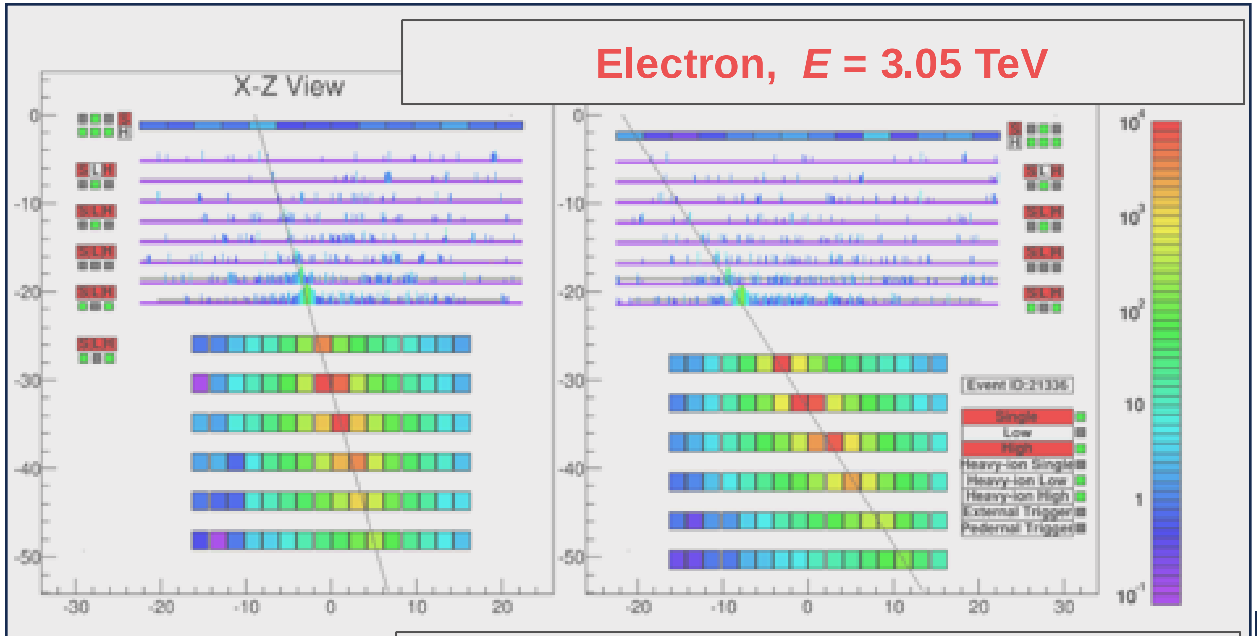

Electron, E = 3.05 TeV

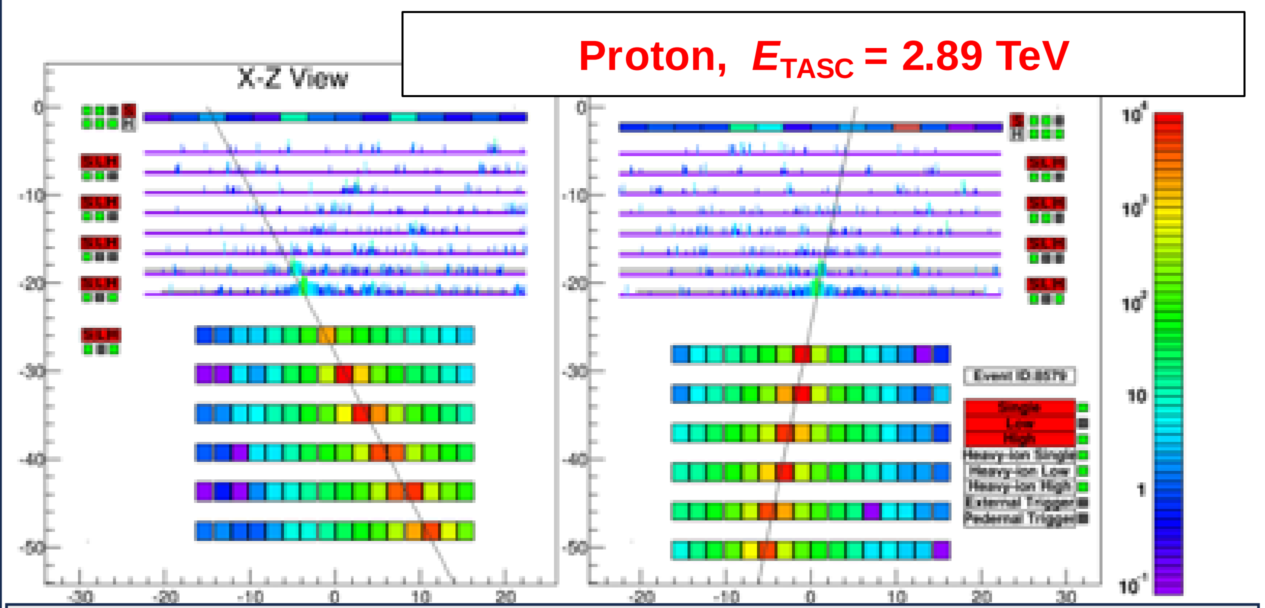

Proton, E_{TASC} = 2.89 TeV

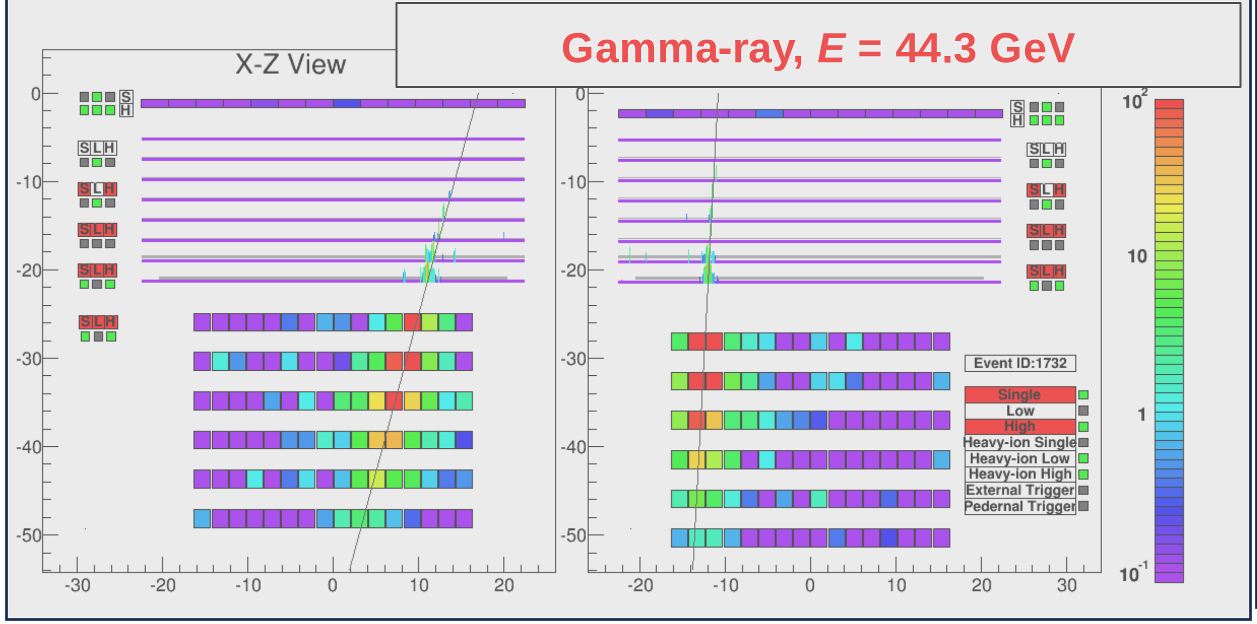

Gamma-ray, E = 44.3 GeV

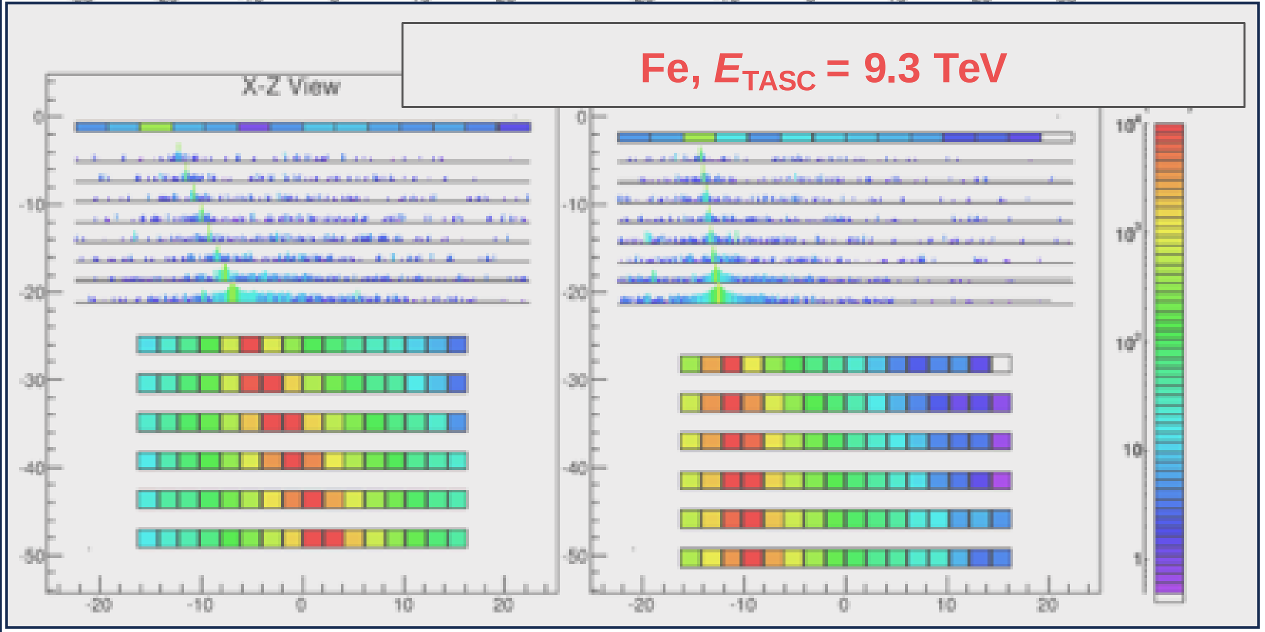

Fe, E_{TASC} = 9.3 TeV

Energy spectrum of cosmic-ray protons

Corr: P.S. Marrocchesi, K. Kobayashi

PRL 129, 101102 (2022)

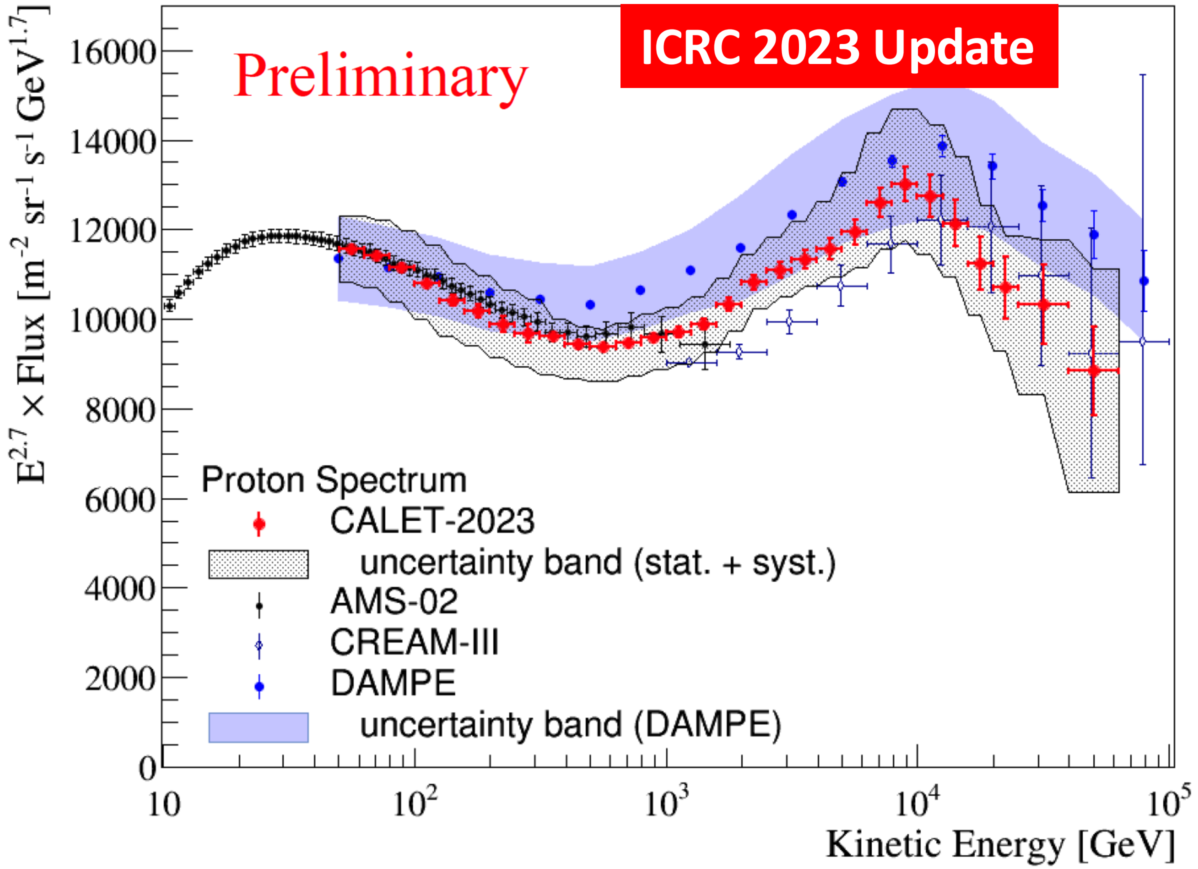

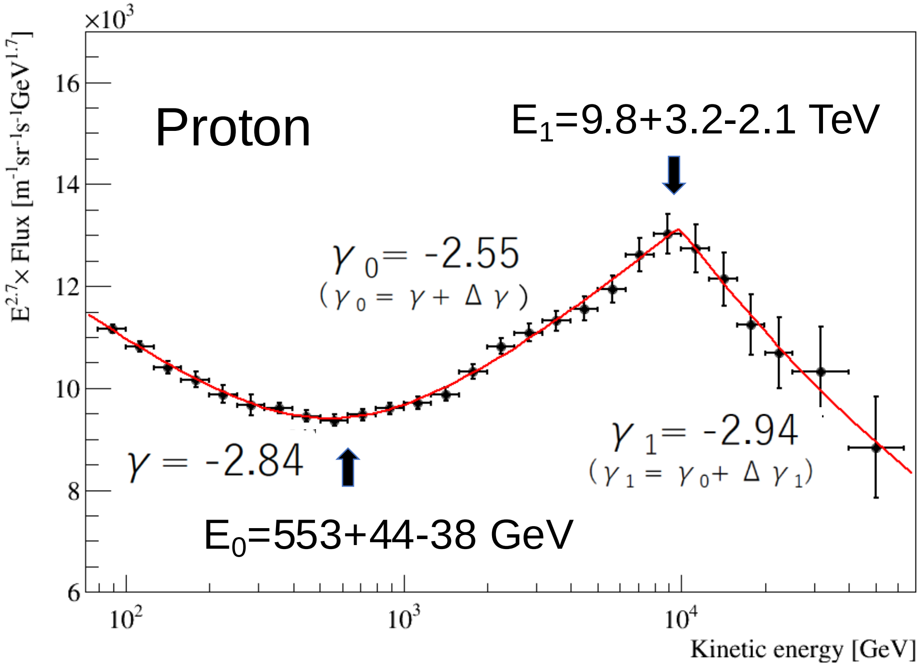

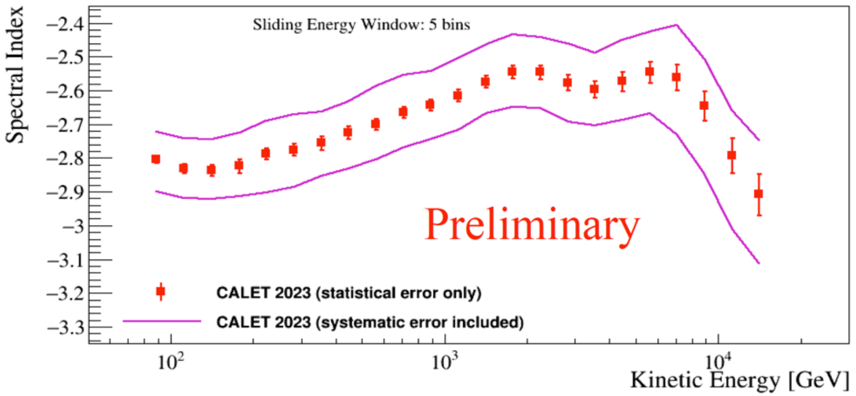

$$\Phi'(E) = C \times \left(\frac{E}{1\ \mathrm{GeV}}\right)^{\gamma} \times \left[1 + \left(\frac{E}{E_0}\right)^{s}\right]^{\frac{\Delta\gamma}{s}} \times \left[1 + \left(\frac{E}{E_1}\right)^{s_1}\right]^{\frac{\Delta\gamma_1}{s_1}}$$

$$\gamma = -2.843^{+0.005}_{-0.005}$$

$$s = 2.1^{+0.4}_{-0.4} \qquad s_1 \approx 90$$

$$\Delta\gamma = 0.29^{+0.01}_{-0.01} \qquad E_0 = 553^{+44}_{-38}\ GeV$$

$$\Delta\gamma_1 = -0.39^{+0.15}_{-0.18} \qquad E_1 = 9.8^{+3.2}_{-2.1}\ TeV$$

Energy spectrum of cosmic-ray Helium

Corr: P. Brogi, K. Kobayashi

PRL 130, 171002 (2023)

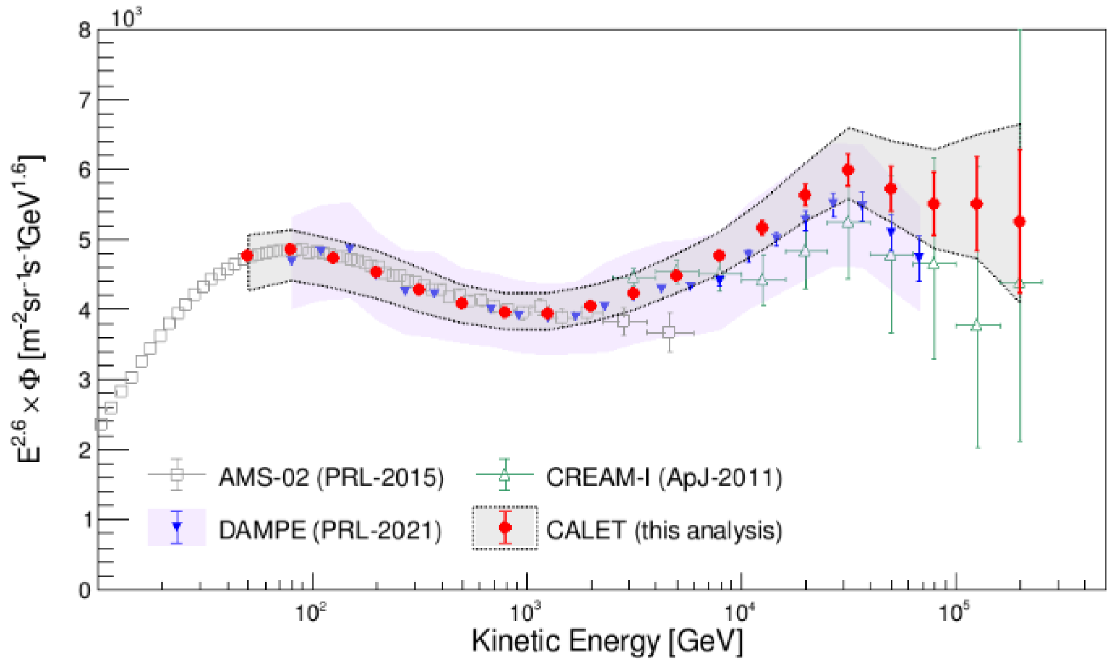

$$\Phi'(E) = C \times \left(\frac{E}{1\ \mathrm{GeV}}\right)^{\gamma} \times \left[1 + \left(\frac{E}{E_0}\right)^{s}\right]^{\frac{\Delta\gamma}{s}} \times \left[1 + \left(\frac{E}{E_1}\right)^{s_1}\right]^{\frac{\Delta\gamma_1}{s_1}}$$

$$\gamma = -2.703^{+0.005+0.032}_{-0.006-0.009}$$

$$s = 2.7^{+0.6+3.0}_{-0.5-0.9} \qquad s_1 = 30$$

$$\Delta\gamma = 0.25^{+0.02+0.02}_{-0.01-0.03} \qquad E_0 = 1319^{+113+267}_{-93-124}\ GeV$$

$$\Delta\gamma_1 = -0.22^{+0.07+0.03}_{-0.10-0.04} \qquad E_1 = 33.2^{+9.8+1.8}_{-6.2-2.3}\ TeV$$

Fitting by Double Power Law (DBPL) function

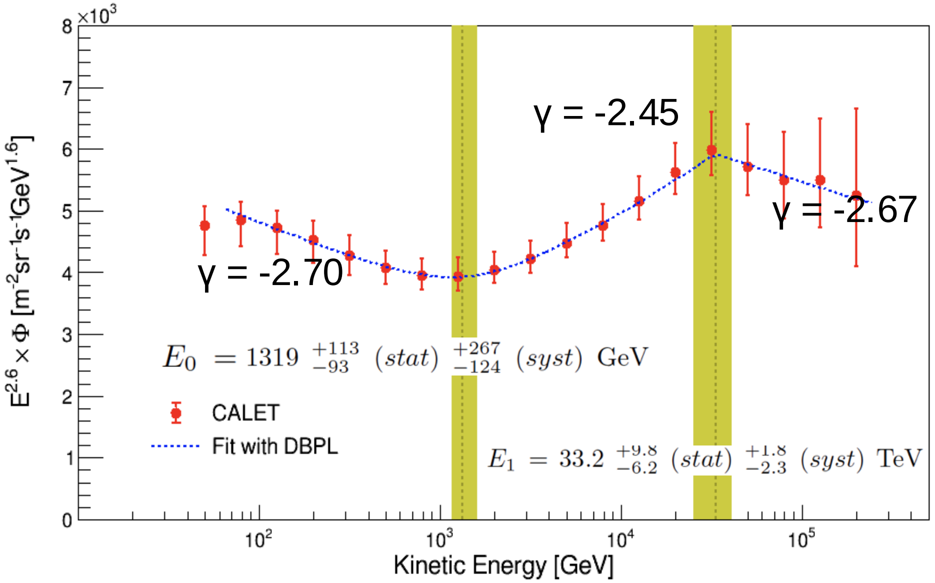

Energy dependence of power index

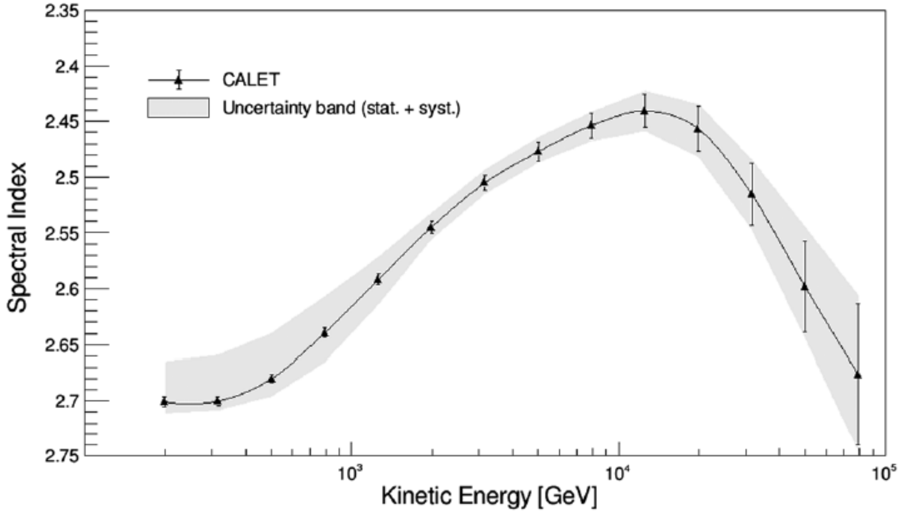

Cosmic Ray Proton/Helium Ratio

PRL 130, 171002 (2023)

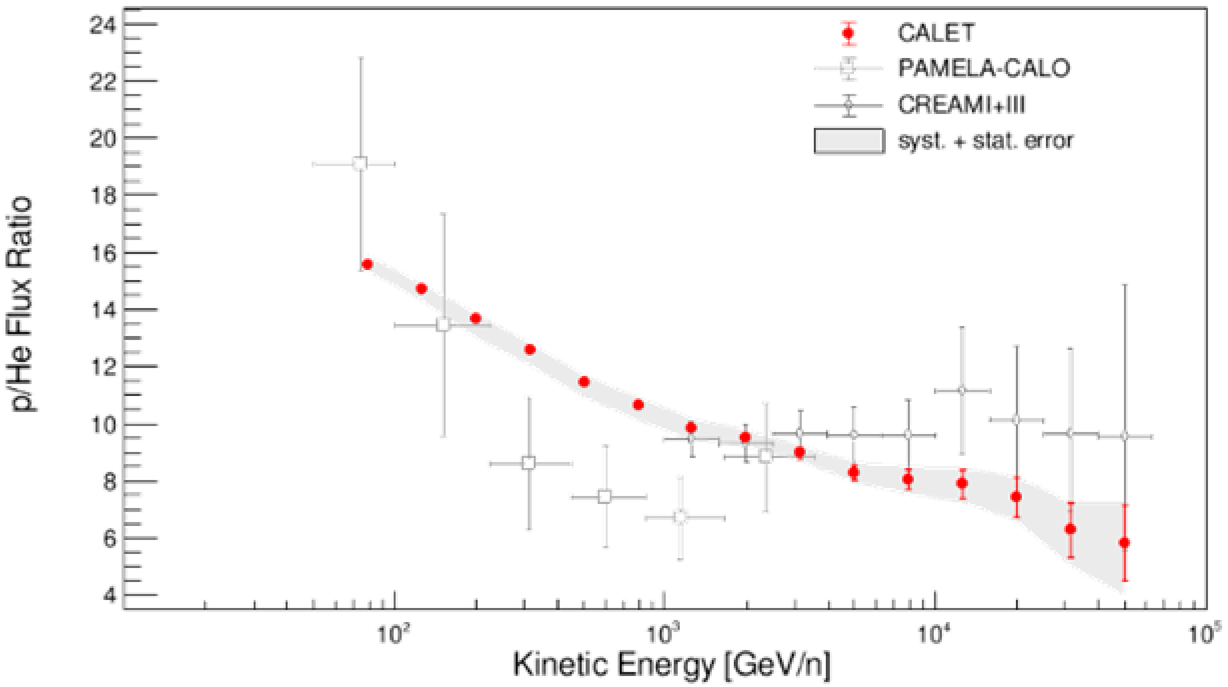

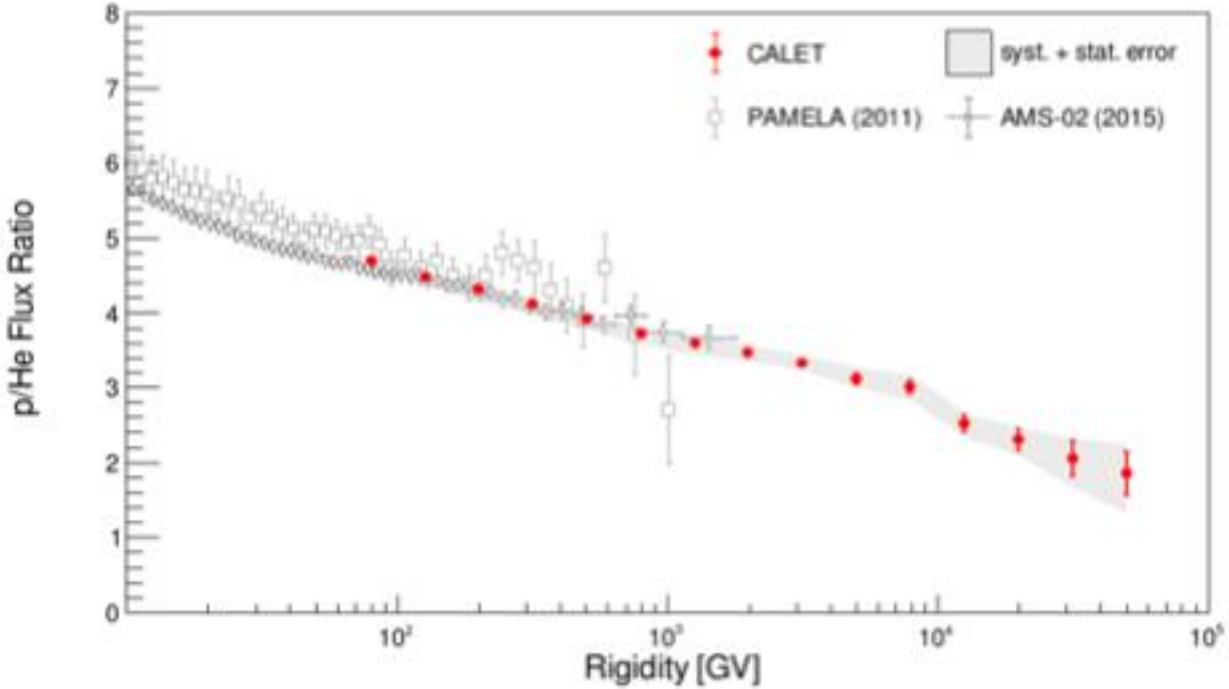

The p/He ratio decreases as a function of Kinetic Energy (GeV/n) and Rigidity (GV)

Observed events in CALET flight data

Electron, E = 3.05 TeV

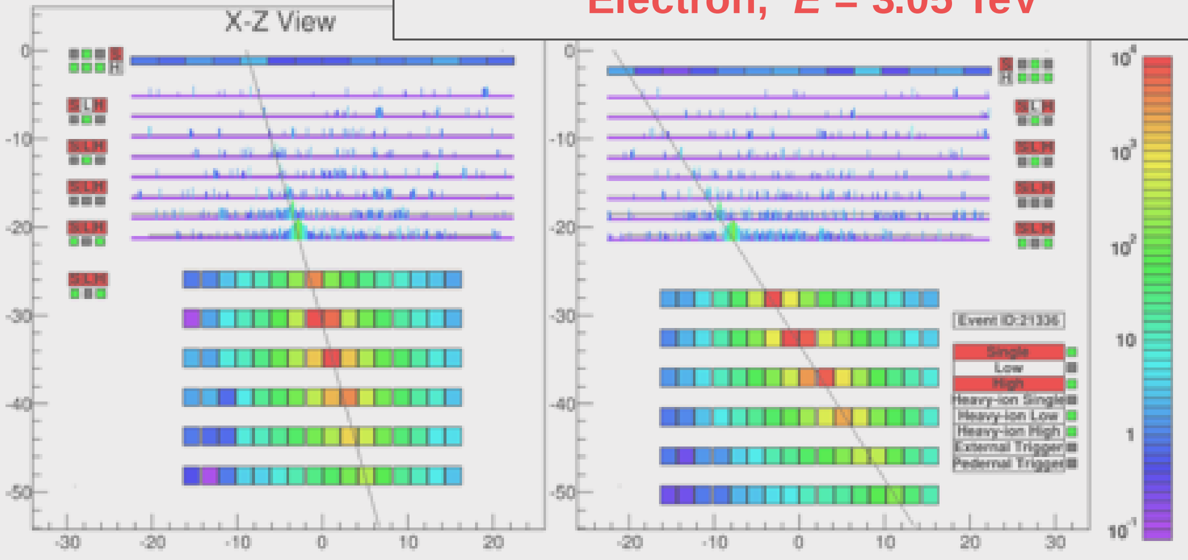

Proton, E_{TASC} = 2.89 TeV

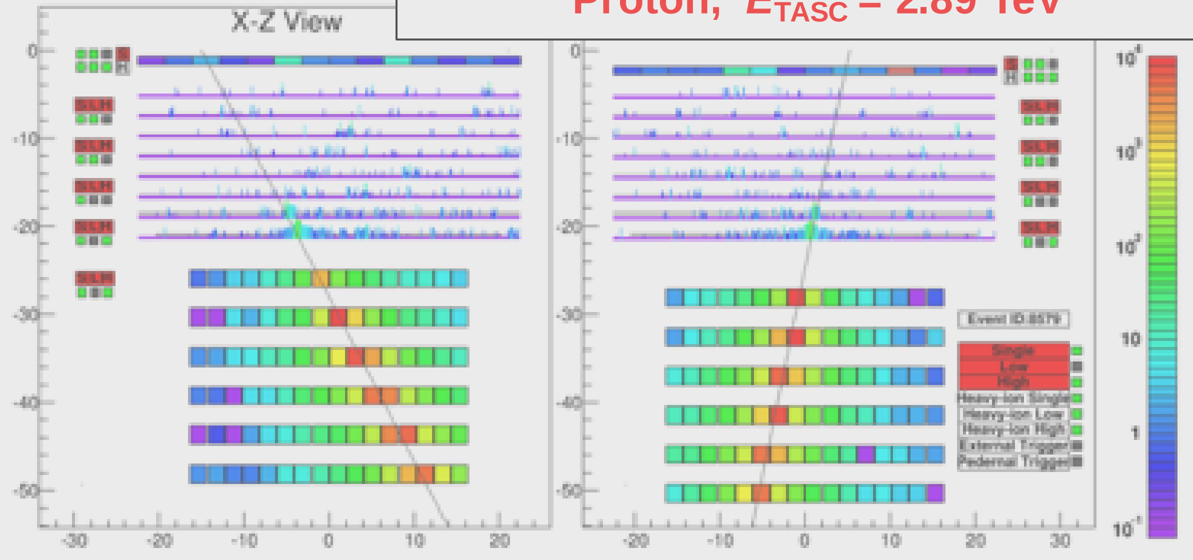

Gamma-ray, E = 44.3 GeV

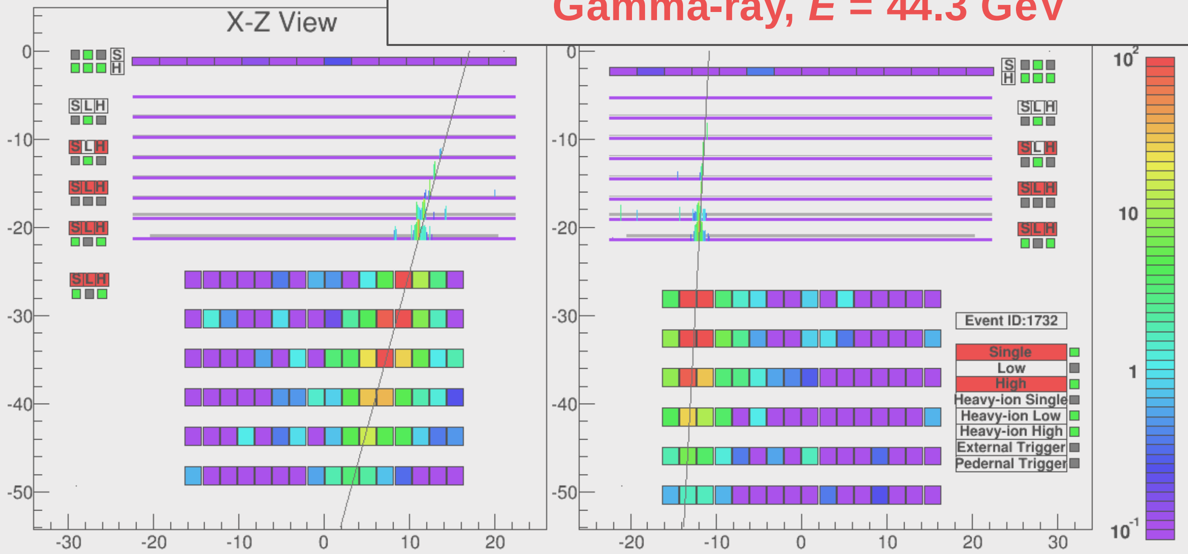

Fe, E_{TASC} = 9.3 TeV

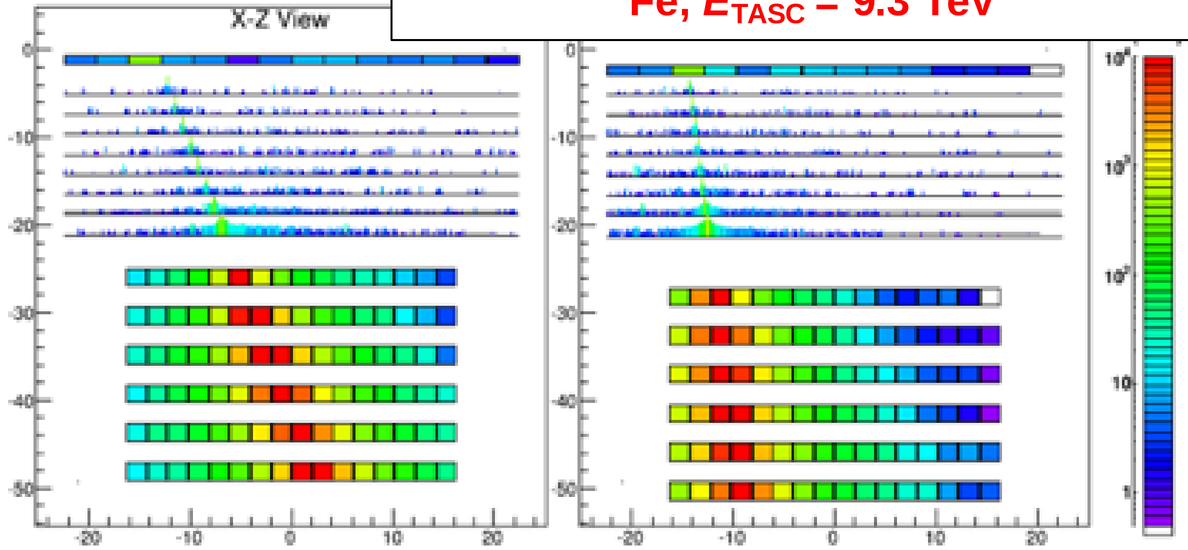

Observations of Cosmic-Ray Nuclei

Preliminary spectra of Carbon – Iron

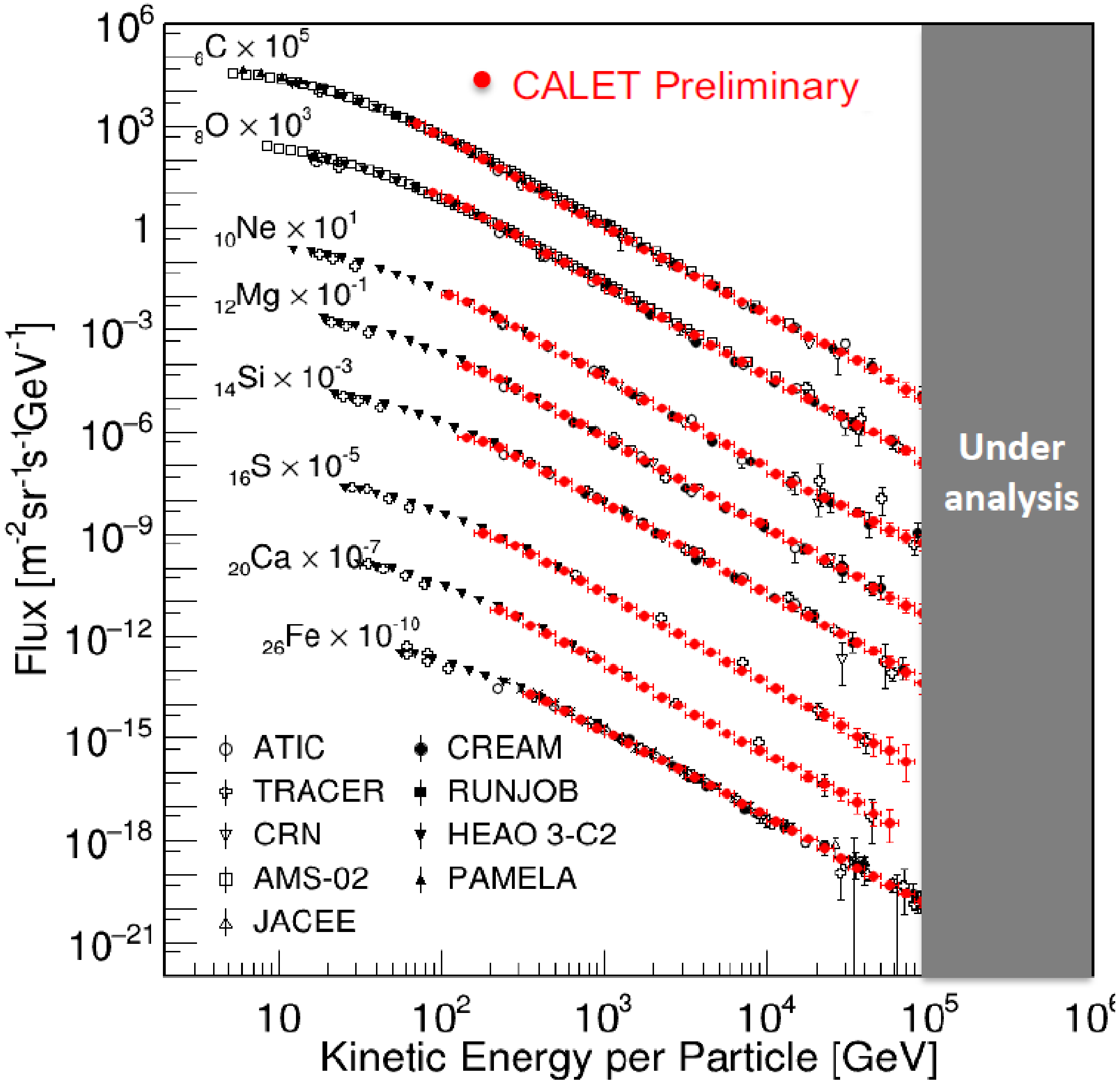

This conference

Dedicated analysis of cosmic-ray nuclear fluxes and flux ratios into the TeV region ongoing.

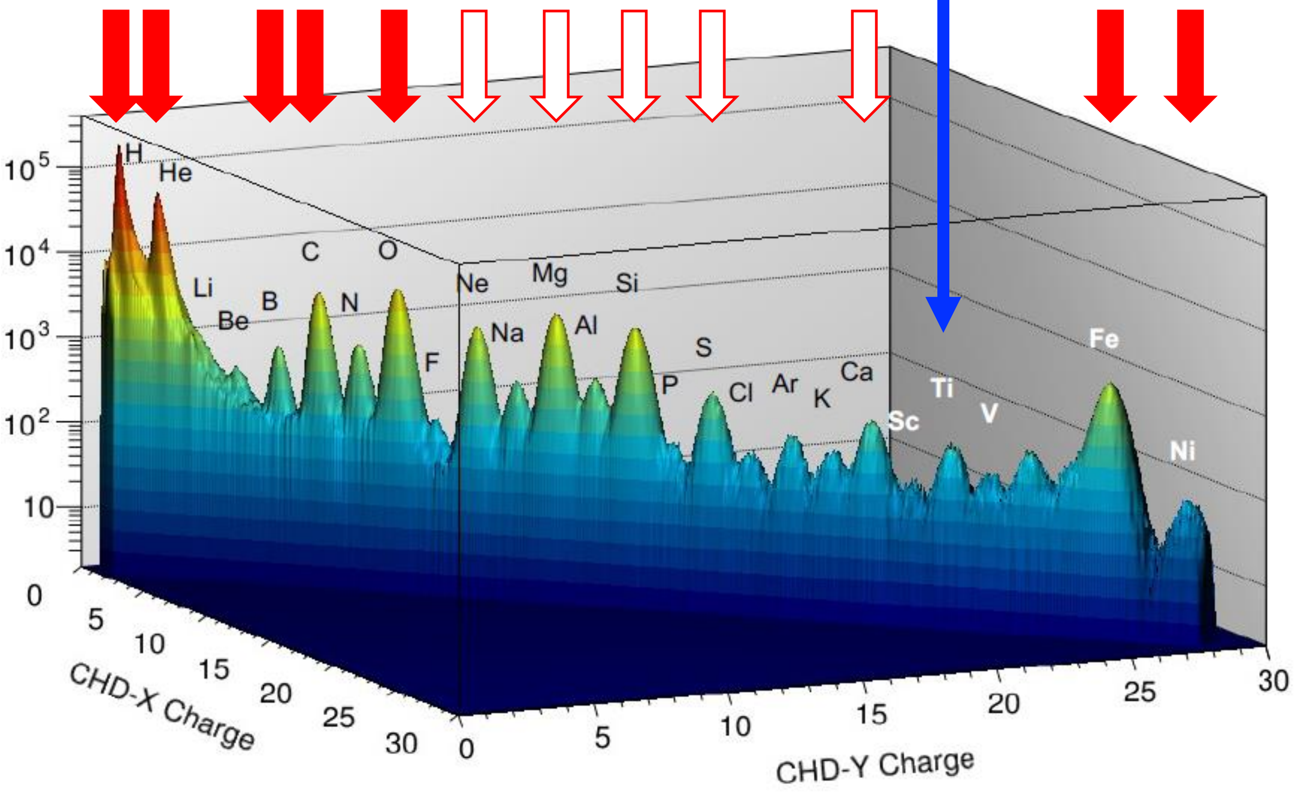

Energy spectra of cosmic-ray BCO

Corr: P. Maestro, Y. Akaike

C&O: PRL 125, 251102 (2020)

B: PRL 129, 251103 (2022)

ICRC 2023 Update

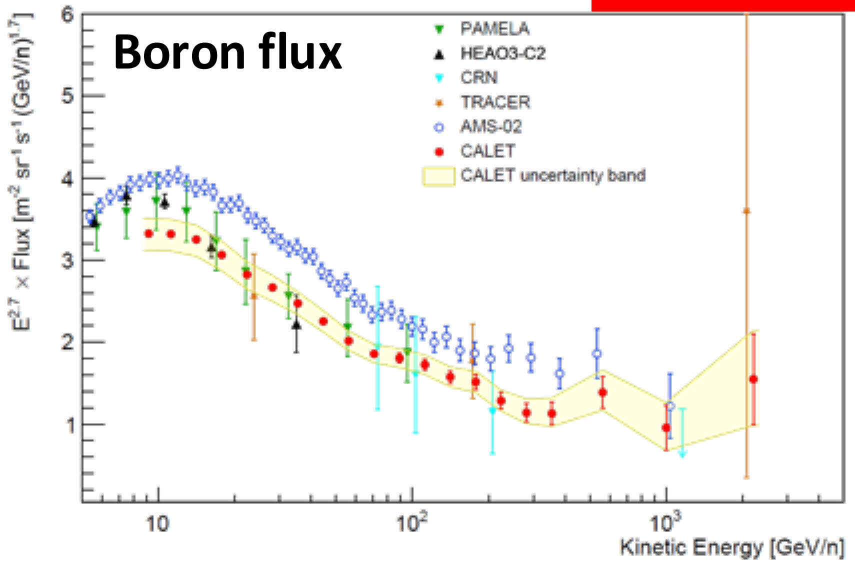

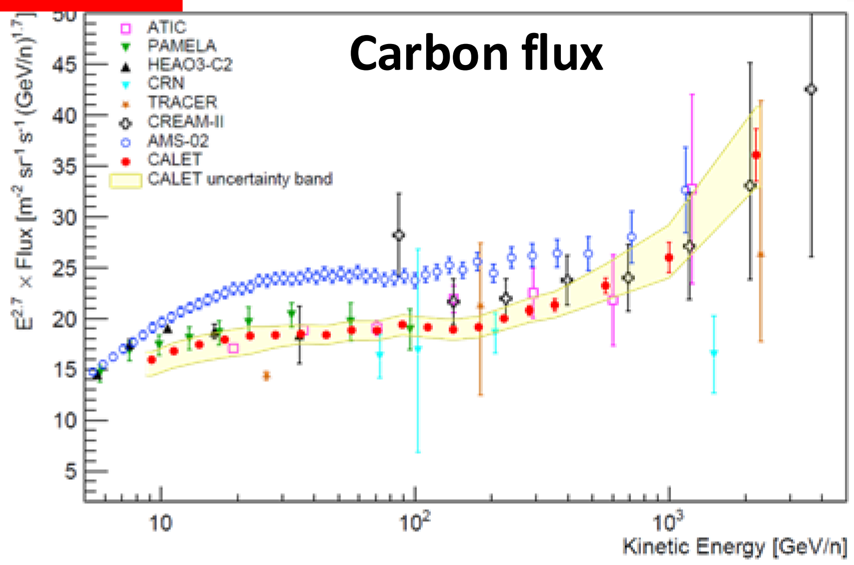

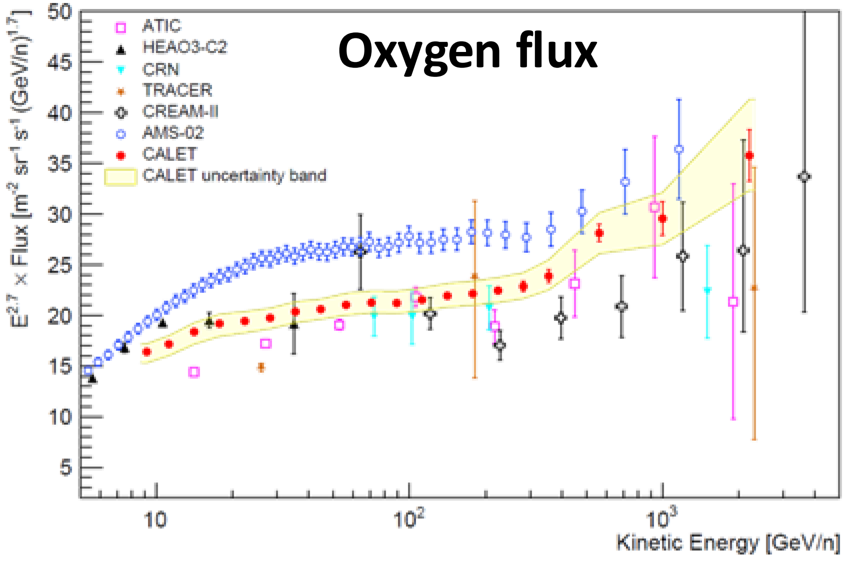

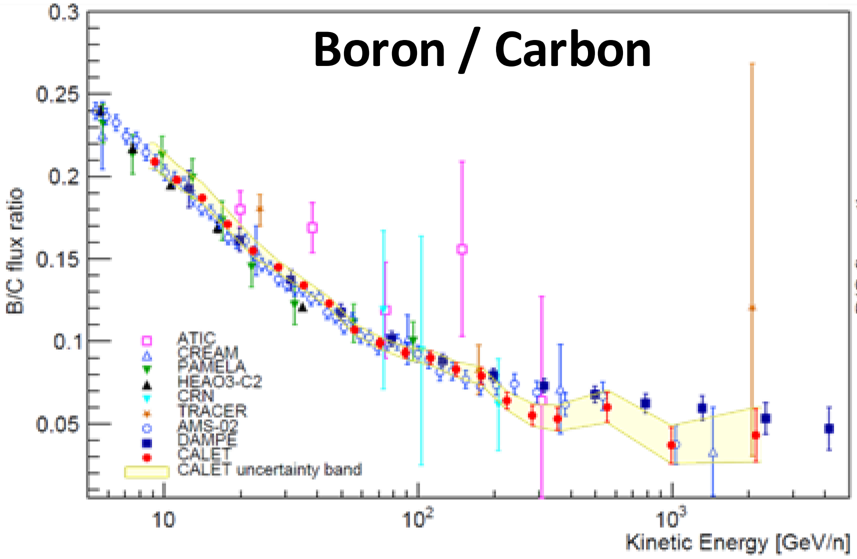

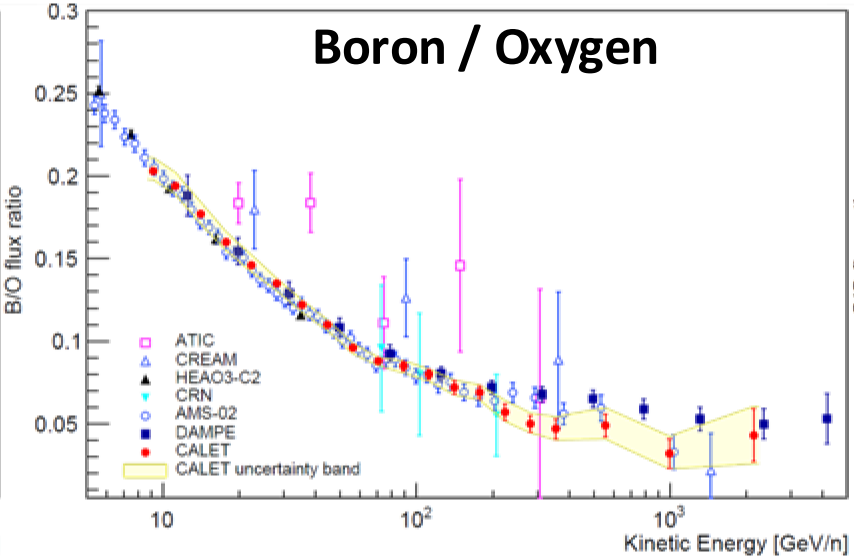

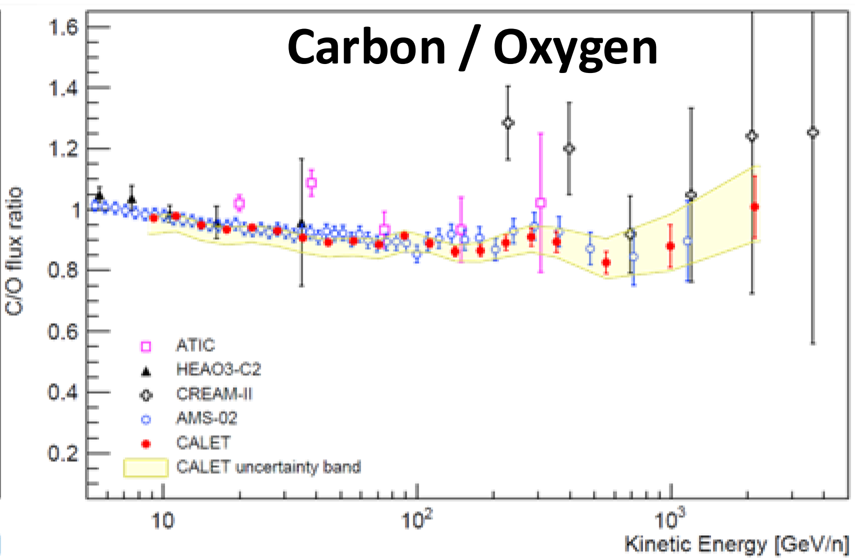

Energy spectra of cosmic-ray Fe & Ni

Corr: C. Checchia, F. Stolzi
Y. Akaike, G. Bigongiari

Fe: PRL 126, 241101 (2021)
Ni: PRL 128, 131103 (2022)

ICRC 2023 Update

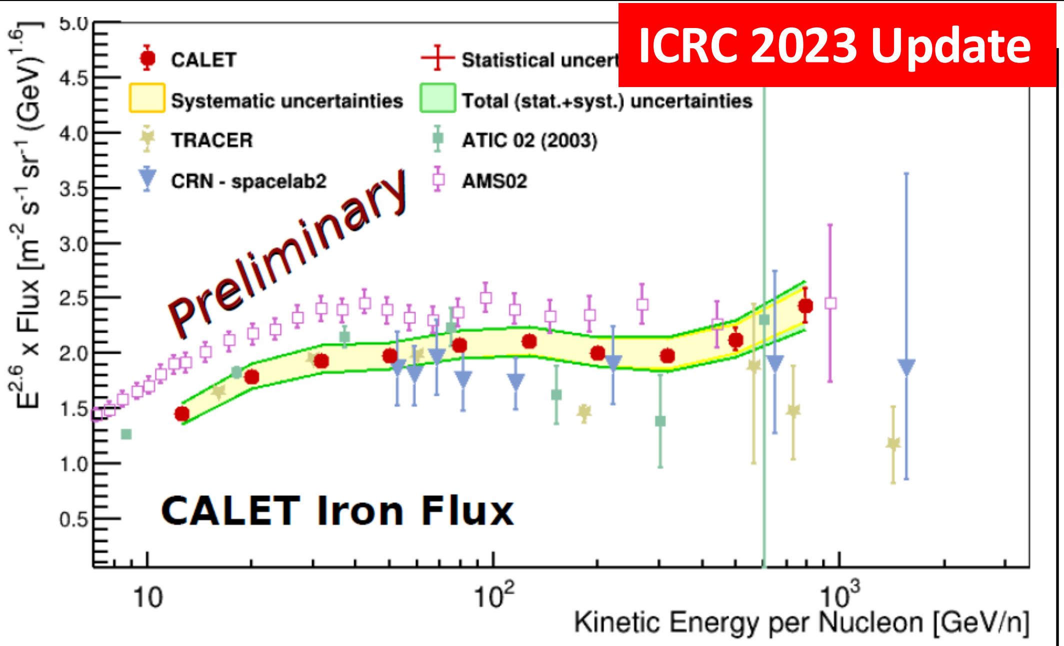

Charge peaks separated and well-reproduced by MC data

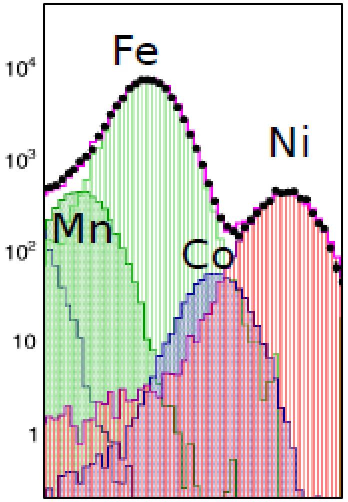

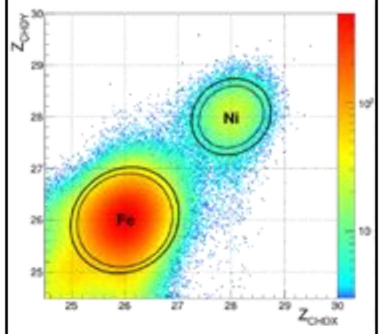

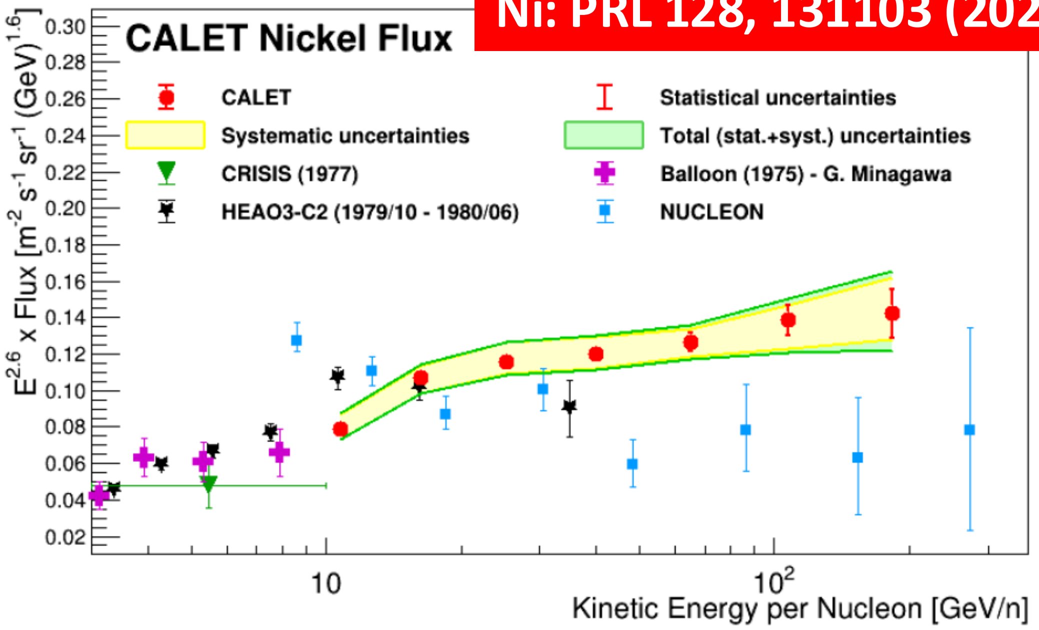

ICRC 2023 Update

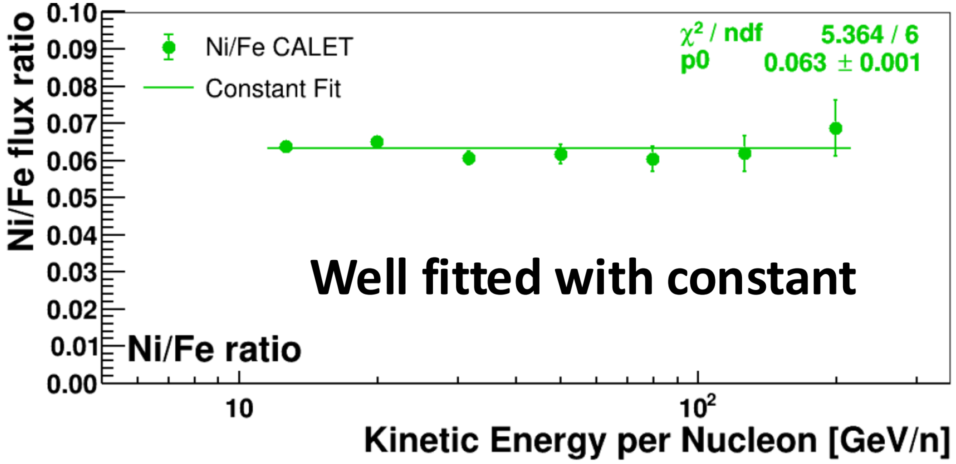

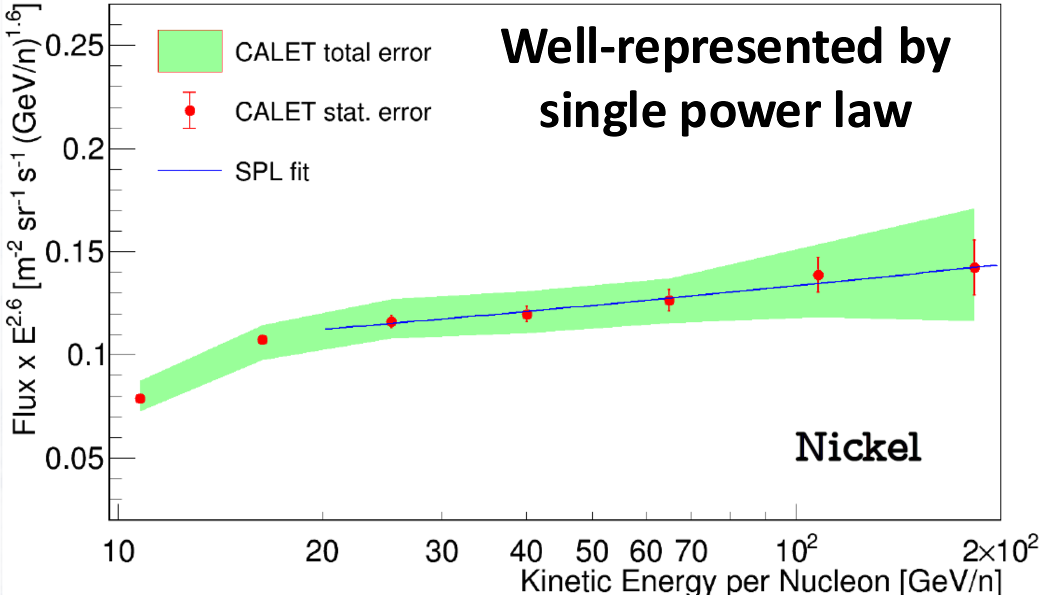

Measurement of the Ti/Fe Ration

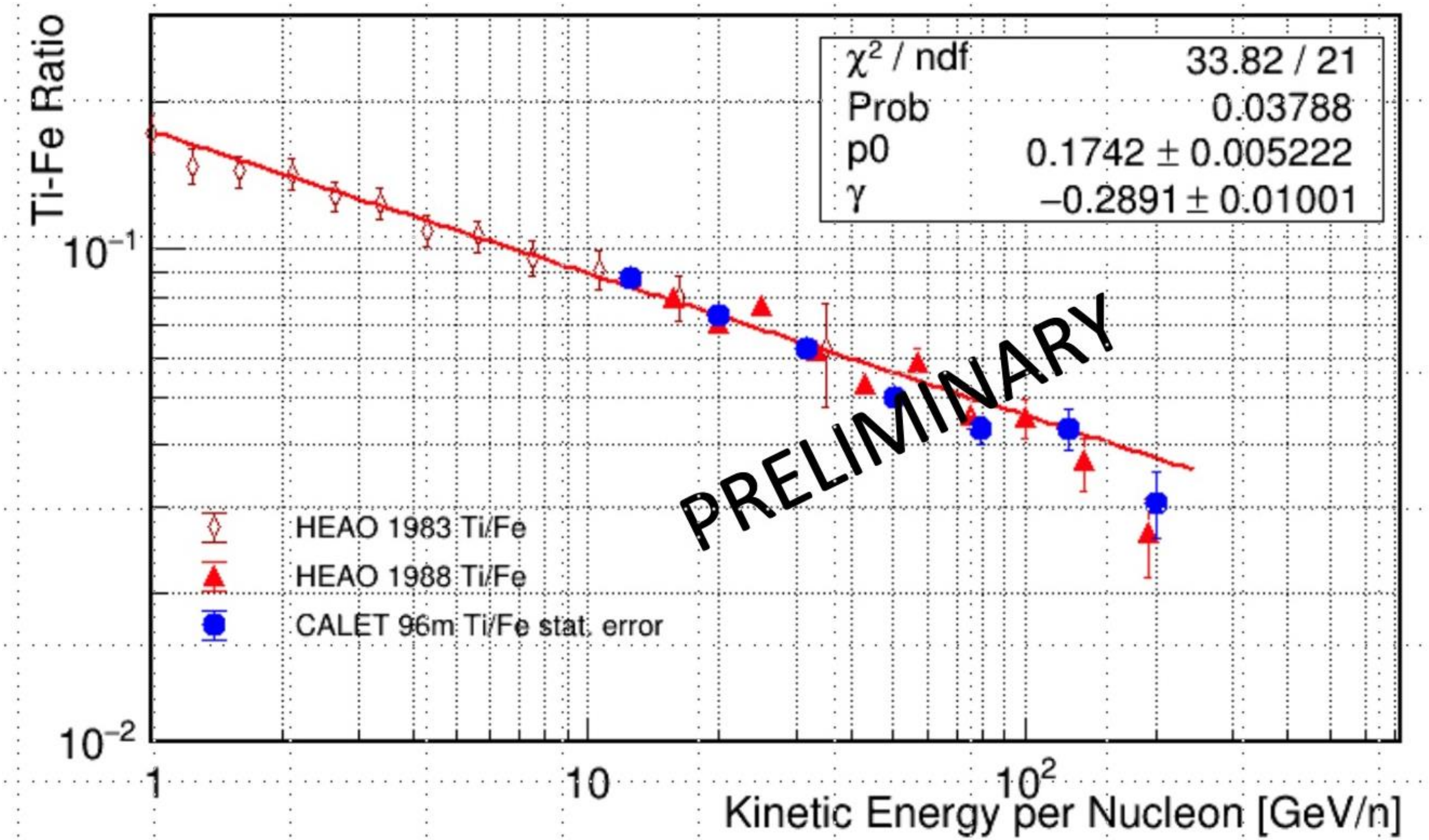

The Ti/Fe ratio as measured by HEAO (red) and CALET (blue) as a function of kinetic energy. CALET uncertainties are statistical only. The red line is a power law fit to the HEAO data.

Measurement of UHGCR Abundances

- 7 years of CALET UH-trigger data from 10/2015 through 06/2023. (~280 million events)
- This analysis: events pass through the top of the TASC. (~70 million events)

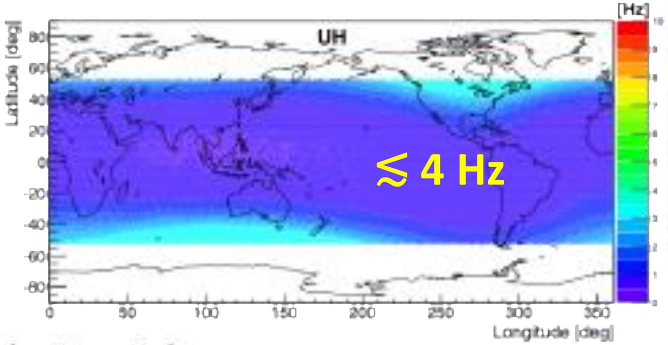

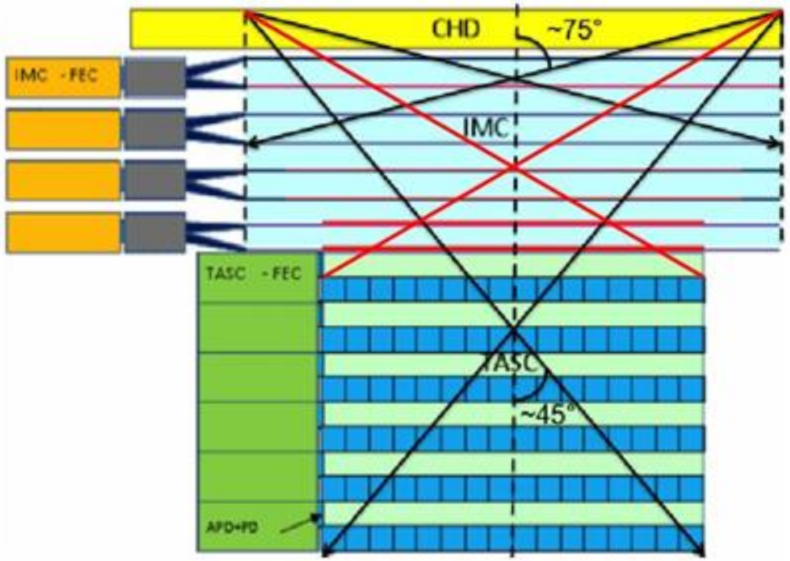

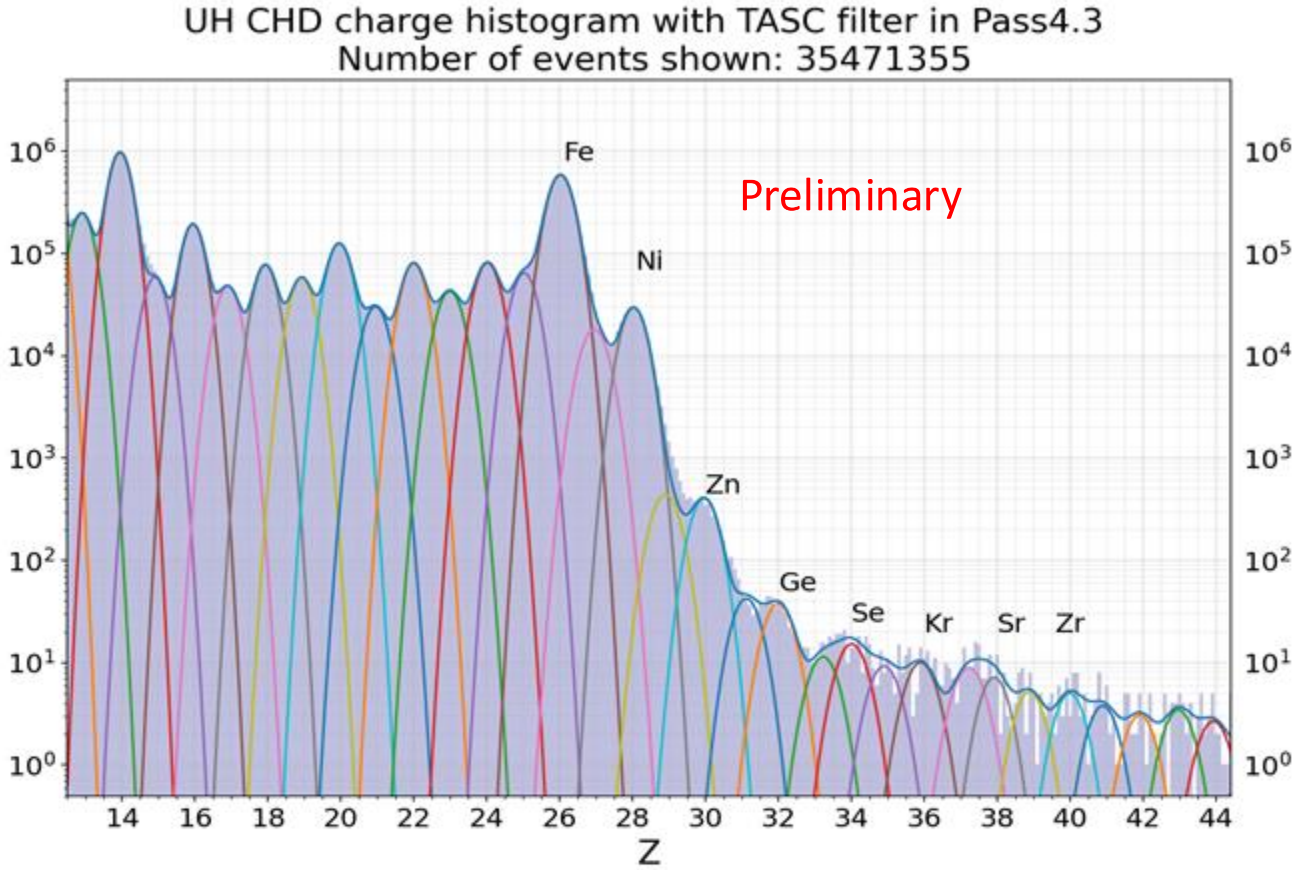

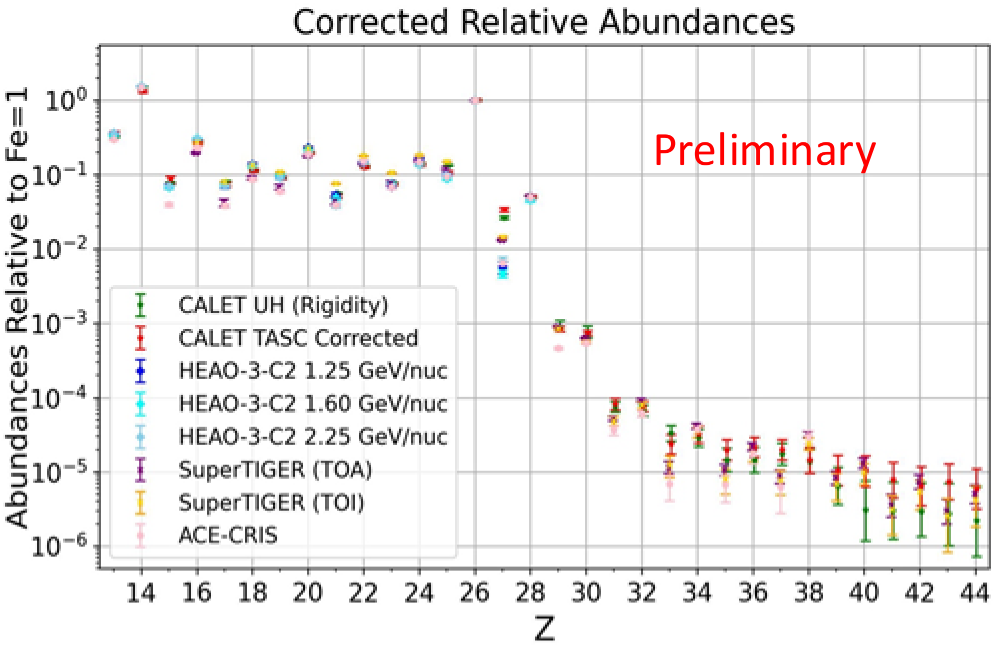

Observed events in CALET flight data

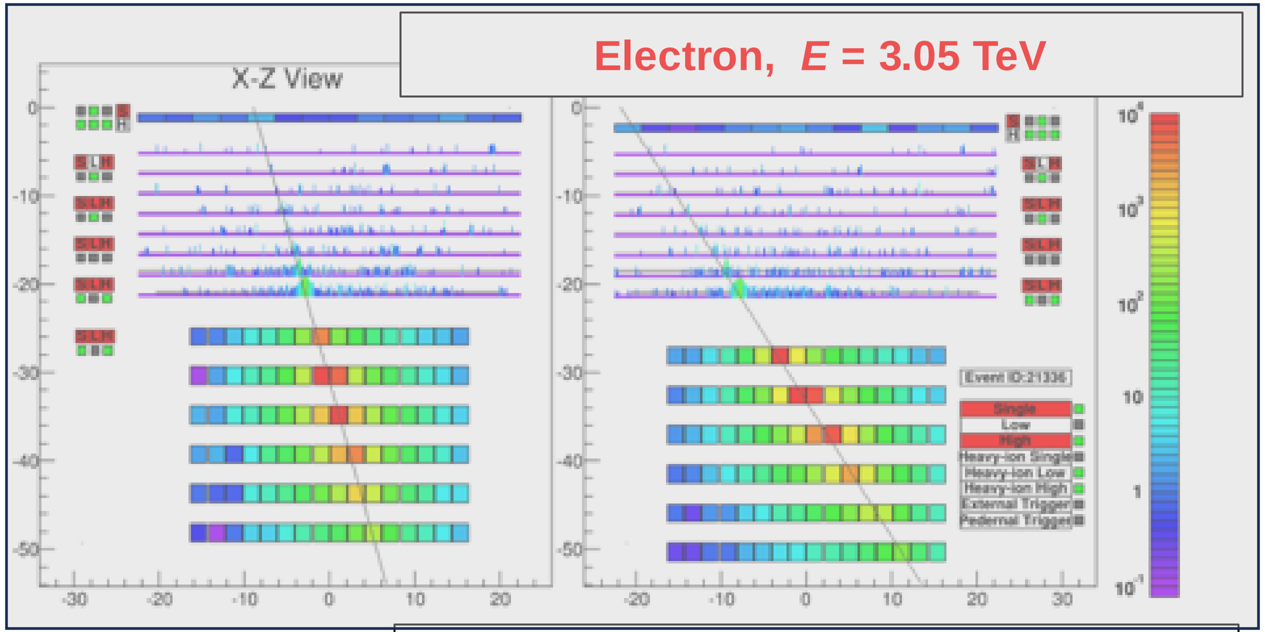

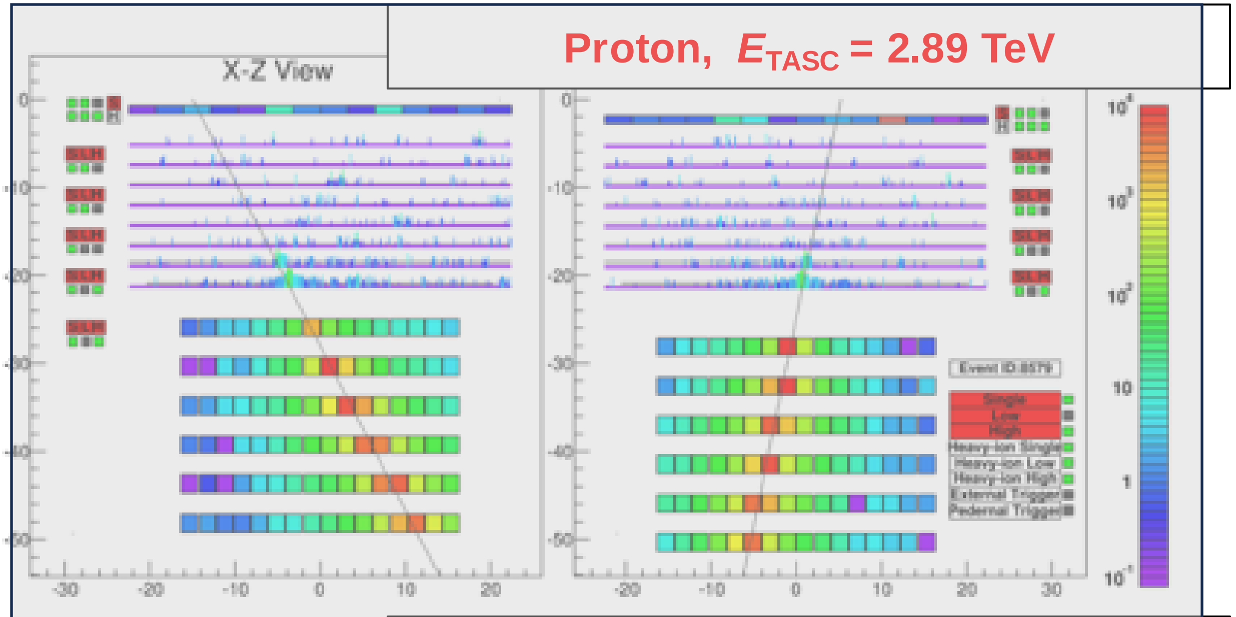

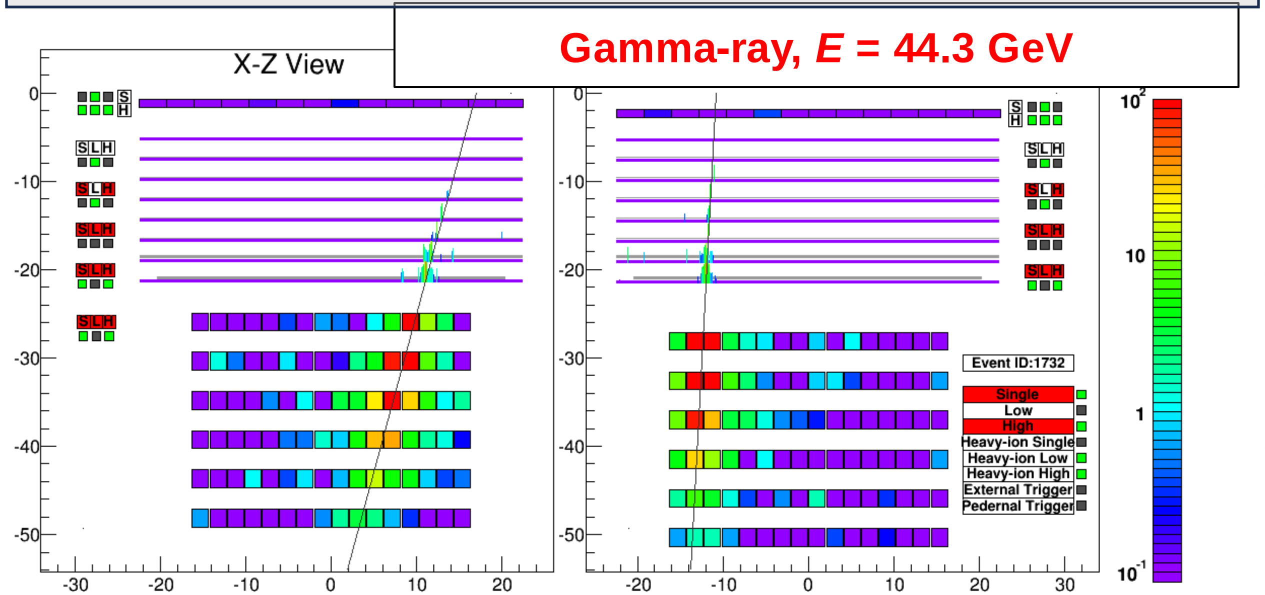

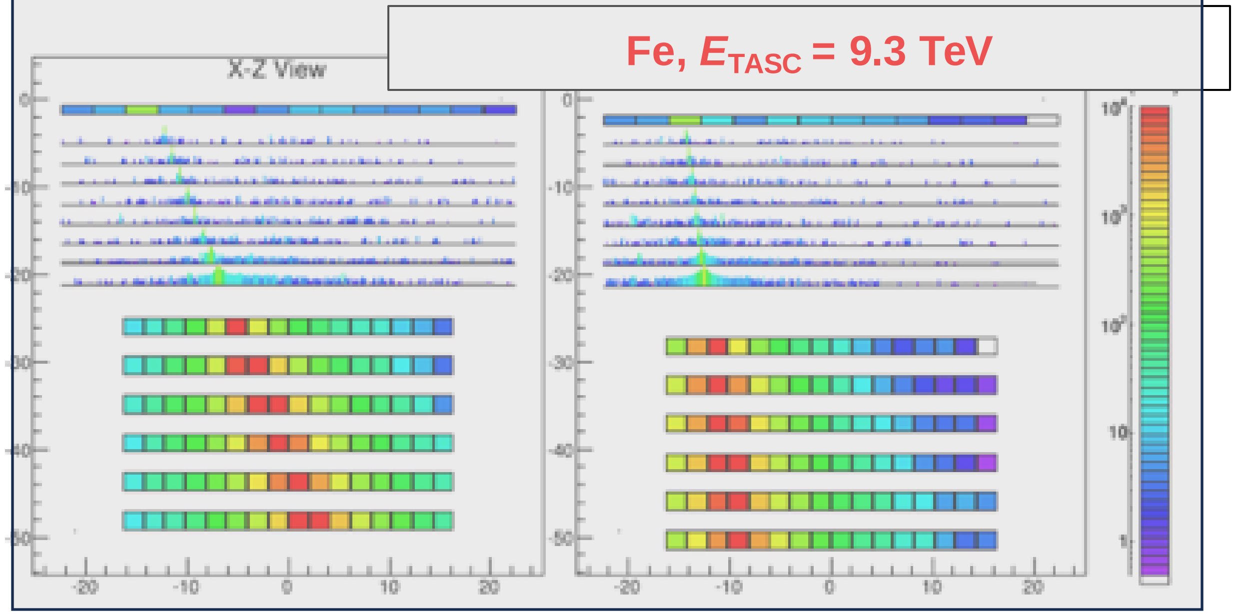

CALET GeV-energy Gamma Rays

Effective area: ~400 cm2 (>2 GeV)

- **Angular resolution: < 0.2° (> 10 GeV)**
- **Energy resolution: ~2% (> 10 GeV)**

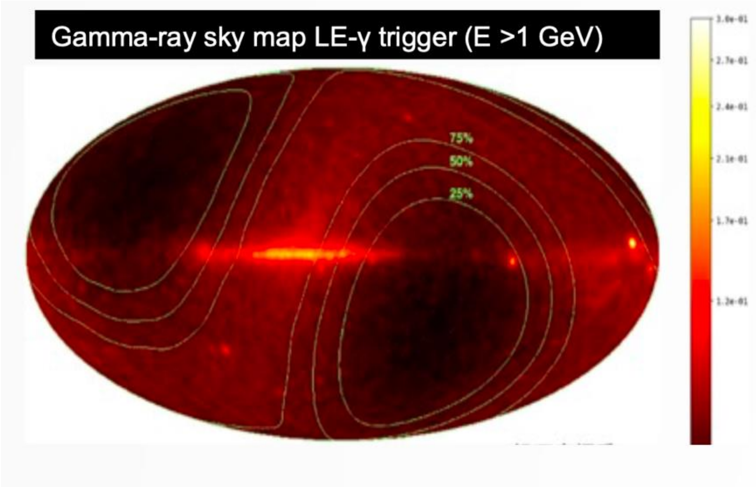

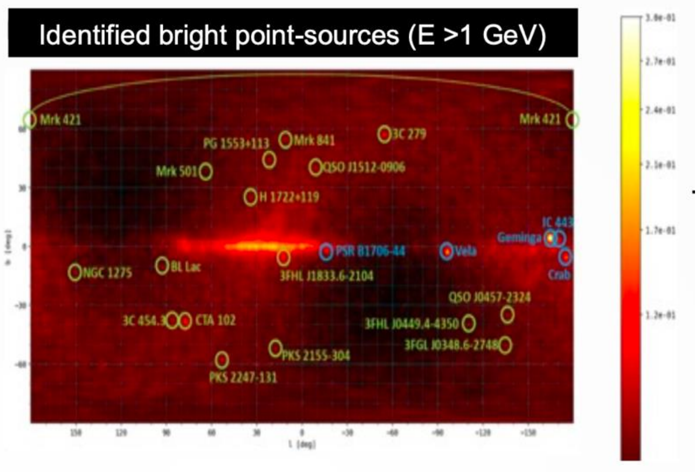

Average galactic spectra

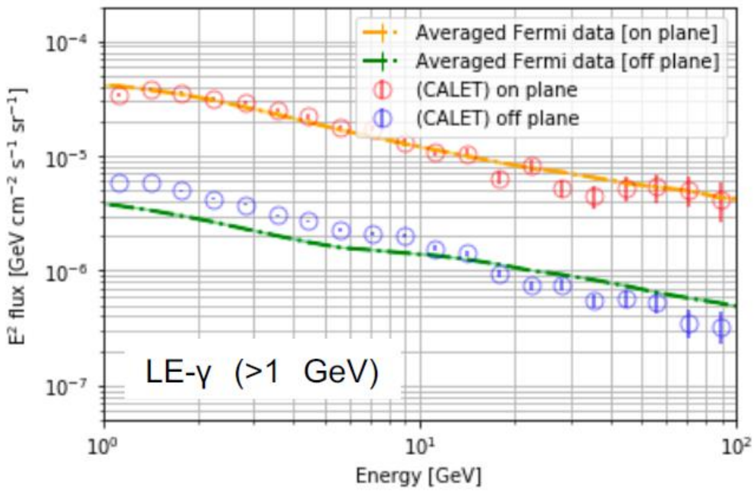

Energy spectra for bright point sources Preliminary

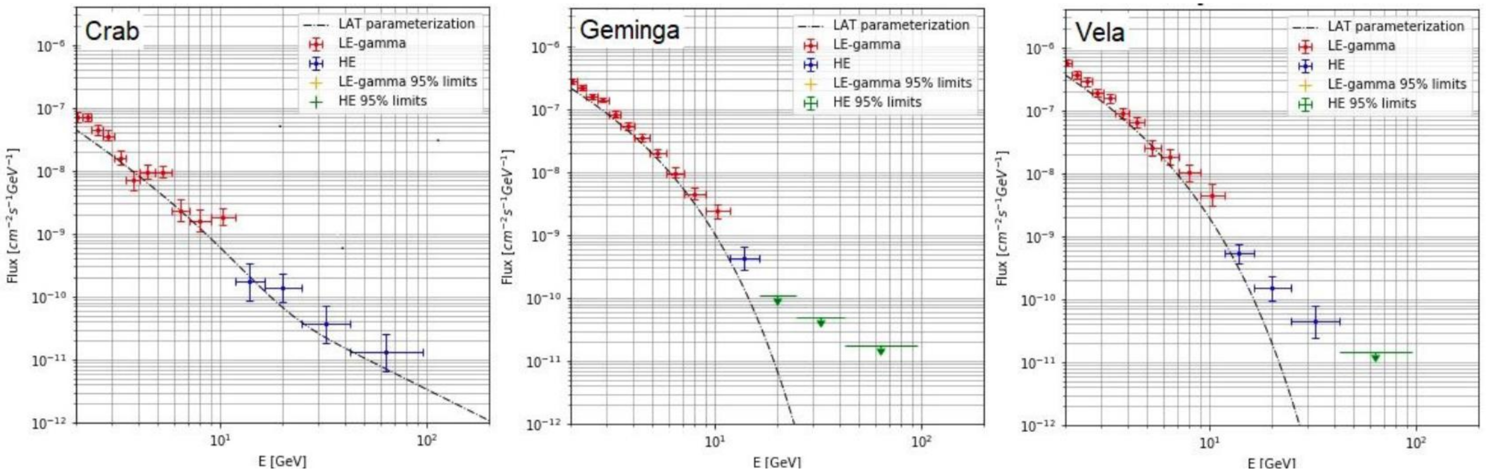

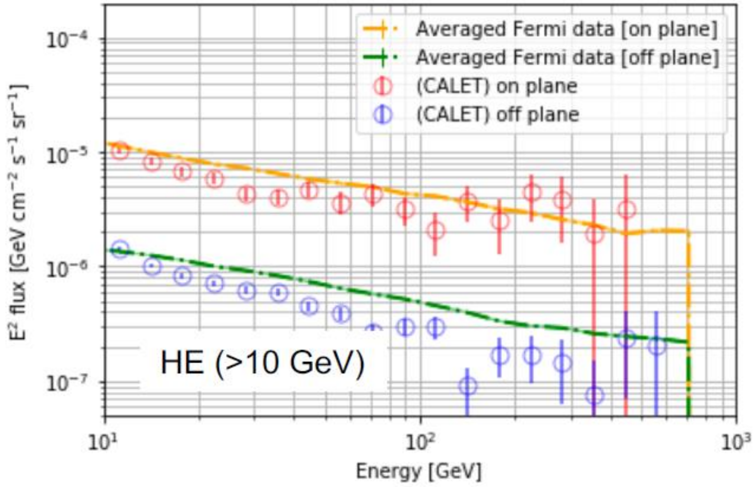

Measurements of energy spectra for point sources and diffuse structures are found to be consistent with those by Fermi-LAT.

On-plane: $|\ell| < 80^\circ$ & $|b| < 8^\circ$
Off-plane: $|b| > 10^\circ$

Gamma-ray Bursts and GW Follow-up

CGBM Specifications

	HXM	SGM
Crystal	LaBr3(Ce)	BGO
Number of detectors	2	1
Diameter [mm]	66.1 (small) 78.7 (large)	102
Thickness [mm]	12.7	76
Energy range [keV]	7-1000	40-20000
Field of view	~3 sr	~8 sr

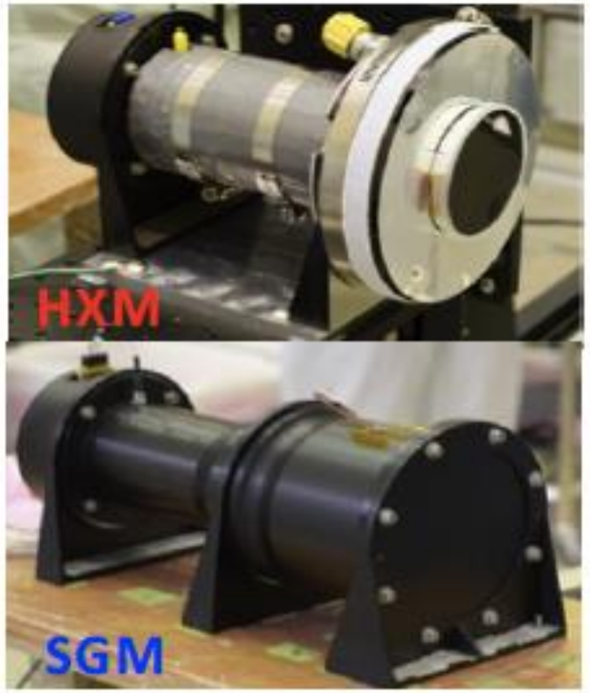

CGBM has detected 367 GRBs as of Aug 2024.

Duration distribution measured by SGM (40 – 1000 keV)

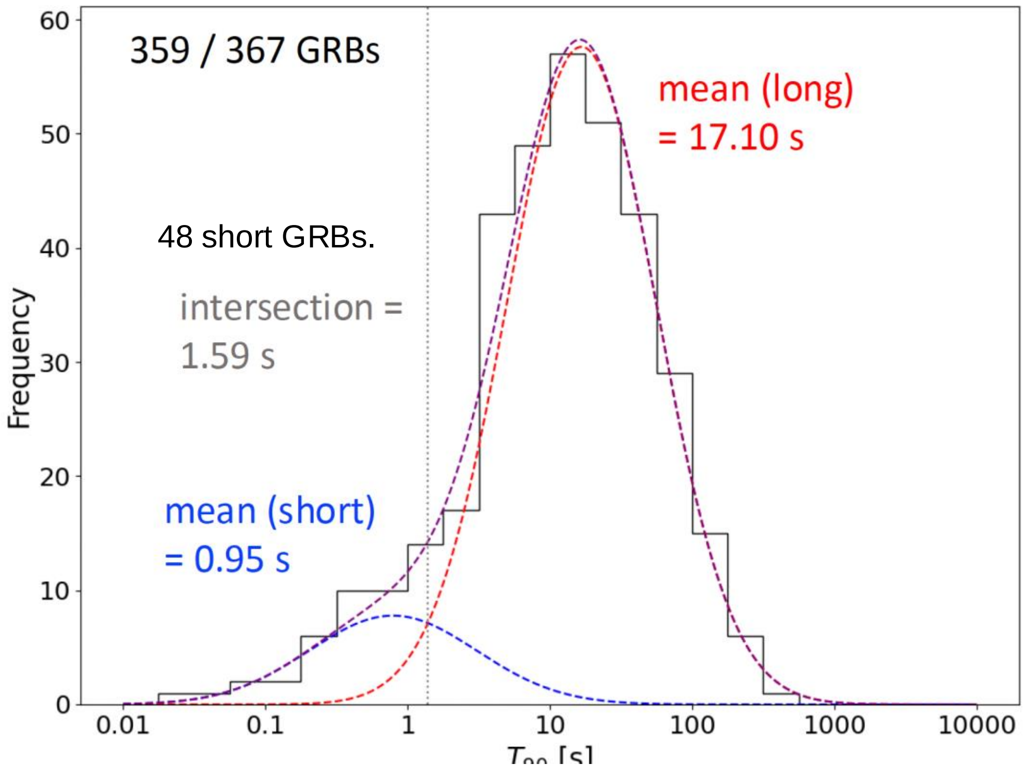

- **Follow-up** of LIGO/Virgo **GW** observations during O3 & O4
  - X-ray and gamma-ray bands
  - High-energy gamma-ray in the calorimeter

- We developed **automatic pipelines to process CGBM and CAL data** to analyze O4 events with higher event rates.
- **169 events have been reported via GCN Notice** in ER15 and O4, and the developed pipelines have been **triggered by LVC NOTICE and processed CALET data**, and enabled us to check many GW events.

Charge-sign Dependent Solar Modulation

PRL 130, 211001 (2023)

ICRC 2023 Update

Solar Modulation during Solar Cycles 24-25 Transition

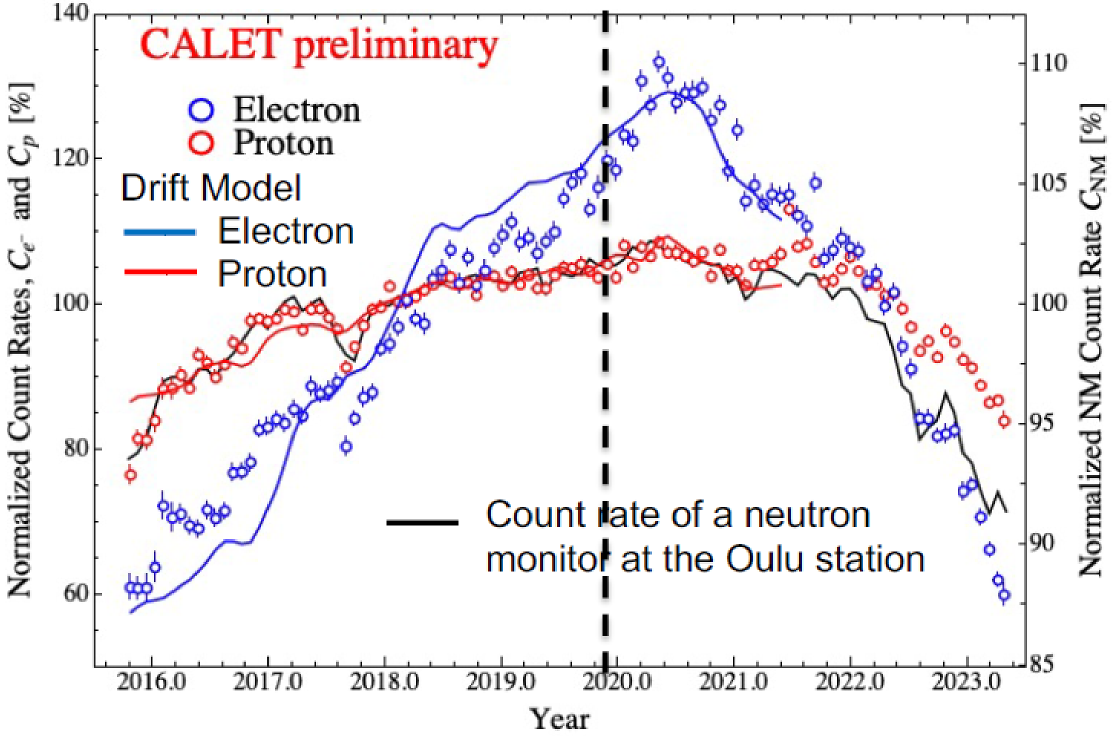

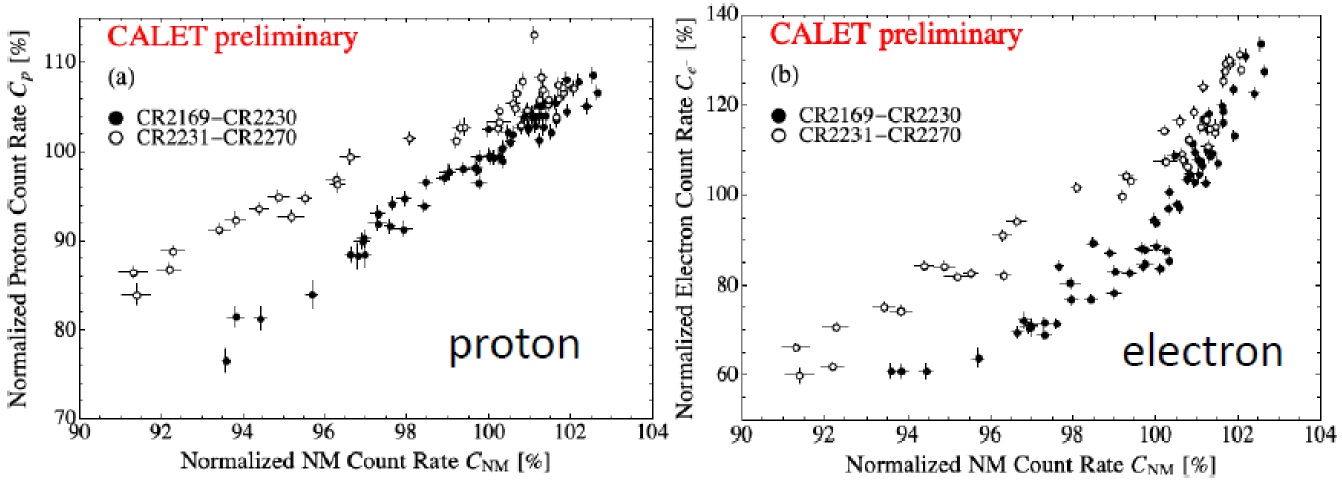

CALET proton (a) and electron (b) count rates at the average rigidity of 3.8 GV as a function of neutron monitor count rates at the Oulu station during the descending phase in the 24th solar cycle (closed circles) and the ascending phase in the 25th solar cycle (open circles).

- We have observed a clear charge-sign dependence of the solar modulation of GCRs, showing that variation amplitude of C_{e-} is much larger than that of C_p at the same average rigidity.
- We also have succeeded in reproducing variations of C_{e-} and C_p simultaneously with a numerical drift model of the solar modulation, which implies that the drift effect plays a major role in the long-term modulation of GCRs.
- We also find a clear difference between ratios, C_p/C_{NM}, during the descending phase of the 24th solar cycle and the ascending phase of the 25th solar cycle.

Space Weather Transients

- Objectives of CALET include continuous monitoring of space-weather phenomena in the LEO radiation environment, including relativistic electron precipitation (REP) from the outer Van Allen Belt
- REP drivers were investigated in magnetically conjugate observations by CALET and Van Allen Probes, showing the role of wave scattering and the contribution of EMIC-wave driven precipitation to radiation-belt losses (Bruno et al., 2021†; Blum et al., 2024‡)

Relativistic Electron Precipitation Events with CALET

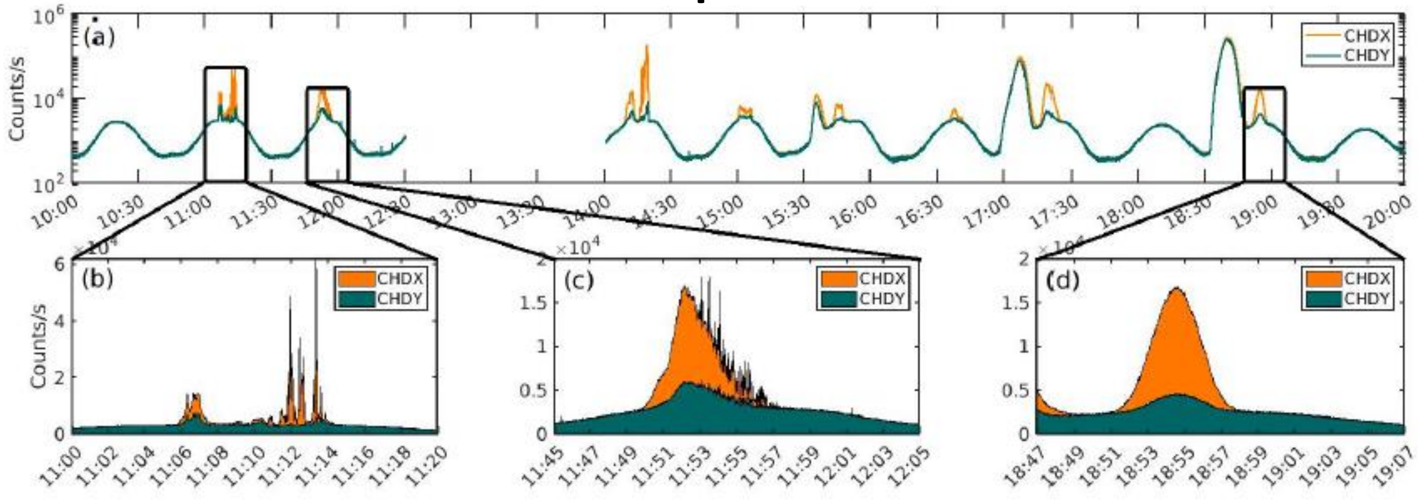

rapid mixed smooth

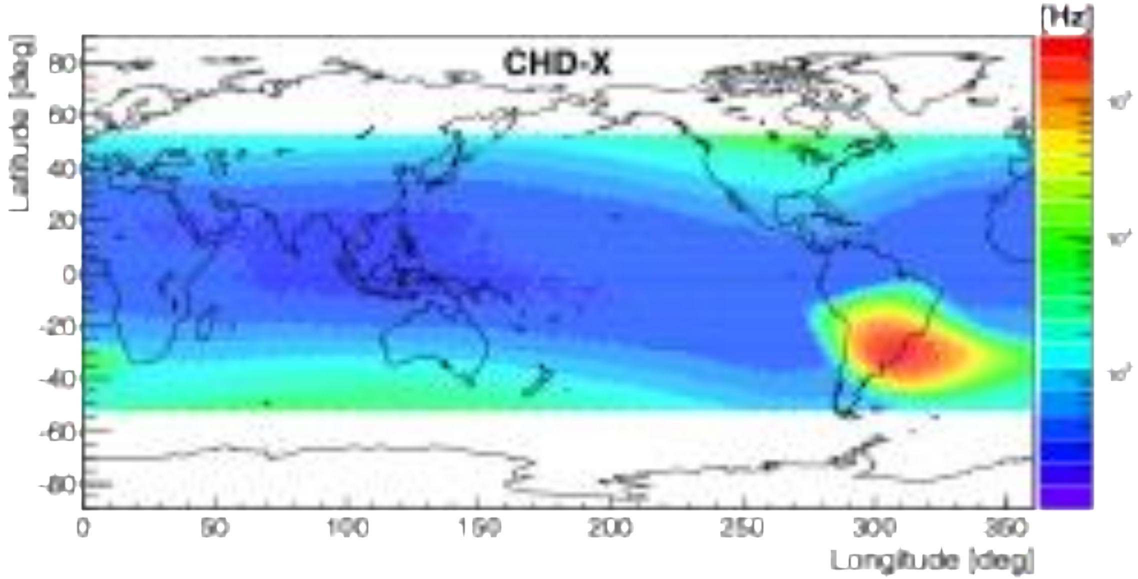

- An automated algorithm based on machine-learning techniques was implemented to identify and classify the REP events collected during >9 years of the mission (Vidal-Luengo et al, 2024a•)
- The large statistical sample allowed to investigate the contribution of REP to the radiation belt dropouts, and the correlations with solar-wind/geomagnetic drivers (Freund et al., 2024*)
- The occurrence of REP events was found to exhibit a semi-annual variation (peaking at equinoxes), in agreement with the temporal periodicity of outer-belt electron intensities (Vidal-Luengo et al, 2024b^)

Space Weather Phenomena with CALET

- To identify relativistic electron precipitation (REP) in the CALET dataset an algorithm was developed which use self organizing maps (SOM), an unsupervised machine learning technique, to both detect and categorize potential REP events.
- For a period from October 2015 to October 2021 this method found a total of 1448 rapid REP events and 21301 smooth profile events.

Relativistic Electron Precipitation (REP) Events with CALET

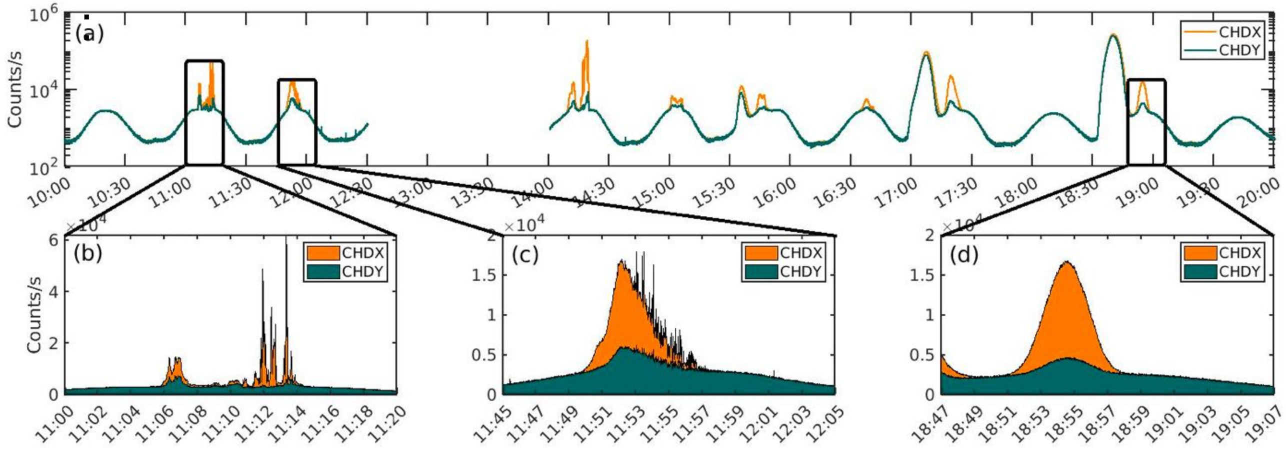

CALET and Radiation Belt Science Probes (RBSP)

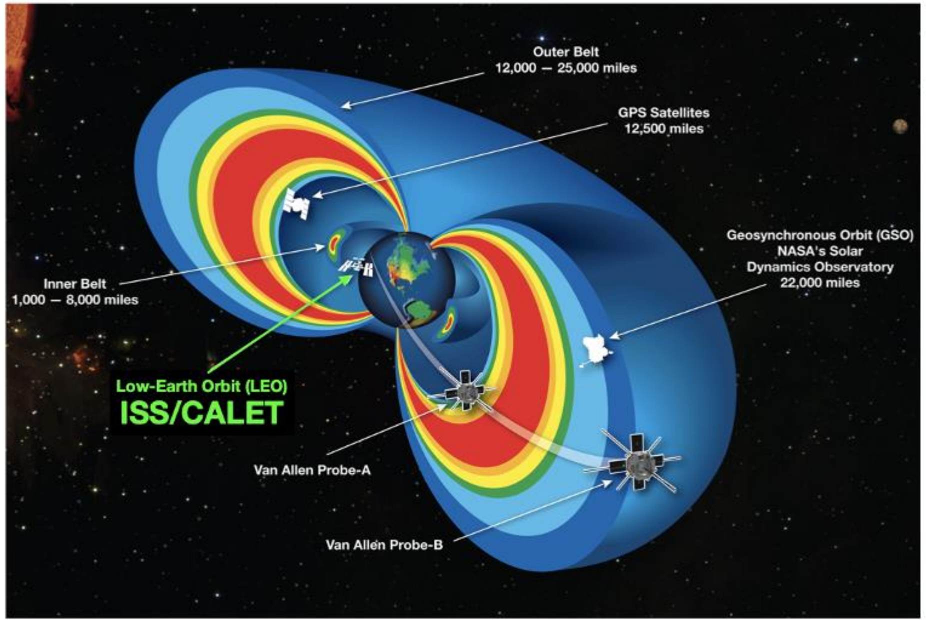

- 664 events were identified in RBSP-A data and 443 events for RBSP-B

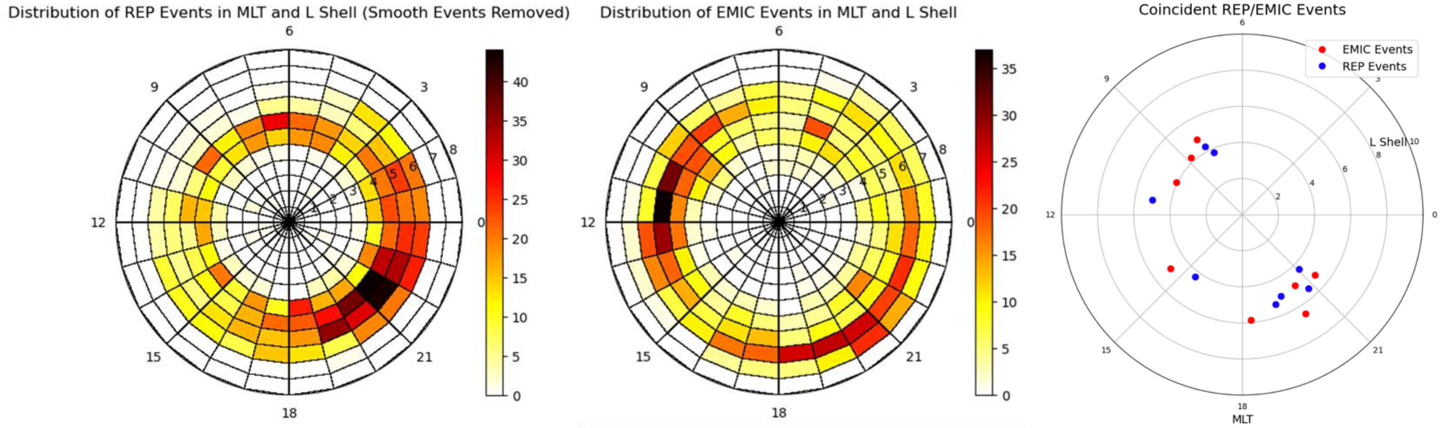

Spatial distribution in terms of magnetic local time (MLT) and L shell for observed REP events (left) and observed EMIC wave events (right).

Spatial distribution of coincident REP/EMIC wave events in MLT and L.

Summary

CALET has been nearly flawlessly recording science data since October 13, 2015

Key results for this conference (Searching for Sources of Galactic Cosmic Rays)

- CALET has measured the all-electron spectrum from 10.6 GeV to 7.5 TeV:
  - Spectrum fits to a broken power law vs single power law by 7.6σ
  - Current statistics do not reveal any local source(s)
- CALET has measured the proton, helium, light and heavy nuclei spectra:
  - The proton spectrum shows a hardening around 550 GeV ($\Delta\gamma \sim 0.29$) and a **softening around 9.8 TeV** ($\Delta\gamma_1 \sim -0.39$)
  - The helium spectrum shows a hardening around 330 GeV/n (1319 GeV, $\Delta\gamma \sim 0.25$) and a **softening around 8.3 TeV/n** (33.2 TeV, $\Delta\gamma_1 \sim -0.22$)
  - *The proton to helium ration decreases as a function of energy and rigidity*
  - Using a joint-fitting approach yields E_0 = 260 ± 50 GeV/n for double power law fit:
    - The carbon and oxygen spectra show a hardening with $\Delta\gamma = 0.25 \pm 0.04$
    - The boron spectrum shows a hardening with $\Delta\gamma = 0.32 \pm 0.14$
    - *The boron/carbon ratio is consistent with a $\lambda_0 = 1.17 \pm 0.16\ g/cm^2$ for a $\lambda(E) = kE^{-\delta} + \lambda_0$ fit.*
  - The UHGCR relative abundances from Z=36 to Z=40 are consistent with previous results, especially SuperTIGER.

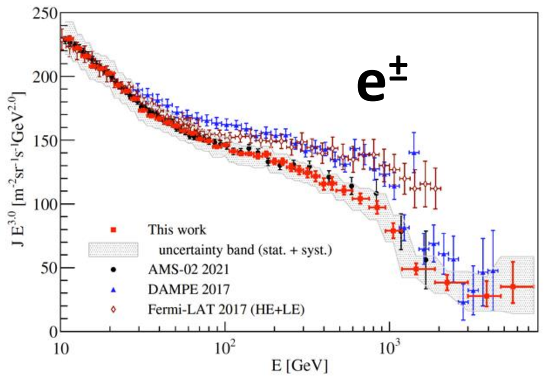

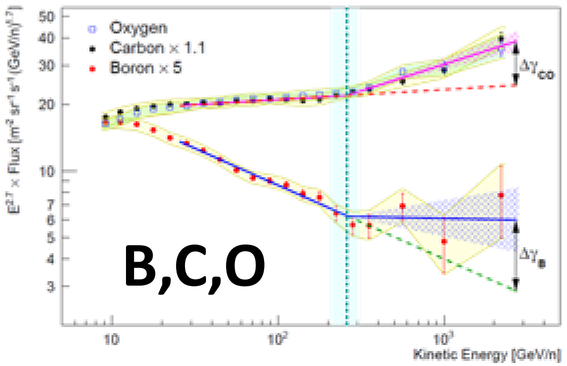

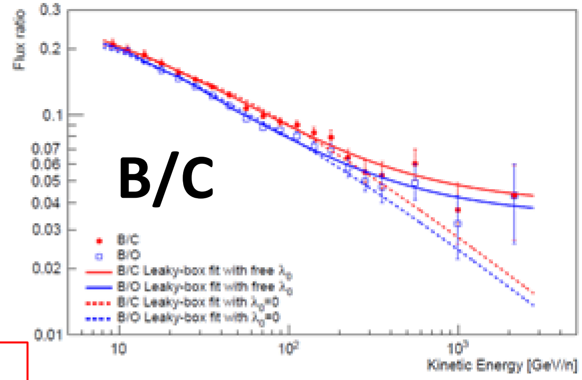

More to come: extended operations approved by JAXA/NASA/ASI through 2030!

CALET Journal Paper Summary

- **CALET was successfully launched in August 2015 and installed on the JEM-EF module on the ISS**
  - Stable operations over a range of observing modes continue — see **Astropart. Phys. 100, 29 – 37 (2018)**
    - Continuous on-orbit updates from ground calibration — see **Astropart. Phys. 91, 1 – 10 (2017)**
    - Operational over 3200 days with 85% live time, total triggers over4.5 billion
- **Analysis of cosmic-ray events continues, extending to higher energies and charges**
  - All-electron spectrum in the range 10.6 GeV – 7.5 TeV — published in **PRL 131, 191001 (2023)**
  - Proton spectrum in the range 50 GeV – 60 TeV — published in **PRL 129, 101102 (2022)**
  - Carbon and oxygen spectra in the range 10 GeV/n – 2.2 TeV/n — published in **PRL 125, 251102 (2020)**
  - Iron spectrum in the range 50 GeV/n – 2 TeV/n — published in **PRL 126, 241101 (2021)**
  - Nickel spectrum in the range 8.8 GeV/n – 240 GeV/n — published in **PRL 128, 131103 (2022)**
  - Boron spectrum in the range 8.4 GeV/n – 3.8 TeV/n — published in **PRL 129, 251103 (2022)**
  - Helium spectrum in the range 40 GeV – 250 TeV — published in **PRL 130, 171002 (2023)**
  - Abundances of heavy and ultra-heavy nuclei ($13 \leq Z \leq 44$) — in preparation for ApJ
- **Analysis of gamma-ray sources and transients continues**
  - Calorimeter instrument response characterized — see **ApJS 238:5 (2018)**
  - GW follow-up and GRB analysis with CGBM & CAL — see **ApJL 829:L20 (2016)**
  - Counterpart search in LIGO/Virgo O3 with CGBM & CAL — see **ApJ 933:85 (2022)**
  - Updates — in progress
- **Analysis of transient heliospheric and space weather phenomena underway**
  - Charge-sign dependence of Solar modulation — published in **PRL 130, 211001 (2023)**
  - Heliospheric transients such as relativistic electron precipitation, etc. — [†]**GRL 49, e2021GL097529 (2022)**; [‡]**GRL 51, e2023GL107087**; [•]**JGR 129, e2024JA032481 (2024)**; ***GRL 51, e2024GL109673**; +1 submitted to ^GRL

Backup slides

Corr: N. Cannady

PoS(ICRC2023)063 (2023)

Field-of-view Obstructions

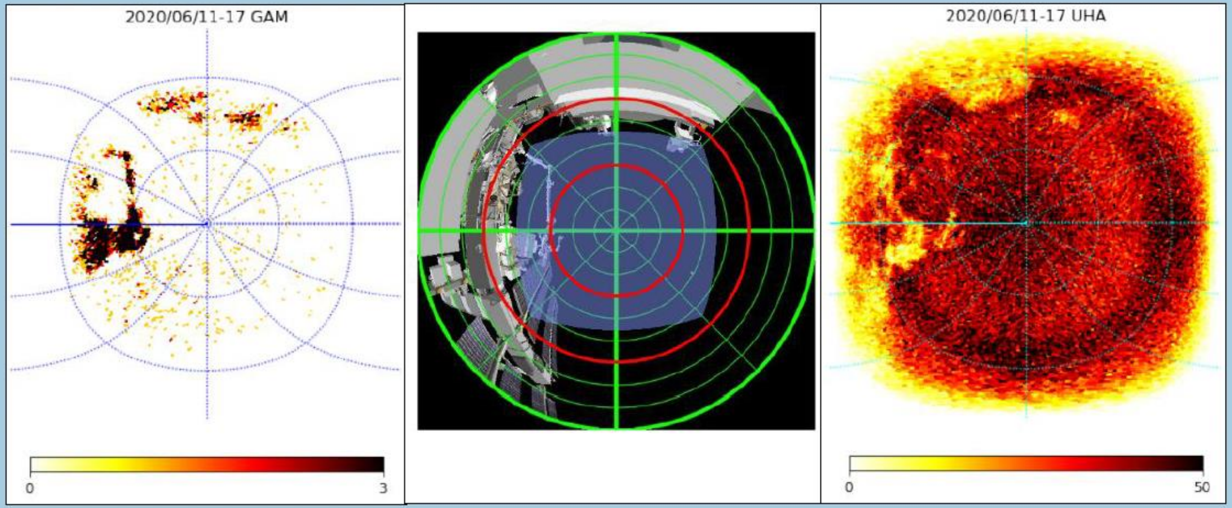

Figure 4. CALET field-of-view during a planned robotic arm active period. From left: (1) bright gamma-ray background; (2) planned arm position; (3) shadow in UHGCRs.

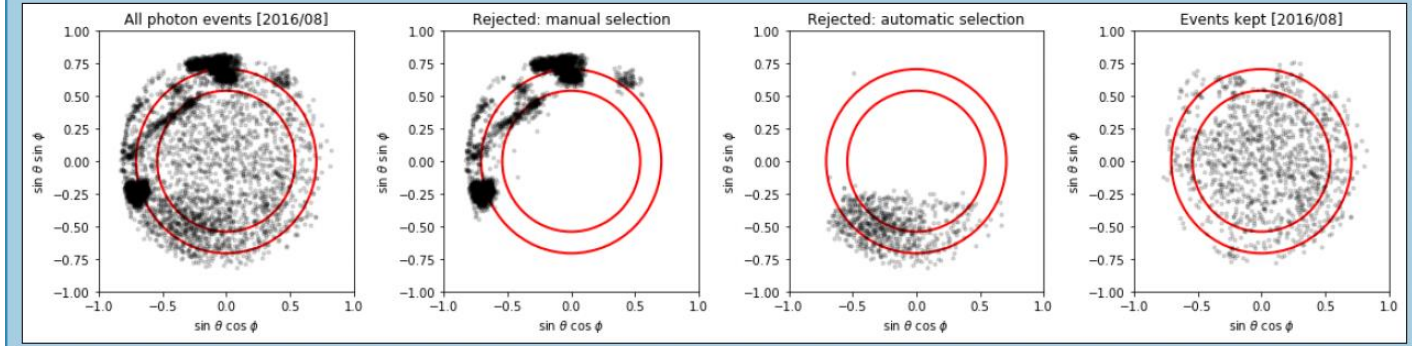

Figure 5. One month of intetegrated low-energy photon events in the CALET field-of-view. From left, the frames show (1) all events; (2) events removed by manual inspection; (3) events removed via modeling of rotating structures; and (4) events remaining after the cuts are applied.

Obstructions appear in the CALET field-of-view and are seen via:

- Low-energy photons (<~5 GeV) produced from cosmic-ray impacts (as seen in Figures 4 and 5)
- Ultra-heavy Gal. cosmic rays (UHGCRs) are shadowed (Fig 4)
- Optical glare from Solar reflection can impact star camera operation

Regularly appearing objects such as Solar panels and radiators are removed via ray-tracing code provided by JAXA

Irregularly appearing objects such as robotic arms and slow-moving objects are removed via manual inspection of field-of-view maps. Cut maps are registered in the calibration DB.

Monitoring of TASC performance on-orbit

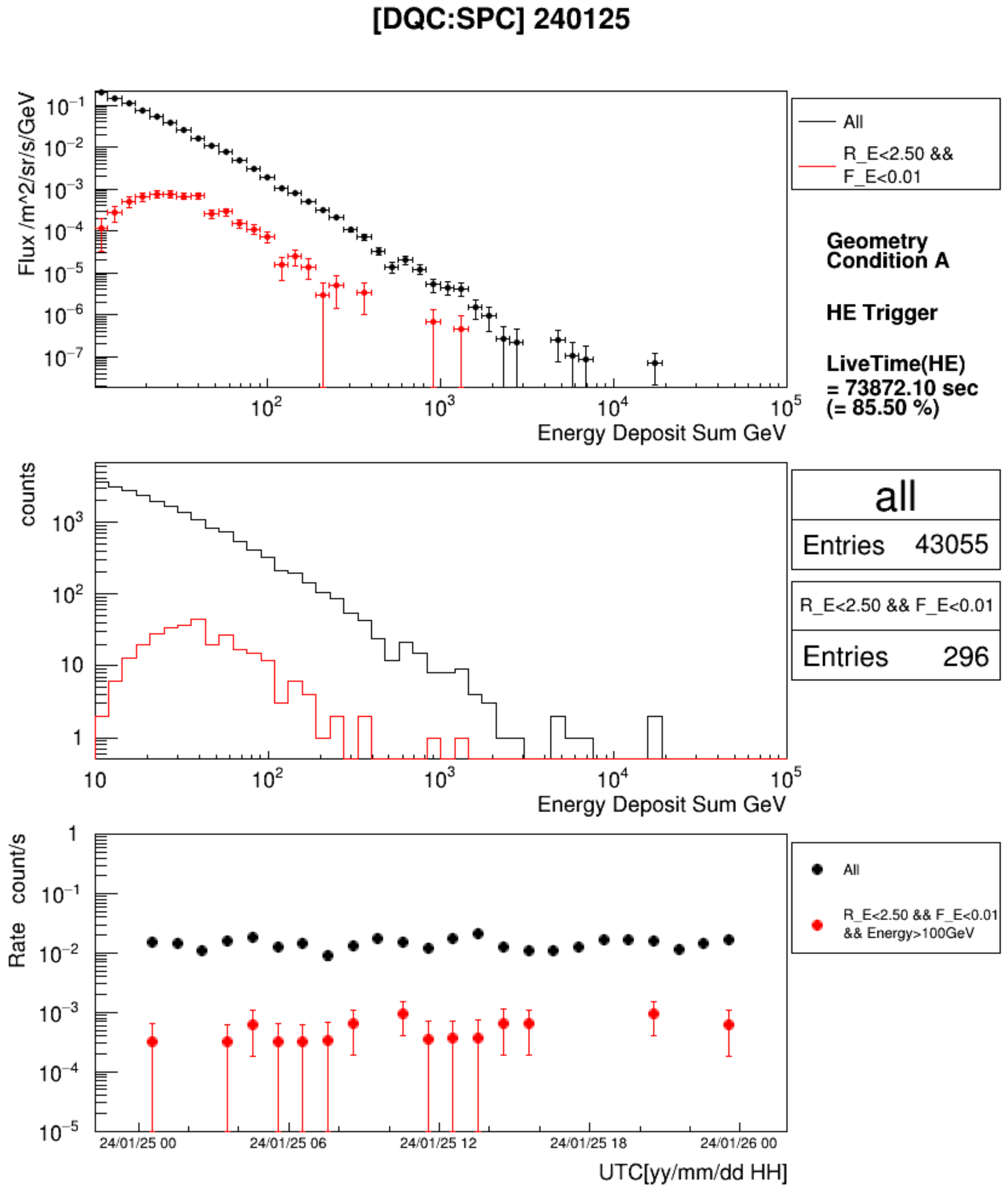

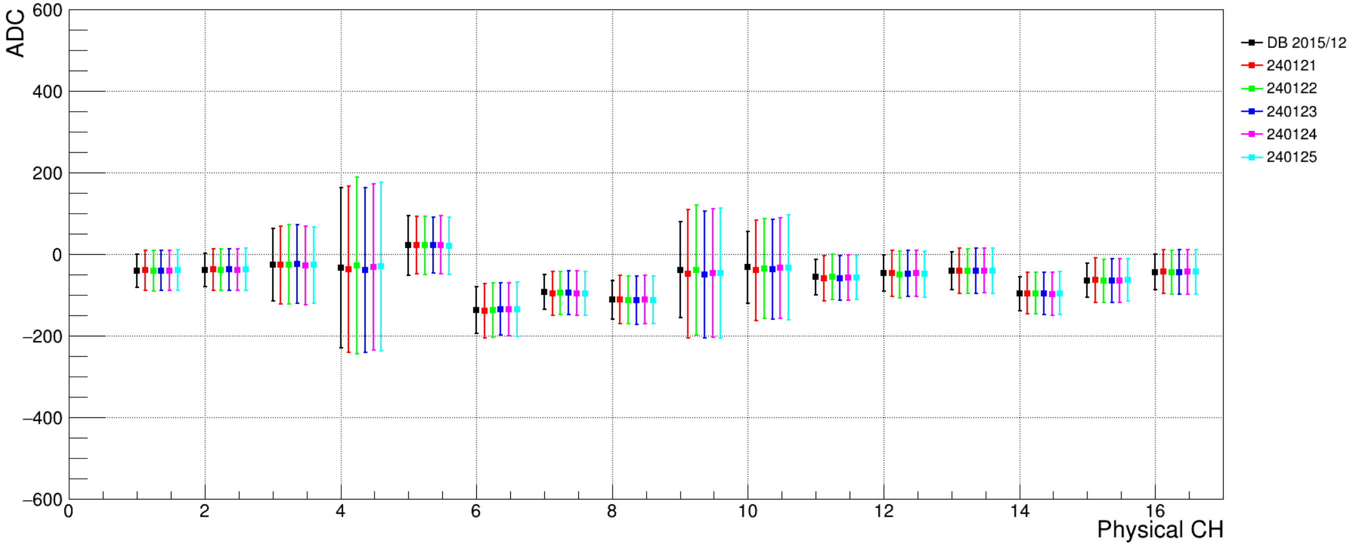

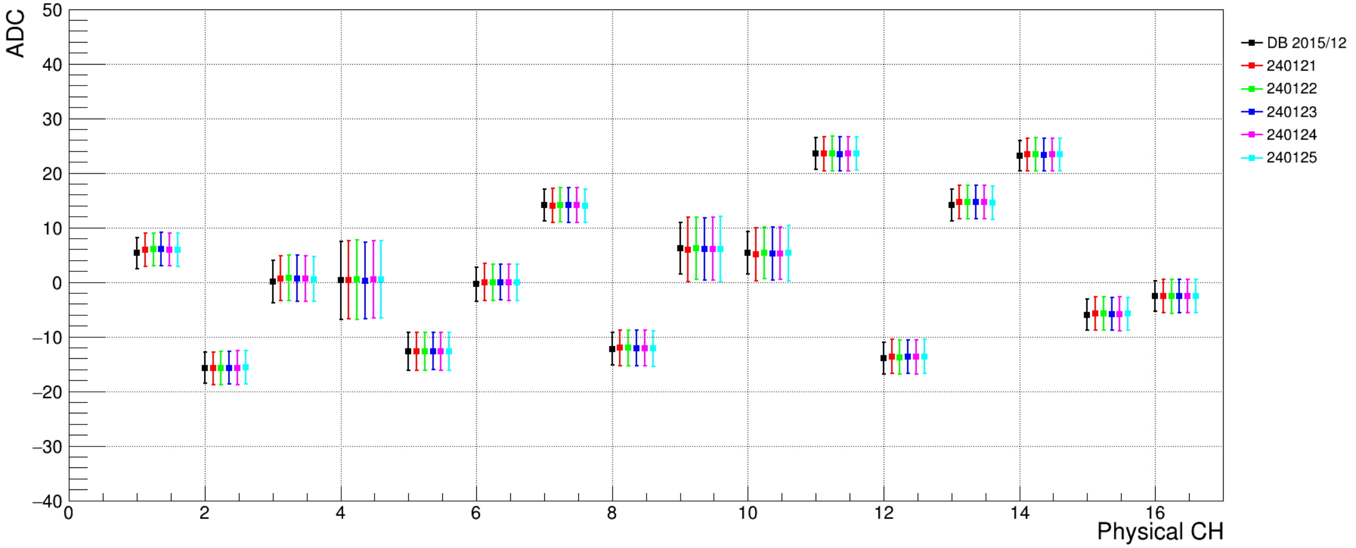

Nuclei Measurement: Charge Identification with CHD and IMC

Single element identification for p, He and light nuclei is achieved by CHD+IMC charge analysis.

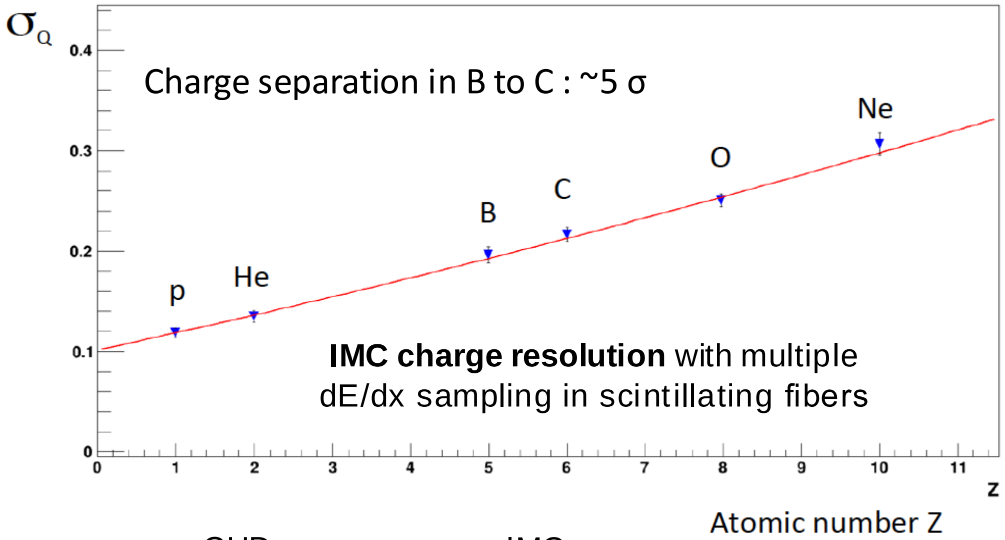

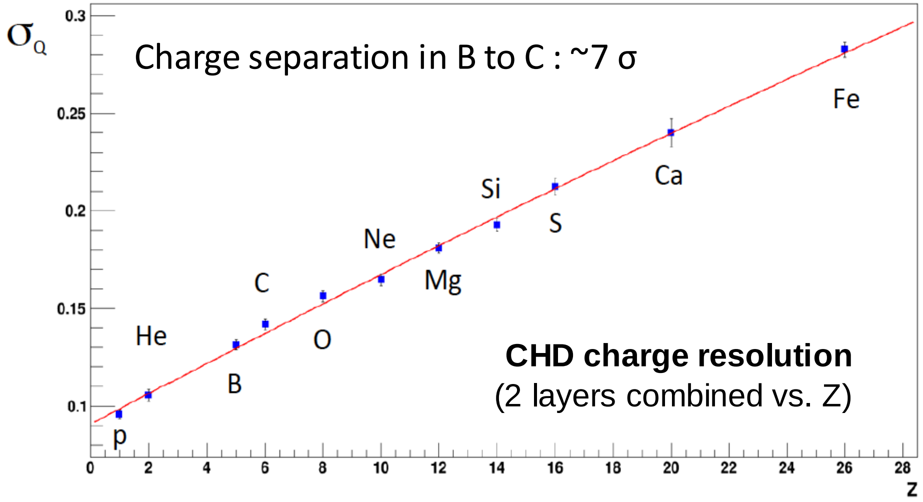

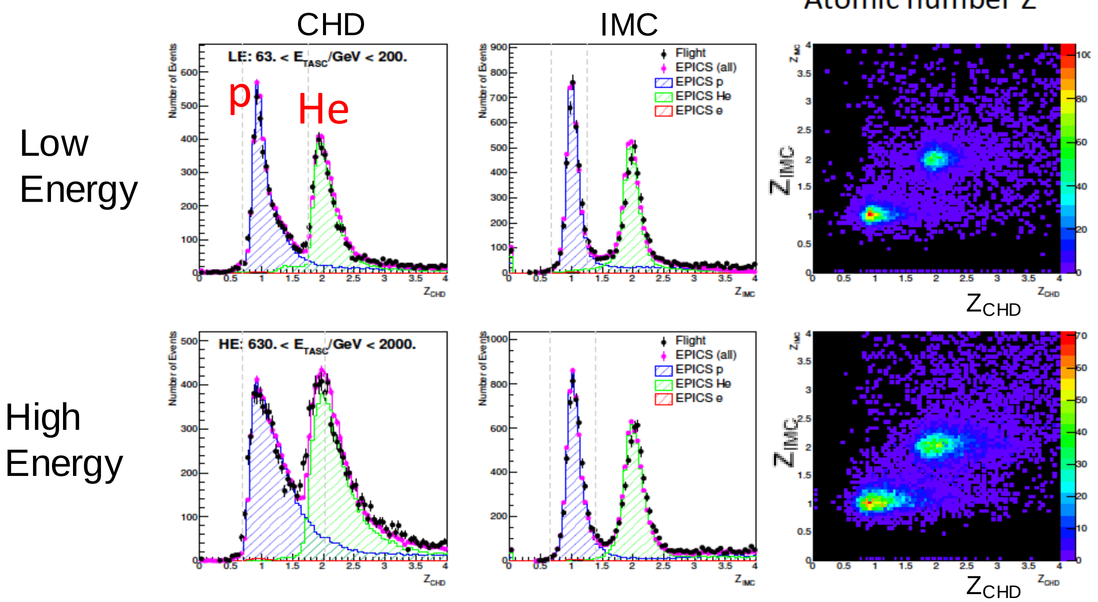

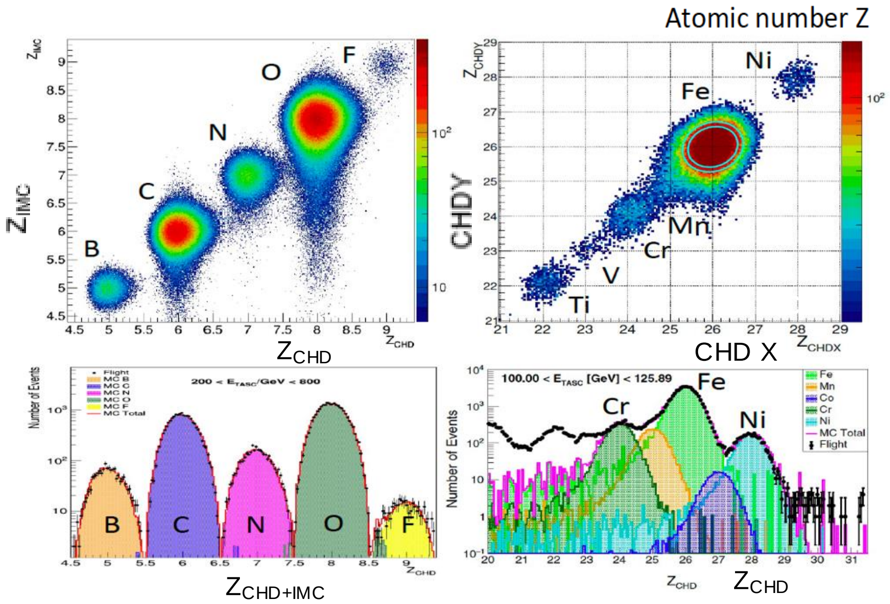

Deviation from Z^2 response is corrected both in CHD and IMC using a core + halo ionization model (Voltz)

Energy spectra of cosmic-ray Fe & Ni

Corr: C. Checchia, F. Stolzi
Y. Akaike, G. Bigongiari

Fe: PRL 126, 241101 (2021)

Ni: PRL 128, 131103 (2022)

ICRC 2023 Update

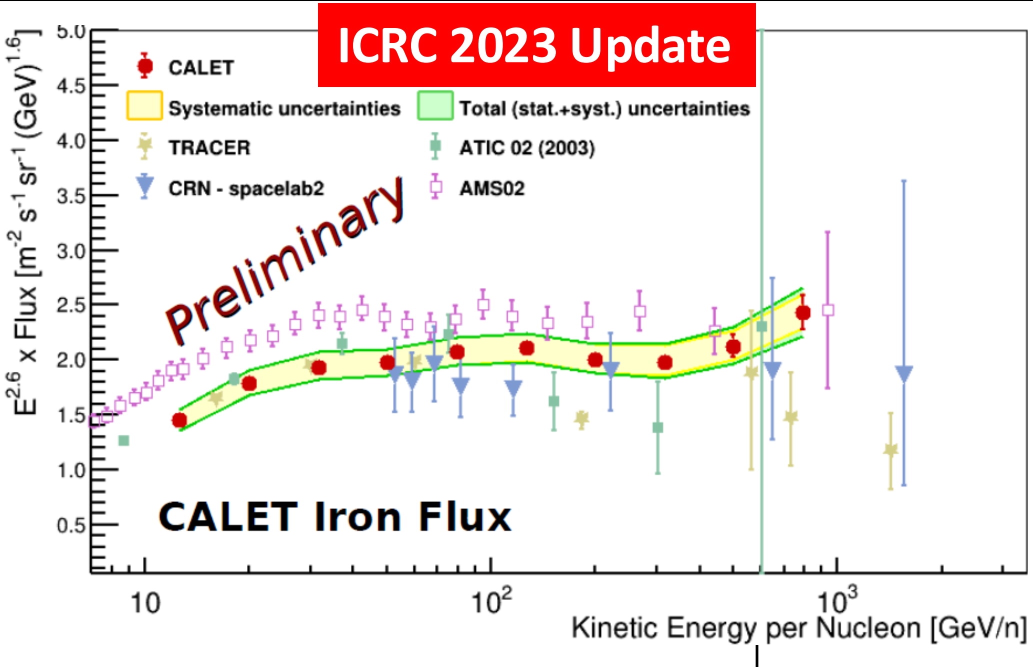

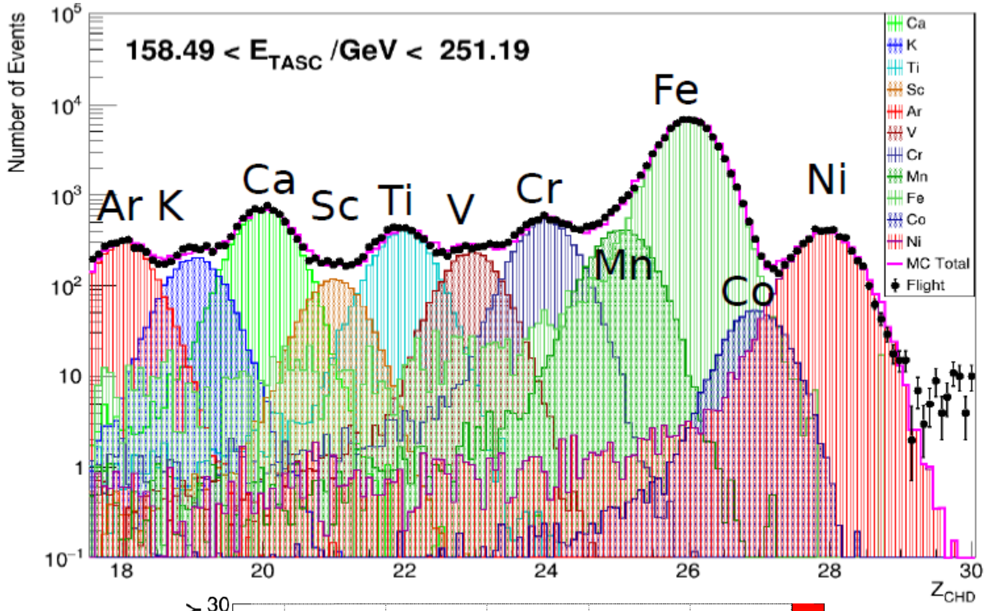

DPL not favored significantly over SPL

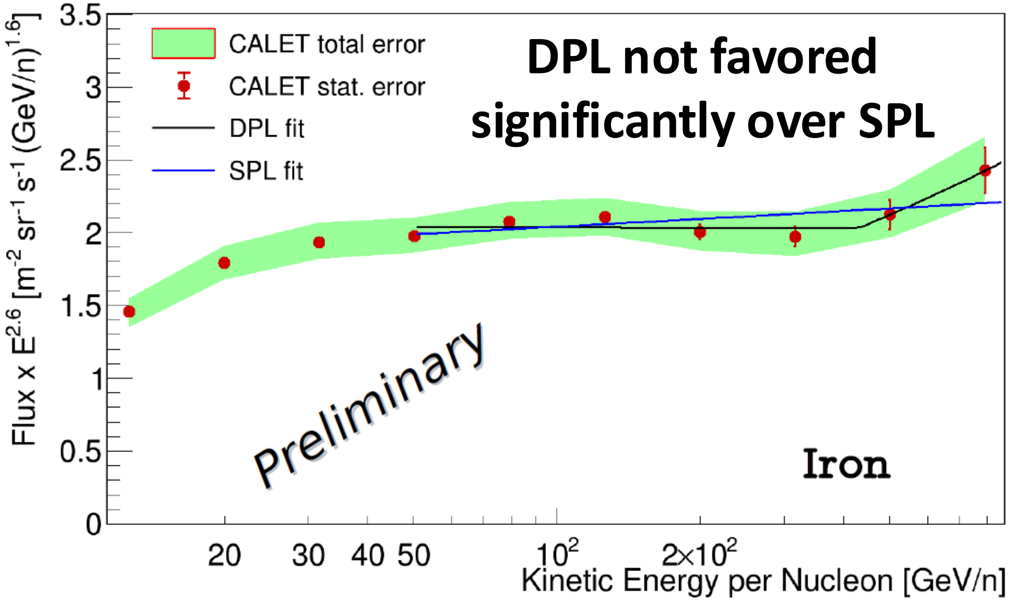

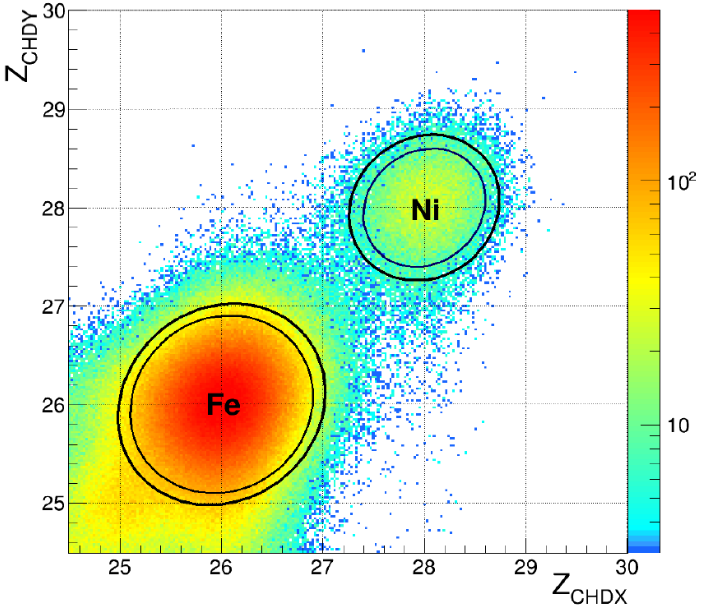

Energy spectra of cosmic-ray BCO

Corr: P. Maestro, Y. Akaike

C&O: PRL 125, 251102 (2020)

B: PRL 129, 251103 (2022)

ICRC 2023 Update

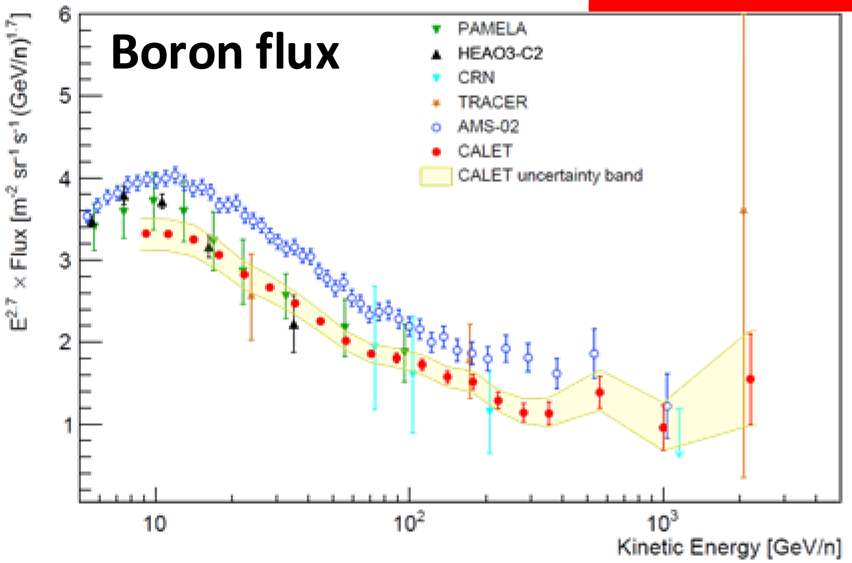

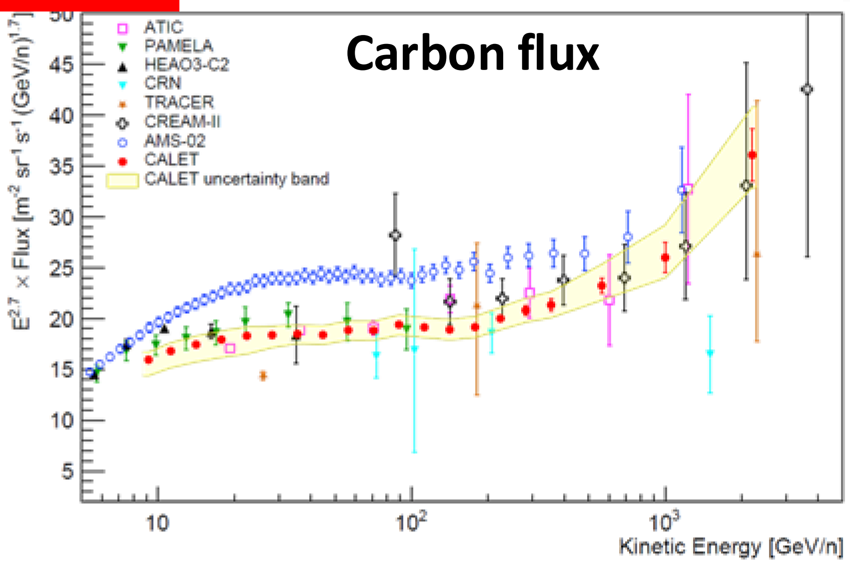

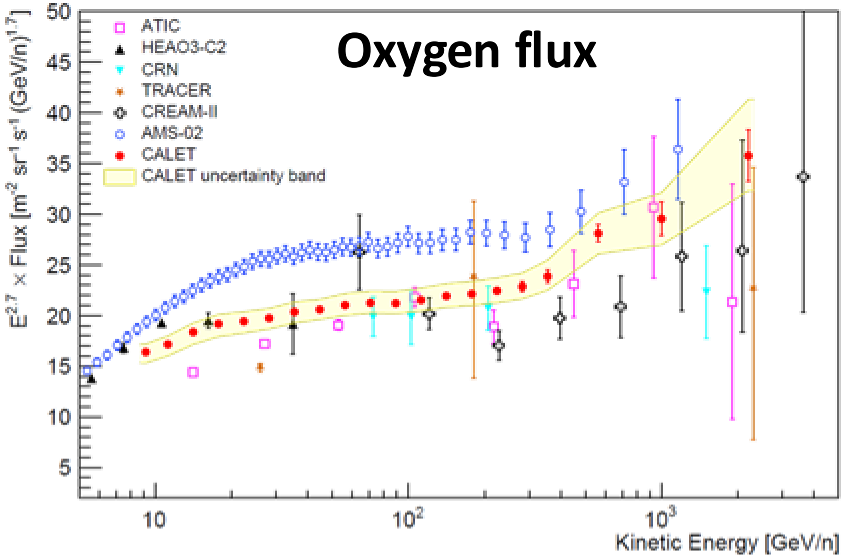

$$\Phi(E) = \begin{cases} C\left(\frac{E}{\mathrm{GeV}}\right)^{\gamma} & E \le E_0 \\ C\left(\frac{E}{\mathrm{GeV}}\right)^{\gamma}\left(\frac{E}{E_0}\right)^{\Delta\gamma} & E > E_0 \end{cases}$$

Boron	Carbon	Oxygen
$\gamma = -3.047 \pm 0.024$	$\gamma = -2.670 \pm 0.005$	$\gamma = -2.637 \pm 0.009$
$\Delta\gamma = 0.25 \pm 0.12$	$\Delta\gamma = 0.19 \pm 0.03$	$\Delta\gamma = 0.158 \pm 0.053$
$E_0 = 220\ GeV/n$ (fixed)	$E_0 = 220 \pm 20\ GeV/n$	$E_0 = 264 \pm 53\ GeV/n$

Flux ratios of cosmic-ray BCO

ICRC 2023 Update

Corr: P. Maestro, Y. Akaike

C&O: PRL 125, 251102 (2020)

B: PRL 129, 251103 (2022)

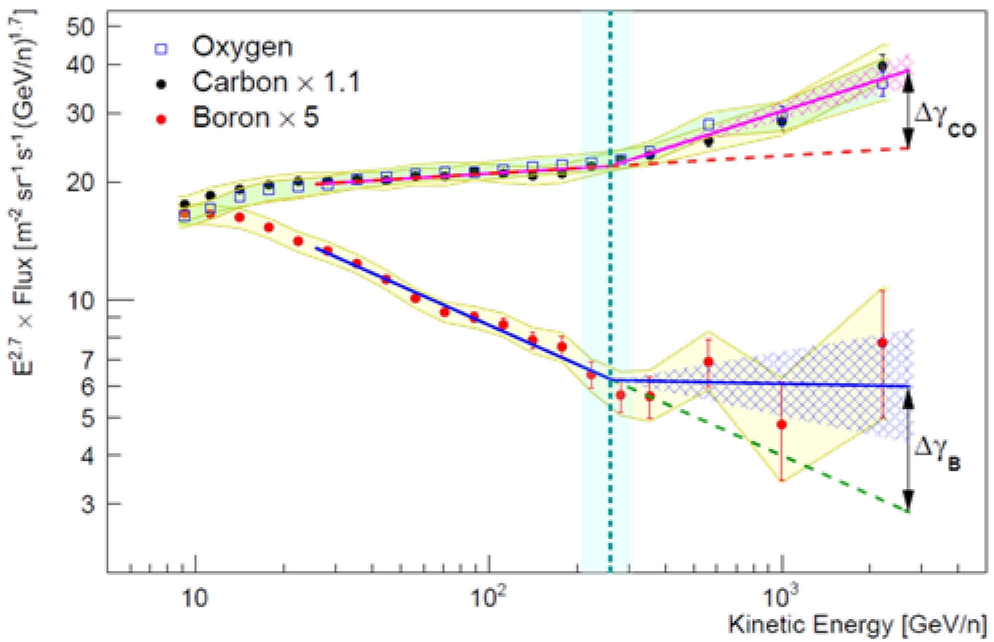

$$\Phi(E) = \begin{cases} C\left(\frac{E}{\mathrm{GeV}}\right)^{\gamma} & E \le E_0 \\ C\left(\frac{E}{\mathrm{GeV}}\right)^{\gamma}\left(\frac{E}{E_0}\right)^{\Delta\gamma} & E > E_0 \end{cases}$$

$\gamma_{CO} = -2.66 \pm 0.02$

$\Delta\gamma_{CO} = 0.19 \pm 0.04$

$E_{0,CO} = (260 \pm 50)\ GeV/n$

$\gamma_B = -3.03 \pm 0.03$

$\Delta\gamma_B = 0.32 \pm 0.14$

$E_{0,B} = 260\ GeV/n$

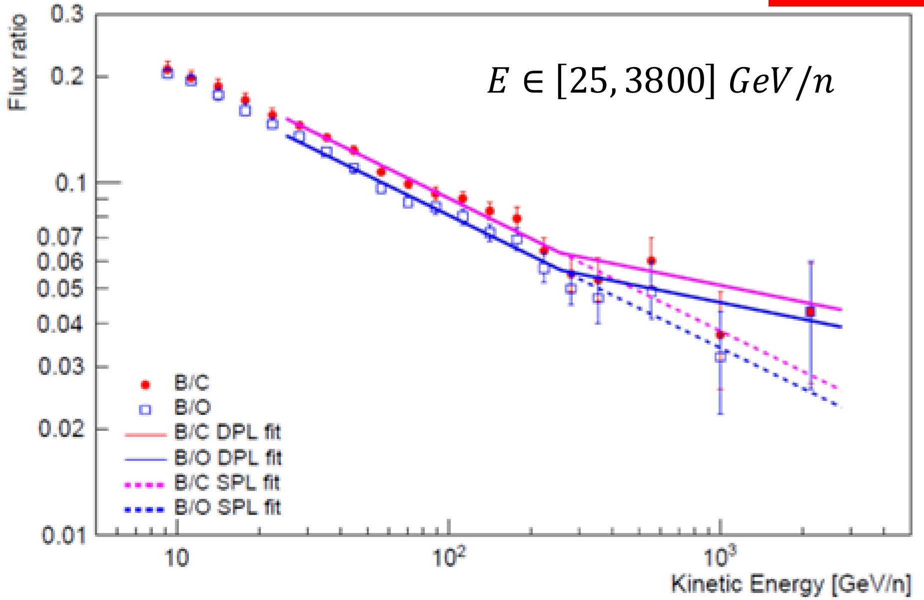

$\Gamma = -0.376 \pm 0.014$

$\Delta\Gamma = 0.22 \pm 0.10$

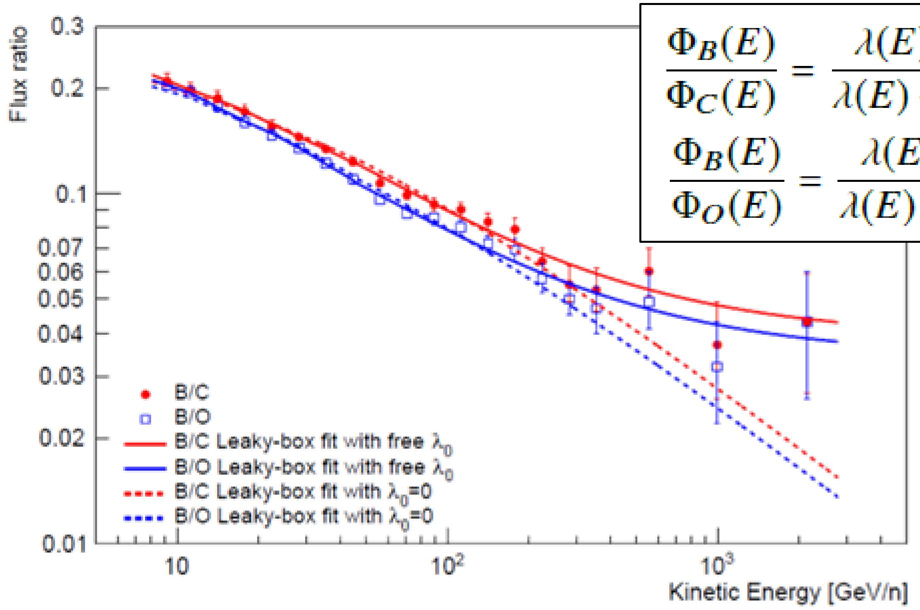

$$\frac{\Phi_B(E)}{\Phi_C(E)} = \frac{\lambda(E)\lambda_B}{\lambda(E)+\lambda_B}\left[\frac{1}{\lambda_{C\to B}} + \frac{\Phi_O(E)}{\Phi_C(E)}\frac{1}{\lambda_{O\to B}}\right]$$

$$\frac{\Phi_B(E)}{\Phi_O(E)} = \frac{\lambda(E)\lambda_B}{\lambda(E)+\lambda_B}\left[\frac{1}{\lambda_{O\to B}} + \frac{\Phi_C(E)}{\Phi_O(E)}\frac{1}{\lambda_{C\to B}}\right]$$

$$\lambda(E) = kE^{-\delta} + \lambda_0$$

$\delta = 0.61 \pm 0.01$

$\lambda_0 = 0$

$\delta = 0.81 \pm 0.04$

$\lambda_0 = 1.17 \pm 0.16\ g/cm^2$